

The Specialist Committee on CFD and EFD Combined Methods Final Report and Recommendations to the 29th ITTC



1. INTRODUCTION

1.1 Membership and meetings

The members (Figure 1) of the Specialist Committee on CFD and EFD Combined Methods of the 29th ITTC are:

- Chair: Sofia Werner, SSPA, Sweden
- Secretary: Ayhan Akinturk, National Research Council of Canada (NRC), Canada
- Secretary: Joe Banks, Southampton University, U.K.

- Kevin Maki, University of Michigan, USA
- Takanori Hino, Yokohama National University, Japan
- Feng Zhao, China Ship Scientific Research Centre (CSSRC), China
- Shin Hyung Rhee, Seoul National University, South Korea
- Hyung Taek Ahn, University of Ulsan, South Korea
- Peter Horn, Hamburgische Schiffbau-Versuchsanstalt (HSVA), Germany
- Tahsin Tezdogan, Strathclyde University, U.K.



Figure 1: The members of the Specialist Committee on CFD and EFD Combined Methods of the 29th ITTC

Four physical meetings were held:

- January 17-19, 2018, SSPA Sweden, 10 members attended
- July 3-4, 2018, NRC, Canada, 9 members attended
- January 22-23, 2019 Yokohama, Japan, 9 members attended
- January 13-14, 2020, Glasgow, U.K. 6 members attended, 1 additional online

1.2 Terms of reference assigned by the 28th ITTC

Combined methods

1. Review recent studies on claimed problems of the current model test prediction methods, for example scale effects. Assess their levels of impact.
2. Review benchmark studies, accuracy achievements and challenges of full scale ship CFD.

3. Review work on EFD/CFD combinations for relevant applications.
4. Suggest ways to improve the current recommended procedures by using CFD in combination with model test. Especially focusing on scaling procedures, starting with but not limited to the calm water speed power prediction.
5. Suggest which other parts of the ITTC procedures that could benefit from combined methods in future work.

Confidence of predictions

6. Review past work and procedures, within and outside ITTC, on CFD uncertainty, validation & verification (V&V), applied to the marine and other business sectors.
7. Suggest practical procedures to ensure the quality of CFD/EFD combined predictions to the end user, especially when applied to speed power predictions. This includes the demonstration of V&V and uncertainty assessment of commercially or legally valid predictions.

Interactions

8. Liaise and cooperate actively with the ITTC TC of related technical areas. Suggest modifications of the relevant Recommended Procedures related to CFD/EFD combinations where applicable.
9. Liaise and cooperate actively with the “CFD Workshop” committee and other groups that deal with CFD benchmark and V&V. Consider their results and suggest further work.
10. Act as a research coordinator for other researchers who wish to contribute: Suggest research topics that lead towards the given committee goals, assembly and review ongoing work.

Presentation of result

11. Apart from the normal committee report, the work should also be presented in a format directed towards the typical receiver of ship

predictions including both ship owners and authorities. This should include discussions on accuracy of respective method (CFD and EFD), reasonable requirements to uncertainty demonstration, and description of new combined methods.

1.3 General remarks

CFD offers new possibilities to improve the EFD based predictions, for example with new treatment of scale effects. On the other hand, we can still not in general rely purely on CFD for ship hydrodynamic predictions for commercial or legal purposes. By using the best combination of CFD and EFD, rather than viewing them as competing methods, we can deliver even better prediction.

New methods based on EFD/CFD combinations need to have the same confidence level as the existing Recommended Procedures give to the end client today.

The purpose of this new Specialist Committee is to initiate and support the process of introducing combined EFD/CFD methods in ITTC’s procedures, with a focus on the predictions confidence level.

2. REVIEW OF RECENT STUDIES ON CLAIMED ISSUES OF MODEL TEST PREDICTION METHODS, FOR EXAMPLE SCALE EFFECTS

Within this section, the focus is laid on calm water speed power prediction based on model tests. Results derived from model tests for manoeuvring, sea keeping or cavitation are not subject to this section.

There are various flaws in current calm water model test scaling methodologies that affect the design of the vessel, credibility of the institute and comparability of results. Some customers see a significant difference among predictions of different model basins. – not only at the trial or ballast draught but also at the load draught. Different model basins have their

individual correlation strategy deviating from ITTC recommended procedures bringing different possibilities for correlations, namely correlation allowance (c_A), form factor ($1+k$), correction on power (c_P), correction on propeller revolution (c_N), correction on friction (c_{FC}) or correction on wake (w_c).

Well-adjusted scaling and correlation strategies and techniques have been established and in the end there is a final correlation allowance derived from model test results in relation with sea trial results. The correlation allowance is therefore only applicable for the scaling method applied to this correlation allowance determination method.

The accuracy of a power prediction depends on the accuracy of the measured values and the complex scaling procedure. Helma et al. (2017) point it out when they say: “An inherent problem of this approach is, that it is virtually impossible to verify each single step, because of the complex nature of the underlying problem.”

Not stated to be complete, this overview shows aspects of experimental as well as computational problems, challenges and hopes in better predictions. Each topic requires more detailed study to conclude with a sophisticated opinion. Some topics are only touched on and not worked out in complete detail.

To each major topic in the ship prediction methods, shortcomings and advantages are noted below for the EFD as well as for the CFD methods. Challenges and dangers in combining them are not fully assessed in this document.

Generally, problems in the model testing procedure or in the evaluation strategies are not always described in detail in published articles. Therefore the following section summarizes also the authors’ experiences and impressions of the latest developments which are not substantiated by scientific investigations.

2.1 Resistance related issues

2.1.1 Froude Scaling, ITTC-1957 correlation line and form factor method (1978 ITTC Performance Prediction Method)

Extrapolating model-scale resistance according to Froude’s Hypothesis follows the principle of scaling the frictional part of the resistance to larger Reynolds number flows by applying friction lines and keeping residuary resistance constant. "A standard extrapolation method applied to the model-scale resistance here underestimates the full-scale resistance by 10%, but the empirical correlation allowance approximately corrects for that difference" (Raven et al., 2008). Raven (2017) claims that extrapolation method according to 1978 ITTC Performance Prediction Method disregards scale effects in form factor and wave resistance, the correlation allowance c_A makes up for this on average. CFD can help to estimate scale effects more precisely and reduce magnitude of c_A . Full-scale CFD calculations claim to be capable of investigating Reynolds scale effects.

Model basins use different scaling and correction methods developed overtime. Some of them have been mutually agreed upon and introduced in the recommended procedures of the ITTC but not all basins following these recommendations strictly. Two major extrapolation strategies exist and are both in use: namely the 2D method (ITTC, 1957) and the 3D method or form factor method (ITTC, 1978).

The ITTC-1957 correlation line was introduced during the 8th ITTC 1957 (ITTC, 1957) as a model-ship correlation line based on empirical investigations. Strictly speaking, ITTC-1957 model-ship correlation line embeds a form factor of about 1.09 which is the reason why it is called the Model Ship Correlation Line, not a friction line. It was stated that this correlation line was regarded only as an interim solution to this problem for practical engineering purposes (Strasser, 2018). It affects the balance between residual and frictional parts of the total resistance and has therefore a

significant impact on the predicted power for the full-scale vessel. Model basins have derived different principles of determining a correlation allowance (C_A) based on full-scale sea trial statistics to overcome this shortage for practical engineering purposes. The method is known to be simple and reliable due to the good database for the determination of the correlation allowance.

ITTC78 overlays yet another form factor. The method of the form factor $1+k$, introduced in 15th ITTC 1978 (ITTC, 1978), is also known as the three-dimensional analysis method because a form dependent factor is included. It claims to comprise the form dependent scale effects into the form factor which is set constant for the model and the full-scale ship. The determination of the form factor, derived from model test, faces significant problems when using the Prohaska method (ITTC, 2017a): submergence of the bulbous bow and the transom, flow separation and the presence of appendages lead to difficulties in a doubtless determination of the form factor (Hollenbach, 2009, Wang 2016a). This uncertainty in the determination of the form factor will directly affect accuracy of the full-scale resistance prediction as the form factor accounts for the relation of the wave and frictional resistance. Experience and impressions from results of different towing tank institutes show a significant spread of the form factor and therefore of the extrapolated full-scale results, when the 3D method is used.

It was found that if ITTC-1957 correlation line is used in combination with the form factor, “ $1 + k$ increases substantially from model to ship. An extrapolation using a fixed form factor would underestimate the ship viscous resistance by 7%” (Raven et al., 2008). García-Gómez (2000), Kouh et al. (2009), Park (2015), Wang et al. (Wang, 2015a), Kinaci et al. (2016), Lee et al. (2018) and Korkmaz et al. (2019a) demonstrate, using CFD, that the form factor is scale dependent if derived using the ITTC-1957 model-ship correlation line (Figure 2). The use of flat plate friction lines (like Grigson (Grigson,

1999), Katsui (Tahara et al., 2003) or a numerical derived friction line leads to comparable form factors for model and full-scale ships (Eça et al. 2005, Eça et al. 2008, Raven 2017, Park 2015).

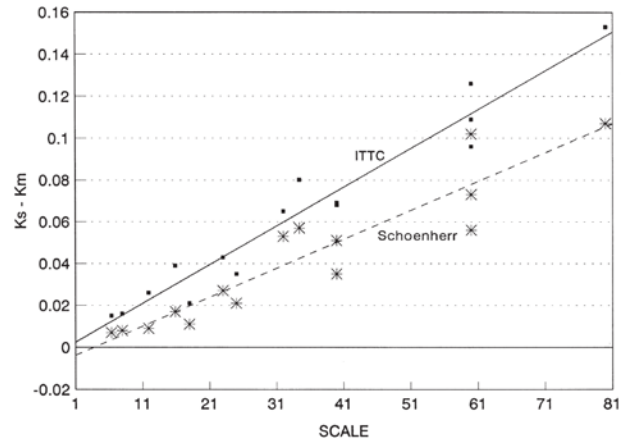


Figure 2: Form factor scale effect dependence on ITTC-1957 correlation line and Schoenherr friction line. K_s is the form factor of the ship and K_m that of the model. García-Gómez (2000).

Determining the form factor with CFD faces problems as well. The handling of the flow separation of an immersed transom or a bulbous bow is still a problem and Pereira et al. (2017) show that the predicted scale effect of a form factor differs depending on which turbulence model is used. The challenges of calculating the form factor with CFD methods is later described in section 5 of this specialist committee report.

When Toki (2008) asked "Should ITTC-1957 correlation line be revised?" they concluded, it is "Yes" in a sense that ITTC-1957 model-ship correlation line, which is prepared for two-dimensional analysis, is used in the three-dimensional form factor method analysis (1978 ITTC Performance Prediction Method). It is "No" in another sense, because towing tanks using the two-dimensional method with its correlation allowance would lose all of the full scale trial basis of making predictions. The expected gain by the revision of the friction line would be almost negligible and we have to expect the setback in power prediction accuracy caused by changing from the well accustomed line to new one.

Raven (2017) concluded that the scale effects of the form factor related to the ITTC-1957 model ship correlation line is not anything physical but an effect of the usage of the ITTC-1957 line. For slender ships the form factor, related to modern friction lines, seems to be more equal for changing Reynolds numbers. For full block vessels with flow separation the form factor changes for a varying Reynolds number and is affected by scale effects. He concluded, that CFD can contribute here to capture this scale effect. Changing to a physically correct flat-plate friction line must be followed by an adjustment of the correlation allowance c_A .

Studies of Kormaz et al. (Kormaz, 2019a, 2019b) was focused on the numerical determination of the form factor and numerical friction lines. They showed that the form factor is scale dependent when using the ITTC-1957 correlation line and scale effects are reduced significantly when a numerical friction line based on the same CFD code is used. A joint research study of 9 different organizations and 7 different CFD codes results in a comparison of the determination of form factors by different approaches (Korkmaz et al., 2020). They showed that the full-scale resistance predictions will scatter less when they used numerically derived form factors for extrapolating towing tank test results. It is shown that the combination of experiments and CFD can provide improvement to the 1978 ITTC Performance Prediction Method (Kormaz et al. 2021).

Wang et al. (Wang, 2015a) calculated numerical friction lines by CFD and compared them with available friction lines from literature. Full-scale resistance values for different hull forms were derived and they showed, that the form factor keeps relatively constant when they use numerical friction lines and bare hull forms, but not for appended hull forms. Generally, they concluded to use numerical friction lines when using form factors based on CFD.

Wang et al. (Wang, 2015c) presents a way of calculating the form factor based on energy conservation of ship wave making.

Wang et al. (Wang, 2016a) investigated the form factor derived numerically for different hull forms at various draughts and compared them with model test results. They concluded that the form factor is in line with the experimental results, when the bulbous bow is totally immersed and the transom not. They claimed that when the bulbous bow is pronounced or the transom immersed and the experimental results are doubtful, numerical results are still reasonable.

Conclusively it can be said that CFD can be supportive in determining the form factor and increasing the accuracy of 1978 ITTC Performance Prediction Method but it is too early to state new procedures and should be re-evaluated when there are more data available. An introduction of a new ship-model correlation line or the revision of the ITTC-1957 ship-model correlation line needs more in depth study as well.

2.1.2 Wave resistance

Raven et al. (2004) show that there is a scale effect on the stern wave elevation, though it is not large for slender ships. Raven et al. (2008) indicates that “the boundary layer around the hull is thin over the forward part of the hull, and in that region the pressure field is hardly affected by viscous effects. On the other hand, along the aft body, the boundary layer thickens quickly due to the decreasing girth length and the increasing pressure towards the stern. The displacement thickness of the boundary layer and wake reduce that pressure increase, and more so at model-scale than at full-scale. The reduced pressure increase in most cases leads to a reduced stern wave generation, again more pronounced at model than at full-scale; but this depends on the stern shape.” Raven (2017) claims that the wave resistance coefficient, C_w , is 20% larger for the full-scale ship than for model-scale. This increase, which is contrary to the common assumption in Froude’s hypothesis, seems consistent with the increase of the stern wave system (Raven et al. 2008) (see also Figure 3).

Van der Ploeg et al. (2011) investigated scale effect of the free-surface and concluded that the scale effects occur only in the stern wave system: namely the stern wave length is longer, the amplitude is larger and waves are less steep in full-scale. Further scale effects are recognized at the transom as the full-scale transom is dry while the model-scale transom is partly wetted.

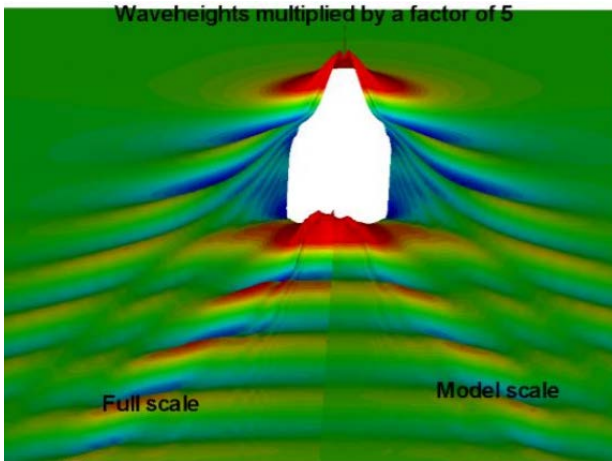


Figure 3: Stern view of computed wave patterns of Hamburg Test Case at $F_n=0.238$, for full-scale (left) and model-scale (right). Wave heights multiplied by 5 (Raven, 2008)

Kinaci et al. (2016) reviewed the determination of the wave resistance by CFD with the use of the form factor method in comparison to the wave resistance derived from model tests. They concluded a different value and slope of the wave resistance over the Reynolds and Froude numbers, was crucial in hull optimization processes.

Farkas et al. (2017) show that there is a scale effect on the wave resistance coefficient for tankers in dependent on the vessel's speed. They concluded that, for the investigated hull form, these scale effects have a minor impact on the final result.

2.1.3 Roughness correction

The roughness correction allowance used in ship powering prediction is based on an empirical formula (ITTC, 1990, Townsin et al., 1984). As experimental results for the determination of the roughness allowance are

challenging to get for full-scale ship Reynolds numbers, this formula is based on extrapolation. Although this formula suffers from an insufficient experimental basis, the common performance prediction method agrees satisfyingly with sea trial results. To overcome the deficiency of the roughness correction method, CFD methods can contribute here as CFD methods are capable to simulate in full-scale ship size, but suffer as well from missing experimental validation data in full-scale.

Full-scale CFD calculations have been performed for ships (Tahara et al. 2003, Eça et al. 2010, Pereira et al. 2017, Ponkratev 2017, Guiard 2017, Kim et al. 2019a) or for full-scale flat plate to derive a numerical friction line (Kouh et al. 2009, Wang et al. 2015a, Korkmaz et al. 2019b). Additional data is required to determine a recommended value for the hull roughness in CFD calculations (Ponkratev, 2017). Guiard (2017) found as well, that applying reasonable values for the roughness in a simulation, the result does not tend to predict the full-scale resistance as expected.

Eça et al. (2010) performed full-scale ship CFD calculations with different roughness values and concluded a good agreement with empirical formula of Townsin et al. (1984). Furthermore, they concluded, that the empirical formula accounts not for different hull forms whereas CFD calculations can make a benefit here in providing hull dependent roughness allowances and therefore improving the full-scale resistance predictions.

Further studies on full-scale CFD computation for ships with implementation of the roughness are currently addressed in the International Joint Research Project (JoRes) workshop lead by Ponkratov (Ponkratov, 2021). Results are expected in 2022.

Mikkelsen et al. (2020) have validated full-scale CFD calculations with sea trial results and have shown that a wall function considering roughness is important to get proper results in this scale.

Demirel et al. (2014 and 2017) as well as Oliveira et al. (2018) investigated the use CFD to predict hull resistance for varying roughness of the hull coating and bio-fouling.

The effect of air lubrication systems on the hull friction was investigated with CFD methods by Kim et al. (2019b)

2.1.4 Transom immersion

The transom immersion is affected by the scale effects. The speed at which a transom runs dry differs from model to full-scale (see also Section 2.1.2, especially van der Ploeg et al. (2011)). These observations are directly connected to the scale effects of the stern wave system. These effects are currently not addressed in the 1978 ITTC Performance Prediction Method (ITTC, 2017b).

Yamano et al. (2000) show that the forward facing breaking wave behind a submerged transom is scale dependent. The resistance coefficient is stated to decrease with increasing Reynolds number and is dependent on the type of stern wave: if it is a forward facing breaking wave or a following wave.

Starke et al. (2007) show that the clearance when the transom gets dry occurs at lower speed in full-scale than in model-scale. They investigated different transom depths, speeds and scales of 2-D transom stern flows. It was shown that this effect is substantially dependent on viscous effects and therefore on the Reynolds number. Due to the velocity defect in the wake of model-scale flows, the trailing wave length is reduced.

A trim wedge optimization study performed by Gornicz et al. (2016) shows that the improvement of the resistance is larger for full-scale flows than for model-scale flows due to transom flow scale effects.

Duy et al. (2017) investigated different transom shapes for the KCS container ship in model-scale.

Song et al. (2019) investigated the effect of a stern flap (or “duct tail”) on the DTMB5415 in model and full-scale in CFD and experiments. They found that the full-scale simulation lead to larger improvements than the extrapolated values from model-scale investigations. They stated that the current model extrapolation method cannot account for the effect of the resistance reduction of the stern flap.

The scale effects of the stern waves seem to be very complex but CFD has already shown that it can provide a good insight in these scale effects. A derivation of correction factors to account for the different scale effects and to improve the performance prediction might be reasonable in the future.

2.1.5 Nominal wake scaling

This section deals with the nominal wake scale effects in the propeller plane. Section 2.2.3 accounts for the scale effects of the effective wake including propeller operation used for the performance prediction.

The Specialist Committee on Scaling of Wake Field of 26th ITTC (ITTC, 2011) made comparisons between full-scale CFD results and extrapolated full-scale wake fields from model-scale according to different methods. The method according to Sasajima and Tanka (1966) was found to be suitable for scaling the model-scale wake. The specialist committee concluded that the best approximation of the full-scale nominal wake can be obtained using high resolution CFD calculations.

Van et al. (2011) use geosim models of KVLCC2 and KCS. They show the scale effect on the flow using CFD. It is shown that for larger Reynolds numbers, the flow near the hull surface around the stern accelerates more and the pressure recovery is larger. This delays the three-dimensional flow separation and reduces the bilge vortex formation. In the wake, the axial flow component is larger and the hook shape disappears for larger Reynolds numbers. This effect is larger on full block hulls.

In a full-scale CFD study with different hull roughness settings, Eça et al. (2010) showed a dependency of the nominal wake on the applied roughness in the calculation.

Wang et al. (2015b) calculated the nominal axial wake fraction of a container ship at different scales and derived a simple relationship to describe scale effects on wake fraction.

Pereira (2017) showed with RANS simulations that the predicted wake scale effect depends on the turbulence model (Figure 4). The difference in wake prediction between the turbulence models is smaller at full-scale. The dependency of the calculated nominal wake on the turbulence model is also shown by Guiard (2017).

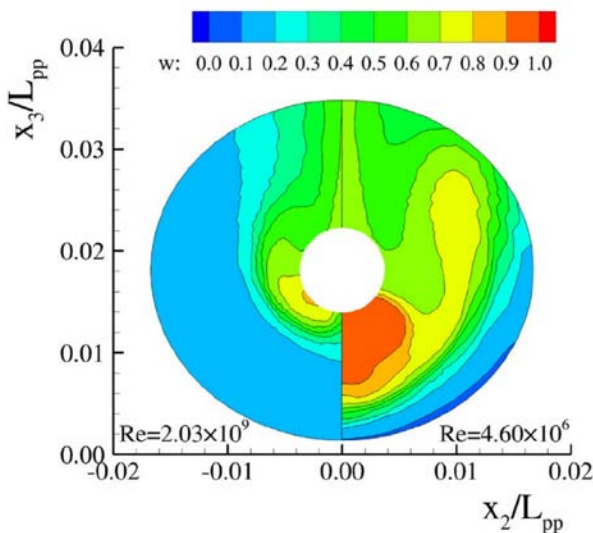


Figure 4: Stream-wise velocity deficit at the propeller at model (right) and full-scale (left) Reynolds number. (Pereira, 2017)

The aim of the international JoRes workshop led by Ponkratov (Ponkratov, 2021) is to measure a full-scale wake and to compare it with full-scale wake measurements. As this will be with an operating propeller, the findings might only be partial beneficial for improving the nominal wake scaling. Results are expected in 2022.

Experimental wake measurements in cavitation tunnels with a model running at larger

Reynolds number than models running in the towing tank can help improve the scaling methods for the nominal wake.

The Tokyo 2015 Workshop on CFD methods in ship hydrodynamics (Hino et al. 2021) indicated that CFD methods can help to understand flow phenomena in the wake.

2.1.6 High Speed Vessels

For high speed vessels like planing boats or catamarans the ITTC provides procedures in 7.5-02-05 “High Speed Marine Vehicles”. In contrast to the classical performance prediction of displacement hulls, the prediction for high speed vessel requires special attention to several aspects which could be challenging during the experimental studies. To list some issues, CFD could assist here to improve the predictions: the wetted area for the scaling process could be estimated, the final dynamic floating position could be predicted to install turbulence stimulators, load cells or other measurement devices properly. For high speed vessels the air resistance plays a substantial role where CFD could help to determine the air resistance during the model tests or for the final full-scale vessel.

Lift producing appendages like foils suffer from scale effects due to different Reynolds number in model and full-scale. Lifting forces could be investigated in CFD in model and full-scale, to adjust the lifting devices for the model-scale experiments to represent the equivalent lift effect as for the full-scale vessel.

A further scale dependent effect is the spray of the bow wave or other waves. Due to the surface tension of the water, the spray requires the attention on other scale effects.

Conclusively it can be said, that the topic of high speed vessel needs further attention on investigating the scale effects of the model test procedure including a literature review and assessing the benefits of possible assistance by CFD calculation methods what might be addressed in future ITTC committees.

2.1.7 Scaling of small appendages

Smaller appendages like small bow thrusters, small bilge keels or sea chests may not be applied on the model for towing tank tests and are included in the performance prediction methods by towing tank facilities differently. Typically, an additional correlation allowance is applied following different principles. A common strategy among the towing tank facilities is not present and detailed studies are not available.

As these appendages have not been present at the model tests, the issue is not based on scaling problems but rather on the estimation of the additional resistance in the full-scale.

However, Krasilnikov et al. (2017) studied scale effects on bow thruster tunnels and found their relative resistance to be twice as large in full-scale than in model-scale.

For a better understanding of the full-scale behavior of these appendages, CFD calculation can assist.

2.1.8 Scaling of large appendages

Appendages typically mounted on the model like rudders, twin screw appendages, stabilizer fins, large bow thrusters or large bilge keels can be scaled individually, partially and independent of the bare hull resistance according to the 1978 ITTC Performance Prediction Method (ITTC, 2017b).

Scale effects on the wake of appendages have been investigated by Visonneau et al. (2006). A scale effect on the resistance of the appendages has not been subject to this study. The Beta-Method (ITTC, 2017b) for predicting the appendage resistance has been reviewed and numerical simulations have been carried out for validation by Oliva-Remolà et al. (2013). They compared experimental and extrapolated results with the results obtained from CFD simulations. They report that due to the complex geometry the validation of the Beta-Method with computational methods has not been successful.

An investigation on the scale effects on rudder lift and drag forces with operating propeller has been performed by Nguyen et al. (2016). Van Hoydonck et al. (2018) investigated the rudder drag and lift on a free-stream full-scale computation and found that the drag values for the full-scale computation are significantly lower than those obtained from the towing tank results.

Sasaki et al. (2019) and Tacar et al. (2019) investigated scale effects on a Gate Rudder.

A proper scaling procedure for appendages of different types at different positions and flow regimes seems not to be investigated very much. A profound understanding of the scale effects require further studies where full-scale CFD calculations can assist.

2.1.9 Flow Separation or vortex generation on the hull

This topic has hardly been investigated towards its effect in the scaling procedure of the resistance. Exemplary, it can be seen in model and full-scale wake calculation, that hook vortices (bilge vortex) will have different extents at different scales. The issue of flow separation on the aft part of the hull has barely been investigated.

To further understand the scale characteristics of vortices and flow separation and their effect on the resistance scaling and prediction, more investigation must be done. CFD methods (RANS) may only be of limited use as flow separation is very complex.

2.2 Propulsion related issues

The performance prediction method according to the 1978 ITTC Performance Prediction Method (ITTC, 2017b) introduces several simplified mathematical formulations to the scaling procedure. It is known that the complex and very diverse flow phenomena at the propeller and the hull will interact with each other and may not be broken down to a

simplified mathematical formulation. Therefore, it could not always be distinguished which part of the scaling process is affected by a minor change in the propulsion settings, for example, a change in the propeller diameter. The changed propeller diameter will modify the wake scaling and the open water test scaling as well. But will they always change the prediction in the same direction? Nevertheless, the following section will focus on specific issues of the propulsion prediction, although it is known that specific aspects that contribute to the overall performance prediction need to be analysed in a holistic way. Subsequently, the final overall performance prediction will always require a certain amount of judgment.

2.2.1 Propeller scaling

The scaling of the propeller open water test results to other Reynolds numbers like those during the propulsion test or those in full-scale are a crucial part of the performance prediction method for ships. Although the 1978 ITTC Performance Prediction Method (ITTC, 2017b) provides simple mathematical formulations to account for scale effects for the full-scale propeller open water performance, other available methods in literature and in use differ in their level of detail. Streckwall et al. (2013) stated that the results of the existing methods differ significantly. In particular, modern blade geometries require modern scaling methods which are using scaling procedures depending on the variation of blade geometry over the radius or even more complex methods. CFD can contribute here to improve the scaling procedure as it gives insight into the flow on the propeller blades on different scales.

As the flow on the propeller blade features the transition of laminar to turbulent flow at model-scale, CFD calculations have to make use of turbulence transition models. Experimental paint flow tests on propeller blades have been performed to validate the findings made in CFD (Figure 5).

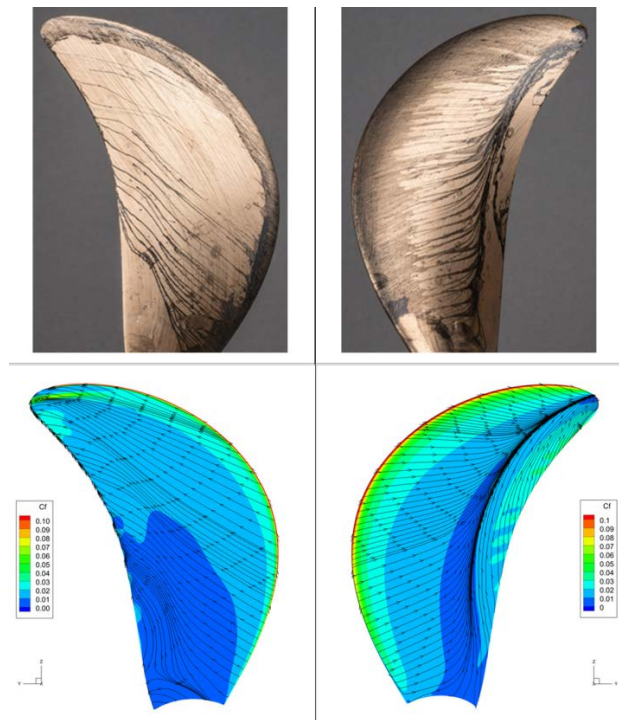


Figure 5: Propeller at low Reynolds numbers. Paint test (row 1) vs. limiting streamlines by CFD (transition γ -model) (row 2). Left: Pressure side. Right: Suction side. (Li, 2019)

Following this approach, Müller et al. (2009) investigated the flow on propeller blades and found that the three-dimensional flow effects play an important role and that a reduction to a two-dimensional problem related to the blade profile will not be sufficient to capture all effects for the scaling procedure. They proposed a scaling method applying a change of the magnitude of the force and the angle at each radius.

Streckwall et al. (2013) developed a “stripe method” to better predict the propeller scaling, especially for modern types of propeller blade profiles.

Rijkema et al. (2015) and Baltazar et al. (2017) investigated different numerical strategies, in particular different turbulence models (including turbulence transition models) for varying Reynolds numbers. They show an increasing thrust and a decreasing torque with increasing Reynolds numbers. Different turbulence models have been investigated by Bonfiglio et al. (2015) especially for transient

flows on the propeller blade. The prediction of the wake behind a propeller open water test with different turbulence closures have been investigated by Guilmineau et al. (2015)

Amadeo et al. (2017) and Quereda et al. (2019) focused on the application of turbulence transition models for unconventional propellers and the resulting performance prediction.

Other unconventional propellers have been subject to the studies of Peravali et al. (2016). The study evaluated propeller scaling procedures with the 1978 ITTC Performance Prediction Method and RANS methods in open water and in-behind condition. They have shown that there is a Reynolds number effect on blade pressure distribution which is not taken into account by the ITTC 1978 method related to the effective wake scaling. This will especially affect unconventional propellers.

The scaling of tip-rake propellers has been investigated by Okazaki et al. (2015), Dong et al. (2017), Shin et al. (2017) and Klose et al. (2017), where the latter proposed a modification to the ITTC 1978 scaling method.

Helma (2015) introduced a new scaling method and compared the results with other scaling methods specifically focusing on the overall performance prediction (Helma et al. 2017).

Hasuike et al. (2017) and Li et al. (2019) investigated the propeller scaling process and recommend using the “2 propeller open water test method” (2POT) introduced by Tamura (1977).

Heinke et al. (2019) showed the application of at least three propeller open water tests to identify the Reynolds dependency of the propeller open water tests performed at very low Reynolds numbers and to improve the performance prediction. This method is supplemented with CFD calculations

By the latest research it is shown that the classical propeller scaling methods do not

properly predict the full-scale open water performance, especially those of unconventional designs like tip modified propellers or small blade area propellers. Many studies mentioned here applied sophisticated CFD methods including transition turbulence models to account for the correct transition of laminar flow to turbulent flow for model-scale Reynolds numbers. Although some flow phenomena have been well predicted by CFD, not all results are fully satisfying when CFD methods are applied. The simulation of the laminar-turbulent transition is still a demanding task. Ongoing studies where CFD methods might be a part of have to be made to possibly conclude with an updated scaling procedure within the ITTC recommendation.

2.2.2 Propeller Hull Interaction

The understanding of the scale effects of the propeller-hull interaction requires model tests or CFD computations of the sailing hull with running propeller. The propeller-hull interaction is expressed by the overall propulsive efficiency (ETAD, η_D) influenced by the hull efficiency (ETAH, η_H , defined by the wake fraction w and the thrust deduction factor t) and the relative rotative efficiency (ETAR, η_R). The scale effects of the rotative efficiency and the thrust deduction factor are defined to be zero or negligible in the 1978 ITTC Performance Prediction Method. The scale effect of the wake fraction has a major influence. In addition to the reference made in this section, studies presented in Section 2.1.5 should be considered as well.

In the report of the Specialist Committee on Scaling of Wake Field of 26th ITTC (ITTC, 2011) participants of a survey stated that the typical scaling on wake was performed for nominal wakes as well as distributions. Effective wake and average values were of secondary importance. Procedures of scaling the effective wake are provided by 1978 ITTC Performance Prediction Method (ITTC, 2017b) or Yazaki (1969).

Numerical and experimental investigations have been performed by Pecoraro et al. (2013) to investigate the effect of the propeller on the detached flow in the stern region of the hull and to quantify the propeller influence upstream.

Krasilnikow (2013) showed that numerical self-propulsion tests in model-scale are suitable to capture the propeller-hull interactions properly.

Hally (2017) showed a method to determine the effective wake by a RANS-BEM coupling method. A similar method has also been used by Regener et al. (2017) to investigate and evaluate nominal and effective wakes in model and full-scale with respect to propeller design.

Sun et al. (2019) performed model and full-scale CFD calculations and investigated the scale effects of the propeller-hull interaction coefficients (Figure 6). They showed that the scale dependency of the wake is one of the main reasons for the propeller working at higher advance ratio and having a lower thrust coefficient in full-scale than in model-scale.

The effect on the rotative efficiency has been investigated by means of experimental data and RANS calculation by Lücke et al. (2017). They recommended an introduction of an efficiency factor η_N in case of rotating wakes in case of using pre swirl stators or asymmetric aft bodies.

Lin et al. (2014) evaluated the scale dependency of the thrust deduction.

By separating the free surface calculation from the propeller calculation, an alternative approach to derive propeller hull interaction and final performance was applied by Giannoulis (2019).

An alternative principle of the computational set up to derive propeller hull interaction and a final performance prediction was applied by Giannoulis (2019).

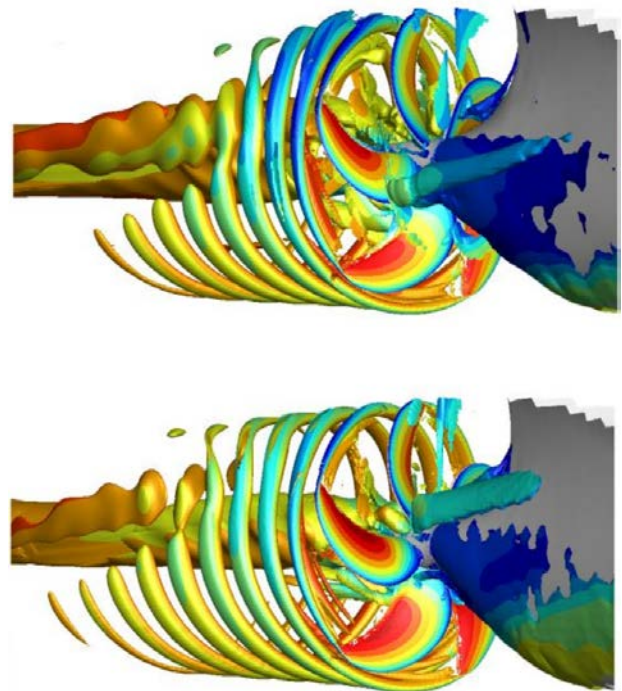


Figure 6: Propeller operating behind a hull. Instantaneous iso-surface of nondimensional Q-criterion, colored by axial velocity ratio. Top: Model-scale. Bottom: Full-scale. (Sun, 2019)

The scaling methods for wake are very basic but directly affect the final performance prediction. Further CFD simulations with propeller operation might be helpful in the future to investigate these scaling issues in more detail and to improve the accuracy of the performance prediction.

2.2.3 ESD scaling

Energy Saving Devices (ESD) or Propulsion Improving Devices (PID) are mostly operating near the propeller and are found to be effective in model tests, as well as full-scale sea trials or monitoring data. As they are working in the wake region of the hull they are affected by Reynolds number effects (scale effects). ITTC provides no standardized procedures to account for these special scale effects (Kim, 2017). A Specialist Committee on Unconventional Propellers at the 22nd ITTC (ITTC, 1999) reviewed experimental methods and extrapolation strategies for different kinds of energy saving devices in detail. Scale effects

mainly due to a modified wake in full-scale are affecting the friction on the device, the modified propeller revolution due to the device or the generation of vortices at the device.

It was shown by Hafermann et al. (2010) that self-propulsion RANS calculations are capable to predict the power gains by a combination of fins and ducts in front of the propeller in model-scale. A closer look on the scale effects of ducts and fins has been made by Heinke et al. (2011) mentioning as well the influence on the cavitation, pressure pulses and design of fins in terms of angle of attack difference between model and full-scale. The need of adapting the design of ESDs towards the full-scale wake is described by Guiard et al. (2013). A design process for pre swirl stators including the validation with trial results was performed by Kim et al. (2012) as well as by Xing-Kaeding et al. (2015). Visonneau et al. (2016) concluded the need for a design of an ESD in full-scale too. They showed as well by unsteady hybrid LES computation an unsteady separation zone characterized by a wake of coherent ring vortices.

A propeller cap fin recovering energy from the hub vortex was investigated by Kim et al. (2016). They pointed out the difficulty to reproduce the cap vortex effects in model-scale (experimental and numerical). They show by computation that the power saving effect is larger in full-scale, a result verified by sea trials.

Kim et al. (2017) proposed an extrapolation method for model-scale results by taking into account the tangential velocity components into account, calculated by CFD methods.

The effect of a combination of different ESDs has been investigated by Okada et al. (2017) and Lee et al. (2017). The latter have shown that the efficiency gain by a combination of three devices is smaller than sum of the efficiency gain by each device.

Further studies on the design, performance and scale effects with full-scale CFD calculations have been made by Wawrzusiszyn

(2018), Krasilnikov et al. (2019) and Sakamoto et al. (2019).

Although it is well known that there are significant scale effects on energy saving devices, not all flow phenomena are fully understood. Therefore suitable and commonly agreed extrapolation methods may not be available. Further studies should be made here including the use of full-scale CFD to better understand the physics and to provide sophisticated power prediction guidelines.

2.2.4 Podded propulsion

Scaling procedures for podded propulsion or azimuthing drive units are addressed in the ITTC Recommended Procedures and Guidelines “Podded Propulsion Tests and Extrapolation” (ITTC 2017c and ITTC 2017d) and its contribution by “The Specialist Committee on Azimuthing Podded Propulsion of the 24th and the 25th ITTC” (ITTC 2005 and ITTC 2008). The Procedure “describes the best possible methodology based on information currently available. However, users should be aware that a clear scaling procedure has not yet been developed due to the lack of model-scale and full-scale supporting data the public domain. The Procedure may be changed when such data becomes available” (ITTC 2017c). Although, commonly agreed procedures have been defined, difficulties are still to fully understand and account for scaling effects of the pod housing resistance, complex pod units (like contra rotating pod units), off-design conditions or aspects of cavitation and manoeuvring. The community was encouraged to investigate more on full-scale problems including the assistance with RANS CFD methods.

Sanchez-Caja et al. (2003) investigated the performance of POD units by means of model and full-scale CFD calculation and found large differences in the scaling of passive components of the thruster showing that the available scaling procedures are not adequate.

Choi et al. (2014) investigated scale effects of pulling type podded propeller with CFD analysis performed at different Reynolds numbers. They concluded that the pod housing resistance under the presence of the propeller slipstream is a major factor of the scale effects. An extrapolation method for these types of podded propulsors is suggested by Park et al. (2016).

Contra rotating PODs (CRP) have been investigated by Wang et al. (2016b). They proposed for the extrapolation and performance prediction using thrust and torque coefficients for the aft propeller to account for the forwards propeller wake and pod blockage effect. Krasilnikov et al. (2017) had a focus on scale effects of a CRP as well performing self-propulsion CFD simulations. They found that propulsive factors do not show large variation with scale, however they suggest performing more investigation on the wake fraction and the thrust deduction factor as they have been under-predicted by the CFD calculations compared to measurements.

A hybrid design of a shaft line propeller in front of a podded propeller has been investigated experimentally by Quereda et al. (2017). They proposed an extrapolation method for these kind of propulsion system.

A POD housing with a nozzle around the propeller and a stator has been investigated by Veikonheimo et al. (2017) using CFD and model-scale test. A new extrapolation method has been introduced for this kind of propulsion system.

To understand the flow physics and provide advanced extrapolation methods for the variety of podded propulsion systems more in depth studies are needed. CFD methods can assist here to understand the complex flow and interaction effect between hull, POD housing and propeller as well as to investigate effects in the scale.

2.2.5 Ducted propellers

The performance of model tests (propulsion and bollard pull) and the principle evaluation of ducted propellers is addressed in the ITTC procedures and guidelines (ITTC, 2017e).

Bulten et al. (2011 and 2017) investigated scale effects on ducted propellers by model and full-scale CFD calculations. Scale effects have been identified and explained based on the theory of loss coefficients and pump efficiency. They stated that the “conventional extrapolation method based on wake fraction, thrust deduction and relative rotative efficiency does not always give clear trends for ducted propellers” and that the “possible differences between laminar and turbulent flow regimes are not explicitly captured in the extrapolation methodology”.

Rijkema et al. (2011) investigated open and ducted propellers with potential flow and RANS methods for different scales (Figure 7). They found, that all open water coefficients increase depending on the propeller loading.

Xia et al. (2012) investigated ducted propellers and was checking the numerical set-up as well as the cavitation and thrust breakdown behaviour.

Bhattacharyya et al. (2015a and 2015b) investigated the laminar turbulent transition of open and ducted propellers with RANS methods including transition modelling. They showed that it is important to use CFD with transitional effects as it directly affects the interpretation of the scale effects. The scale effects were found to be similar for different duct designs. They found significant scale effects for the duct thrust depending on the propeller loading. The interaction between the propeller tip and the duct is important because it influences the scale effects due to propeller tip loading.

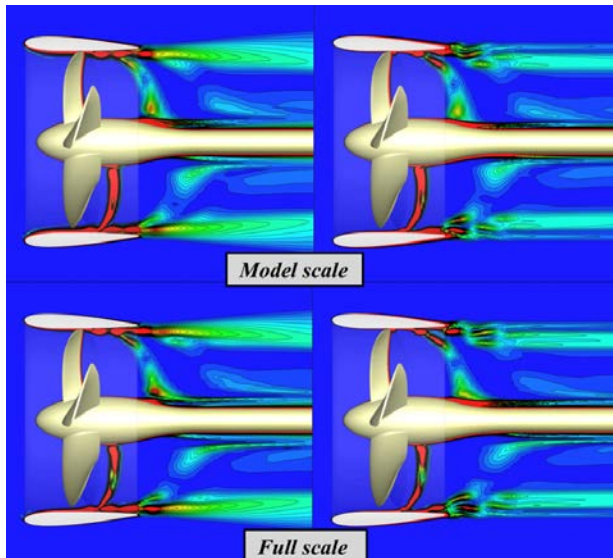


Figure 7: Slice of vorticity field for $J=0.30$ (left), $J=1.0$ (right). Model-scale results (top) and full-scale results (bottom). (Rijkema et al. 2011)

Zondervan et al. (2019) compared the performance of ducted controllable pitch propellers calculated with BEM and URANS including sliding interface. They found that BEM method is an adequate choice for the design of ducted propellers in reasonable calculation times although it has its limitations.

The complex flow of the propeller interacting with a duct can be further investigated with CFD calculations to better understand the flow phenomena and scale effects and to improve the extrapolation methods for ducted propellers.

2.3 Assessment of Level of Impact on Speed Power Prediction

The following chapter is based on literature review, as well as own experience from commercial work and interviews with yards, propeller designers, ship owners. The aim of this chapter is to identify the different mentioned difficulties with the scale effects and their “level of impact” towards the general performance prediction of vessels.

The impact can be judged in different ways. For example:

1. Impact on trends in full-scale performance. When the optimum design in model-scale is not the optimum in full-scale. The prediction in model-scale drives the design in the wrong direction, leading to ships that work not in the optimum in reality.
2. Error in predicting the energy saving of new concept.
 - a. Show large potential in model-scale, but gives no gain in full-scale. Leads to increased energy consumption.
 - b. Show no potential in model-scale, but gives in fact good saving in full-scale. Leads to missed opportunities, since these concepts are not realized.
3. Error in predicting the absolute value of power. This leads to issues for the next link in the chain, for example that cavitation tests are done at incorrect condition which may lead to unnecessary safe propeller or opposite, propeller damage because risk was not detected. It can give error in selecting main engine and other design choices depending on the total power. It affects the regulations like EEDI, EEXI and contracts.

The following paragraphs summarize the “level of impact” for some of the individual topics mentioned in the forgoing chapters.

Hull friction determination using alternative friction or correlation line

On average level, the effect of using an unsuitable friction or correlation line and the form factor concept is small. If a model basin uses similar scale factors and similar type of ships, the average error is well corrected with correlation factors. For individual ships deviating from the standard and for model basins without extensive correlation statistics, the error might be larger.

Determination of the form factor

Difficulties to determine the form factor due to the applicability of the experimental procedure (Prohaska method) can fail for some ship types and lead to errors in the magnitude 5% even up to 10% on total power. It can affect

the trends so that the best hull form is not selected, for example when balancing the wave resistance against viscous resistance. This effect can be significant for some ship types operating at Froude numbers around 0.2-0.3, like RoRo, LNG-carriers, container vessels, but less important for tankers, bulk carriers and others operating at lower Froude number. It has also consequence on defining the EEDI as the form factor has a large effect here.

Wave resistance and transom drag

Scale effects of wave resistance could also affect the trends, for example comparing ship hulls forms with different stern shape. This is linked to the transom resistance scaling, since the scale effect on wave resistance occurs mainly in the aft body. The magnitude of the error could be significant and affects ship types like RoRo or container vessels.

Roughness allowance

The roughness allowance is applied on all full-scale ship prediction procedures. As the overall frictional resistance due to roughness is rather small compared to other parts of the resistance the impact on trends and absolute power is low when improving this issue.

Appendage resistance

Appendages could be very different and scaling procedures are not individually enough to account for different scale effects. Therefore there might be an impact on trends, optima of designs and overall power consumption. For a better understanding of the full-scale behaviour of appendages and the flow, CFD calculation can assist. Proper scaling procedure for appendages of different types at different positions and flow regimes can be investigated.

Flow separation or vortex on the hull

For models of full ships, there may be flow separation or string bilge vortices, which do not occur in full-scale. Sometimes this is stronger in towed condition during the resistance test but

less so in the self-propelled condition. These phenomena may lead to:

- Form factor can be too high, which may give too optimistic power prediction.
- A duct ahead of propeller stabilizes the flow and reduces separation what affects the evaluation of this energy saving device.
- Separation around U-shaped aft body with flow separation in resistance test underestimates the thrust deduction coefficient t and overestimates of wake fraction w , leading to too optimistic power prediction.

Propeller Open Water Scaling

Several propeller designers express their concern that some actors (always the others) deliberately optimize propeller blades for model-scale condition. One example is the problem of a possible laminar boundary layer in self-propulsion test and the usage of two propeller open water test (POT) at different Reynolds number to overcome this. It is claimed that this method can be utilized to achieve higher efficiency on paper. On the other hand, others claim that the 1978 ITTC Performance Prediction Method (ITTC, 2017b) with one POT penalizes low blade area propeller.

In both ways, this may lead to suboptimal propeller designs. The magnitude is approximately up to 3% and can affect most common ship types.

Effective wake scaling

The scaling according to 1978 ITTC Performance Prediction Method (ITTC, 2017b) is sometimes claimed to penalize some concepts:

- Unconventional propellers
- Increasing propeller diameter

Energy saving devices

Different ESDs recover energy from different sources to improve the performance. The individuality of the devices makes it difficult to find common scaling procedures and to predict the absolute power level. The influence on the optima in design between model and full-scale is noticeable.

Ducted propellers

This is indicated here as an example where the usage of model tests may hinder the possible development of energy savings due to significant scale effects. It is suspected, that ducted propellers perform in general better in full-scale than in model-scale.

2.4 Ranking of the level of impact

The committee has proposed a ranking of different challenges in scaling to determine the future focus for investigations. The choice of issues to rank has been mutually agreed upon. For this ranking, three different criteria have been evaluated for each issue separately. A rating of zero to two has been applied after a common discussion in the committee. These ratings have been summed up equally weighted to get an overall ranking and to find the issue most suitable for future investigations. As the ranking is based on personal impression and experience of each committee's member daily work and the input of interviews made by the committee, the result is quite subjective and controversial to a certain degree. Nevertheless it was found that this is a simple, practical and good starting point to get a ranking at all.

The three criteria are:

1. Impact on trends and design
2. Impact on absolute power
3. Frequency of occurrence

Criteria one and two have been discussed in the introduction of this chapter. The ranking for the third criteria "frequency of occurrence" tries to classify how often this issue is coming up

during typical daily work for performance prediction of ships. Therefore, more frequent issues are rated higher than more seldom issues what addresses the urgency for further improvement.

A table giving an overview of these rankings is found in the appendix of this chapter (See Appendix A). From this tabular overview the committee concluded to suggest the community to focus on five different issues:

- Numerical determination of the form factor
- Full-scale calculations of energy saving devices
- Improving wake scaling methods
- Improving propeller open water scaling methods
- Understanding scale effects of transom immersion (linked to wave resistance scale effects)

In addition to this ranking, the possibility to improve each issue with CFD methods was classified. This result is included in the table as well and, as for the other ranking, is strongly based on personal impressions and experiences.

The committee decided to investigate whether a modification of the 1978 ITTC Performance Prediction Method (ITTC, 2017b) regarding the possibility to use CFD for the form factor could be beneficial. The motivation for selecting this issue from the list is that it was regarded as a major error source in EEDI and contract power prediction, and it is believed to have a potential to be improved with CFD, since state-of-the-art CFD can handle model-scale resistance computations well.

The community is not bound to this ranking and classification and could make their individual ranking based on their experience and therefore their choice of the path of future investigations.

2.5 Issues not considered

There have been many issues reviewed in this chapter in detail having more or less a significant effect on the speed power performance prediction. Nevertheless, some other issues do affect the prediction methods as well and are influenced by scale effects. But it was found that these issues have a minor effect on the speed power prediction and will therefore only be mentioned here shortly.

Some of the issues are from the perspective of sea trials. Sea trials are important to mention here, because they are the basis for the correlation strategy of model tests. The following three topics are mostly vessel specific issues and are determined individually to correct sea trials properly. These are:

- Added resistance of wind
- Added resistance of waves
- Added resistance due to shallow water

There are suitable methods either empirically or by means of CFD methods, to determine the value of these added resistances. These fields already have or will have a certain potential where CFD methods could improve the sea trial evaluation and therefore the correlation of model tests.

There are further model test procedures affected from scale effects:

- Sea-keeping tests
- Manoeuvring tests
- Cavitation tests

These tests have not been part of the review as they are not part of the calm water speed power prediction. Nevertheless, these methods already do or will benefit from the application of CFD methods.

2.6 Advantages of model tests

Experimental model tests are still the most trusted method for power predictions for ships.

This is mainly due to the profound experience for the application of performance prediction methods applied among different towing tank facilities. Based on these experiences, good correlation strategies are available giving reliable prediction for the absolute powering of ships. A good correlation between sea trials and scaled tank results has been established over the decades. Werner et al. (2020) shows that towing tank predictions and corresponding sea trials match within 1% on average for a population of 183 ships. (Figure 8). Furthermore experimental tests will still benefit from the inherently correct physical water properties like turbulence, boundary layer development, flow separation or vortex generation where CFD methods may suffer from the necessary approximations.

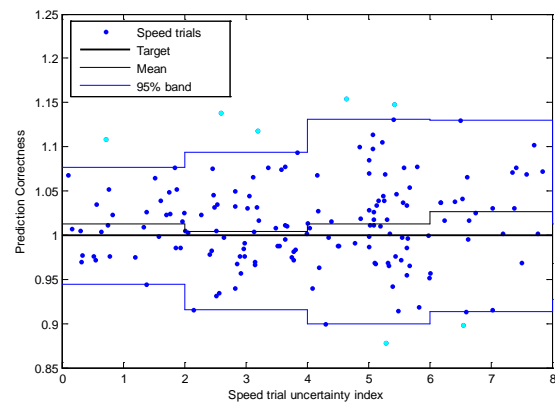


Figure 8: Confirmation of model test power prediction correlation show that the average difference is about 1% on the power. (Note that the spread is due to precision error in speed trial test and building process.) (Werner et al. 2020)

2.7 Outlook

Besides the aforementioned encouragement in further CFD investigation in model and full-scale for the variety of different issues of the scaling and performance prediction methods, a certain focus should be laid on the checking and adaptation of the correlation allowance of an individual towing tank facilities by applying new methods like CFD. The link to the ITTC Guideline on the determination of model-ship correlation factors (ITTC, 2017f) is made here. Currently there is no procedure indicating when

a correlation factor has to be adjusted when changing scaling procedures.

The committee identified scaling processes to be addressed in future for the consideration if CFD methods can be used in assistance for a more precise speed power prediction. These problems are:

- Numerical determination of the form factor
- Full-scale calculations of energy saving devices
- Improving wake scaling methods
- Improving propeller open water scaling methods
- Understanding scale effects of transom immersion (linked to wave resistance scale effects)

Unless these emphasized scaling issues, all other items mentioned in this chapter merit more in-depth investigation with CFD methods. CFD tools can be useful for understanding scale effects and will give an insight into flow superior to that obtained from experimental model tests alone. The items that need more in-depth investigation are:

- Appendage drag scale effects
- Nominal wake scale effects
- Ducted propeller scale effects
- Podded propulsor scale effects
- High speed vessel scale effects
- Flow separation and vortex generation scale effects
- Full-scale roughness effects
- Application of numerical friction lines within the 1978 ITTC Performance Prediction Method

It should be kept in mind that these individual problems should not be considered separately. There might be scaling problems interacting with each other. The indication of interaction effects should be addressed in further studies as well.

Besides the scaling problems in the calm water speed power prediction, scaling problems

in the fields of manoeuvring, sea keeping and cavitation are worth more detailed investigation. Determination of added resistance due to wind, waves and shallow waters is needed to properly evaluate sea trials and should be investigated in detail. From these investigation, updated procedures and guidelines should be worked out by the ITTC to address the potential which CFD methods can provide.

The committee concluded to keep on working on the above mentioned fields. The committee can liaise benchmark cases of CFD methods which can be used for the power prediction. Other committees should have a task to review possible application of CFD methods within their field of work. They should contact the EFD/CFD specialist committee and inform them on these possibilities and EFD/CFD specialist committee summarizes these methods.

2.8 Conclusion

Model tests are still an accurate reliable way to predict the speed and power for ships. Nevertheless the computational methods can truly assist to improve the applied methods during the general scaling process by assisting and improving an individual scaling problem.

To identify which of the scaling problems would be the most suitable to be used for applying a CFD method to its improvement, it is necessary to organize these individual problems and rank them on different aspects. Different individual scaling problems for the calm water speed power prediction have been identified and their general uncertainty has been assessed to the level of impact on the prediction of correct trends in design as well as on the absolute powering level. The scaling problems have been rated on their frequency of occurrence in the typical business of towing tank facilities. The CFD method, which could be used in a certain scaling problem, has been assessed if it is easy to be used and state of the art for industrial CFD application. The possible improvement of the accuracy of a certain scaling problem by using CFD methods was judged as well.

All these aspects have been collected in a matrix-like overview. The determination of the form factor was addressed to be the most valuable one for further investigation to be used in combination with CFD methods.

It has to be noted here, that scaling effects and their possible assistance by CFD methods have been investigated separately here and not the combination of different scaling processes. It is known that scale effects have impact on the ranking: some scale effects are over predicting and some are under predicting. Effects are mixed and can interact in the end of a complete speed power prediction process and CFD methods could help to become aware of these effects. Picking out one scale effect and make it more robust by insights from CFD methods can result in that the final speed power prediction is not even more correct, because all scaling effects are mixed and working together hand in hand. The use of a correlation allowance finally corrects it. You have to be very careful by changing single scaling methods without checking the overall accordance with a modified correlation allowance value. Methods for checking and adapting the correlation allowance have to be available when changing individual parts of the scaling process.

The work on determining the form factor by CFD methods and comparing these results with the form factor derived from towing tank showed a good agreement. Despite that, a quite significant spread was observed among the participants. That shows that CFD methods are promising but results have to be handled carefully.

The committee identified further scaling processes to be addressed in future for the consideration if CFD methods to be used in assistance for a more precise speed power prediction. These problems are: propeller-open-water scaling, effective wake scaling, scaling problems of immersed transoms and scaling of energy saving devices. Besides the scaling problems in the calm water speed power prediction, scaling problems in fields of

manoeuvring, sea keeping and cavitation are also worth to look into them more in detail.

3. REVIEW OF BENCHMARK STUDIES, ACCURACY, ACHIEVEMENTS AND CHALLENGES OF FULL-SCALE SHIP CFD

3.1 Scope

In this section, a review of the full-scale benchmark studies is outlined. Emphasis is placed on the achieved predictive accuracy. Studies reporting on the challenges associated with performing full-scale simulations are also given. The purpose of doing so is to enable a summary based on a broad overview of the current progress within the community.

3.2 Achievements of full-scale CFD with focus on Lloyd's Register 2016 workshop.

In view of the constant increase of available computational power, several workshops have been organized to gauge the performance of modern computational tools. Accurate prediction of ship hydrodynamics has come a long way in recent years, especially with the advent of Computational Fluid Dynamics (CFD). However, confidence in this technique is not sufficient, particularly for full-scale predictions, which is what the 2016 Lloyd's Register workshop aimed at improving. Full-scale data is notoriously difficult to obtain, for this reason, the abovementioned workshop focused participants investigations in this direction. The organisers (Ponkratov, 2016) provided the required characteristics and 3D model of the ship and received sixty sets of results with varying degrees of setup complexity. For instance, some included surface roughness, superstructure aerodynamics, while others made simplifications. The workshop also included propeller cavitation comparisons.

Challenges associated with full-scale CFD computations are discussed starting with the 3D laser scan of the ship, which revealed some

small deviations between the original drawings and actual ship. High curvature areas, such as bilge keels, were manually adjusted because the scanning method ran into difficulty when applied to these features. The adoption of similar corrections was necessary to ensure the accurate description of the propeller geometry, where the scan showed the four propeller blades are not identical – an assumption usually made in hydrodynamic analysis. This same assumption was made during the workshop for the sake of simplicity. All sensors had to be checked against each other and verified for the correct outputs.

As part of the workshop, submitted resistance calculations were compared to established methods to determine each model’s suitability. While most research into the resistance of ships is focused solely on the underwater shape, the organizers included the vessel’s cranes and superstructure. The former was shown to be negligible. These parameters are expected to be strongly dependent on the ship characteristics and can be excluded if their contribution is known to be small. Furthermore, neglecting the superstructure was shown to influence dynamic trim, which, if ignored, can also impact predictive accuracy. The received trim amplitudes were very small and scattered, while the sinkage values agreed well between participants. This suggests that trim is more challenging than sinkage to capture numerically in full-scale.

In terms of self-propulsion simulations, it was established that allowing the ship to surge freely can be beneficial in cases where propeller RPM cannot be gradually adjusted to achieve thrust/effective resistance balance. One set of submitted results employed a novel approach where the setup is split into four stages, each with a different turbulence treatment. However, this methodology is more resource consuming, thus recommended in cases where no alternative is available. In terms of accuracy, the participants reported values with a scatter between -30% and +10%. An assessment of the

CFD power predictions, compared to the sea trial data is shown in Figure 9.



Figure 9. CFD error of predicted power for a given speed compared to sea trial result.

Overall, based on the scatter of results submitted by the participants, it is not possible to conclude that current CFD practices are sufficiently mature to be applied directly at full-scale with confidence. Further investigations are required to determine the best approach to achieve a good prediction. For example, a fine mesh of as many as 35 million cells and a small time step were not sufficient to capture propeller tip vortex cavitation detaching from the blades. Only the early stage tip vortex detachment was resolved. Thus, further efforts are required to establish higher predictive capabilities and increase confidence to allow routine applications of full-scale CFD. An example of such research is the work of Starke et al. (2017), who participated in the full-scale workshop. According to their study, the free surface fitting method was not capable of capturing overturning bow wave features. Thus, making the Volume of Fluid (VOF) method more applicable to full-scale ship CFD.

3.3 Challenges of full-scale CFD

One aspect reported as a challenge in much of the research work reviewed in this section relates to the number of cells required to perform a full-scale simulation. For instance, as stated earlier, the full-scale workshop, organised by Lloyd’s Register, received submissions ranging from a few million to 35 million cells. Thus, the approaches to full-scale CFD relating

to mesh vary significantly across the research community. One approach to circumvent large cell numbers was devised by Haase et al. (2016). Specifically, Haase et al. (2016) proposed the validation of a grid in model scale Reynolds numbers, which is then scaled solely by a change in the value of viscosity.

Sezen and Cakici (2019) re-constructed the near-wall mesh in order to match the y^+ values in model- and full-scale. They determined that the method exhibits slight variations in the computed residual resistance coefficient. According to Terziev et al. (2019) such differences in the residual resistance coefficients may safely be attributed to scale effects. The procedure of Haase et al. (2016) can be implemented in multiphase and double body conditions, even when the mesh is kept identical between model- and full-scales, as shown by Terziev et al. (2019). Thus, computational savings are possible when adopting this technique. However, further studies are required to determine the confidence levels attributable to this technique.

To alleviate the computational load, a widely resorted to assumption is that of double body flow. Indeed, several RANS-based works referred previously have made use of this simplification. The literature also offers examples of full-scale computations which have modelled all physical phenomena. For instance, Tezdogan et al. (2016) provided a useful starting point for full-scale simulations in the arguably more complex unsteady case of shallow water vertical motions due to waves. Recent work exploring the added layer of complexity introduced when considering calm shallow water cases at full-scale can be found in Garenaux et al. (2019) and Terziev et al. (2020). The apparent scarcity of experimental data did not allow comparisons in these cases. Therefore, no validation was made against full-scale measurements.

In cases where self-propulsion is modelled, a variety of simplifications are applied by researchers to reduce the computational load required in discretising a ship's propeller (K. S.

Kim et al., 2019). The accurate modelling of the propeller is critical to assess performance and devise intervention strategies, such as the inclusion of an energy saving device, to improve performance (Gudla et al., 2019; Huang and Lin, 2019).

Near-wall cells are of particular importance in resistance predictions, especially in full-scale. The aspect ratio of cells within the boundary layer of a ship can be too large, causing stability problems. For this reason, most researchers opt to use wall functions and prescribe the near-wall mesh so that wall functions are used (Peric, 2019). Although the computed forces can be predicted with reasonable accuracy when using wall functions, the flow properties within the wake field may not be modelled accurately. Therefore, a comparison between the wall function, and the resolved approach is necessary at full-scale to determine the former's suitability.

Turbulence modelling is typically a source of modelling error, which is difficult to quantify at full-scale (Bhushan et al., 2009, 2007; Duvigneau et al., 2003; Pereira et al., 2017). Thus, alternatives to RANS techniques, which resolve at least part of the turbulent kinetic energy spectrum have emerged and are rapidly gaining popularity. In this respect, Liefvendahl and Fureby (2017) estimated that a full-scale Large Eddy Simulation (LES) for the Japan Bulk Carrier (JBC) would require between 9.7×10^9 and 67×10^{12} cells, depending on the approach (wall-modelled LES vs. wall-resolved LES). For example, Fujisawa et al. (2020) resolved the flow around a model-scale propeller in open water via the LES approach using grids numbering between 0.1 and 6.4 billion cells. Such grids are difficult to handle, even in academic contexts, demonstrating that resolving the turbulent kinetic energy spectrum in full-scale is not currently practical. According to Pena et al. (2019), the bridging alternative, known as Detached Eddy Simulation (DES), can be successfully employed to predict full-scale ship performance. For instance, the

authors gave Figure 10 as an example of the generated vortices in the aft region of the ship.

Zhang et al. (2018) summarised the challenges related to full-scale simulations of ship hydrodynamics as follows.

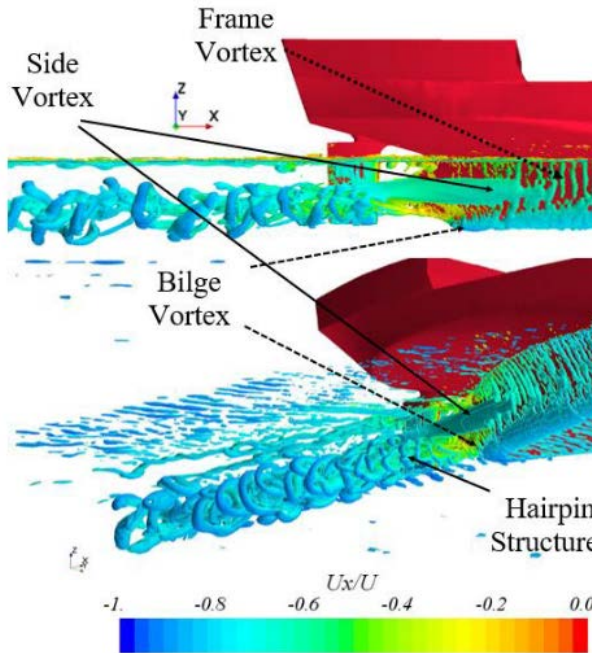


Figure 10: Iso surfaces of the Q-criterion showing the existence of different vortex systems. Adopted from (Pena et al., 2019).

1. The thickness of the boundary layer, which reduces with an increase in Reynolds number requires a fine near-wall mesh to capture well the viscous effects.
2. The unsteady nature of the ship resistance problem, which may be modelled with time-averaged approaches.
3. The neglect of surface roughness, which becomes more significant at full-scale.

The final point (3) has been investigated by numerous researchers, and is an active field of study at present. Recent contributions include K. Kim et al., (2019) and Song et al. (2019), where the authors investigated the drag penalty resulting from surface roughness, and confirmed the RANS approach is capable of modelling the thickening of the boundary layer as a result of fouling. The authors performed model- and full-

scale simulations of the KCS in calm waters and assessed the effects of different levels of hull fouling on ship resistance. A review on the effect of surface roughness and fouling on ship resistance (Andersson et al., 2020), however, found disagreements in the academic community with respect to the approach to model roughness. This stems from the difficulty in relating CFD roughness parameters to a physical measure of roughness. Therefore, although modelling a rough hull condition is not challenging per se, it is difficult to know what that corresponds to in reality.

Computational studies in full- and model-scales are useful to determine flow features that may dominate at low Reynolds numbers, but are reduced in importance at high Reynolds numbers. For instance, the strength of the bilge vortex, as well as wake gradient are reduced at full-scale (Farkas et al., 2018; Zhou et al., 2019).

Niklas and Pruszko (2019) and Terziev et al. (2019) used double body and multiphase simulations to demonstrate the sensitivity of full-scale total resistance predictions on the choice of methodology. Specifically, approach taken to predicting the wave resistance, form factor, and frictional resistance can lead to a high scatter in full-scale, depending on the approach.

Full-scale experimental and combined EFD/CFD studies (Hiroi et al., 2019; Inukai, 2019; Mikkelsen et al., 2019; Niklas and Pruszko, 2019; Sakamoto et al., 2019) have become more frequent. However, a greater number of openly available full-scale trials are required, accompanied by CFD studies into the optimal set-up to establish greater confidence in the method. For example, Sun et al. (2020) presented a set of numerical simulations which compared well with sea trial data. They compared different modelling strategies, featuring the inclusion and omission of surface roughness and its effect on the predicted power. A sample of the results reported in Sun et al. (2020) is shown in Figure 11.

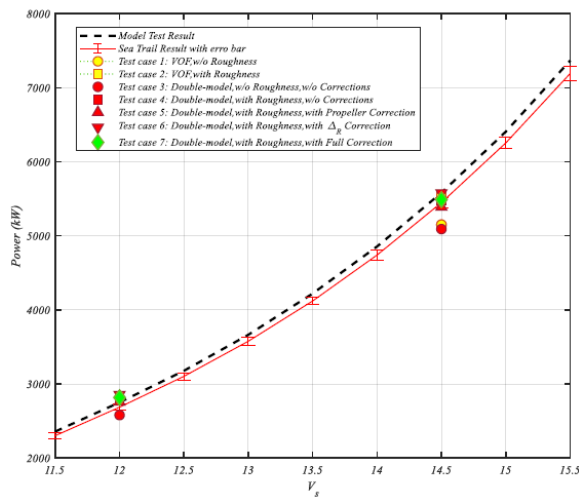


Figure 11: Power predictions compared to sea trial data. Adopted from Sun et al. (2020).

Alternatively, the study of Orihara and Tsujimoto (2017) and Tsujimoto and Orihara (2018) show a promising approach. In their studies, the authors predicted the full-scale ship performance and validated the resulting data by fitting the ship with on-board monitoring equipment. The findings of the studies include that further work is required to improve the speed-power predictions in conditions that do not closely match the scale. The authors point out that the parameters are highly affected by encountered waves. For this reason, the performance prediction technique requires that the encountered conditions are similar to the ones assumed in the computations. This may be taken as an indication that idealised conditions, necessary for validation purposes are difficult to achieve in full-scale.

3.4 Conclusions

Several trends can be identified in the field. The number of studies into the prediction of full-scale ship performance prediction have increased noticeably in the recent years. These are coupled with the increase in the availability of computational resources. However, the currently reported cell numbers are not thought sufficient to allow higher fidelity modelling (LES) of turbulent quantities in full-scale. A bridging alternative between RANS and LES has been demonstrated to be capable of providing accurate results when compared to

full-scale sea trial data. One of the main issues in the accurately performing full-scale simulations, the lack of validation studies, is being addressed (Ponkratov, 2016). To further facilitate developments in the field and provide further insight, open source data for a range of hull forms and conditions are necessary to test available techniques. Such data would enable the determination of best practices in all areas examined above: near-wall grid topology, surface roughness, as well as turbulence modelling approach. It is therefore of critical importance that the number of benchmark cases increases. In this respect, contributions in the form of the JoRes project, whose completion is expected in April 2022 will undoubtedly aid the wider field. It is important to evaluate whether any lessons learned from the first round of the project (Ponkratov, 2016) can translate into a smaller scatter of predicted data. This will also assist in setting the groundwork towards pinpointing the most suitable computational approaches to predict full-scale flows. Below, the main conclusions are summarised.

- Work in the field of full-scale ship performance prediction is accelerating, based on the number of recent studies.
- Confidence in full-scale CFD simulations must be increased by demonstrating good predictive accuracy over a range of conditions, consistently.
- At present, the scatter predictions submitted to the Lloyd's register workshop suggests further work is needed to identify best practices in full-scale simulations.
- The main challenges are associated with the grid resolution, turbulence modelling, and surface roughness treatment.

4. REVIEW OF EFD/CFD COMBINATIONS FOR RELEVANT APPLICATIONS

The most frequent example of combined methods is the use of EFD to validate CFD methods. Examples of this are widespread and form part of best practice guidelines for the

effective use of CFD. The topic of CFD validation is covered in more detail in Section 7 and therefore will not be discussed further here. These examples are predominantly focused on building confidence in a CFD method which is then used in isolation and therefore do not fully explore the potential of what could be achieved with combined methods. This chapter will therefore focus on how a combination of EFD and CFD has been used to provide greater insight than either could do in isolation. Two such examples are given in Wang Z-Z et al (2015a) and Eça, et al (2010) for numerical friction line and surface roughness on ship viscous resistance, respectively. These will be elaborated further below.

4.1 Investigating empirical relationships to be used within the scaling process

Several studies have been carried out recently using CFD to investigate the dependency of skin friction coefficient with Reynolds number and compared this to empirical friction lines.

Wang Z-Z et al (2015a) derive through very careful CFD computations a numerical friction line which can be used when scaling resistance from a model test. The Reynolds number dependency of the form factor, vanish almost completely when the numerical friction line is used instead of the traditional ITTC-1957 model-ship correlation line. This is an example on where CFD has been used to improve the scaling methods. However, it should be pointed out that other empirical friction lines (Grigson and Katsui) also has this advantage over the ITTC-1957 line, and that the latter is not a pure friction line but include full scale correlation as well. A potential pit fall is the laminar to turbulent transition at the lower Reynolds numbers, which is notoriously difficult to predict with RANS computations.

Eça, et al (2010) use CFD to investigate the effect of hull roughness on the resistance. They were able to conclude that the Townsin formula, currently in the ITTC Recommended

Procedures, is the most appropriate of several investigated empirical formulations. The study is a good example of how CFD can be very useful to evaluate empirical relations. Apart from that, the study also gave deeper insight into the effect of roughness on friction and viscous pressure and how that differs depending on hull shape. This may inspire to even better formulations in the future.

They find that very fine grid close to the wall is needed when analysing roughness effects. Even with careful grid convergence work, the numerical uncertainty is larger than that obtained from smooth surface computations. Another uncertainty is the conversion between equivalent sand grain roughness and the mean apparent amplitude, which is what is used in ship practice and in the ITTC equations for roughness allowance. This relation is, as the authors point out, a research topic of itself, and should be addressed in further studies.

Remolà (2014) attempt to verify the method for scaling of appendage viscous drag recommended in ITTC, the so-called beta-method. This method is in short, to estimate the drag of appendages from resistance test with and without appendages, and reduce the drag coefficient by a factor and add it to the full scale resistance of the base hull. This is criticized to be a very crude method with large uncertainties. Using CFD to examine and perhaps refine the method would make a great contribution. Unfortunately, the CFD computations in the referenced work were not successful and no conclusions were made. However, the attempt is interesting and should be considered for further studies.

Wang et al. (2016a) develop a new method for scaling model test of CRP (contra rotating propeller) using CFD. The CFD computations reveals in detail the scale effect for the various components and this knowledge is used when the authors suggest scaling equations for the influence of the first propeller on the pod house resistance and the propulsion coefficients of the second propeller. This is a good example of where CFD has provided deep insights which

would not be possible before, and how this is transferred to a scaling equation that can be used without CFD.

4.2 CFD derived components used within the scaling process

Raven et al (2008) were one of the first to explicitly suggest “replacing parts of the extrapolation procedures by CFD computations”. Since then several authors have investigated the use of CFD to derive the form factor.

Raven et al (2008) suggest to use double model computations to derive the viscous resistance, and from that derive the form factor using a friction line. Since the form factor is shown to be Reynolds number dependent when the ITTC-1957 model-ship correlation line is used, they recommend using a numerically derived friction line. Wang Z-Z et al (2015a) come to the same conclusion.

Raven et al (2008) mention that care has to be taken with the CFD setup when deriving the form factor in this way. The same applies to investigating the scale effects in general using CFD. The viscous pressure resistance is especially sensitive to incomplete convergence, boundary conditions etc. Grid type, grid density, discretisation scheme and domain size also influence the result.

Wang et al (2016b) suggest deriving the form factor without a friction line by defining $k=C_{pv}/C_f$, where C_{pv} and C_f both come from CFD double model computations. They point out that grid type and turbulence model can affect the results. However, it is unclear how their form factor is meant to be used for full scale resistance, if no friction line is to be involved.

More recently a wider study investigating the use of CFD to obtain the form factor was initiated by this specialist committee. Seven codes and six different turbulence models were used to determine the form factor for the KCS and the KVLCC2 using double body

simulations. This study further confirms the speed dependence of form factor derived using the ITTC-1957 model-ship correlation line but shows that this significantly reduces using the Katsui line and is nearly eliminated using numerical friction lines (Korkmaz et al 2021a).

The benefits of using a CFD determined form factor within the power prediction process have been investigated further by applying this method to a wide range of model scale tests and comparing the results against sea trials data Korkmaz et al 2021b. They conclude that generally powering predictions are improved by the use of CFD based form factors but crucially no deterioration was observed. The impact of a wide range of numerical settings are investigated allowing general recommendations to be made about implementing this method in the future.

The benefit of using CFD for the form factor (regardless of which friction line to use) is especially apparent for ships where the Prohaska method fails due to wave making even at low speeds. For such cases, the derivation of form factor is very problematic using the standard EFD methods.

4.3 Use of CFD to provide greater insight than the one obtainable from EFD alone

With increased numbers of simulations of the flow around full scale ships being conducted, CFD can be used to investigate scale effects by comparing flow fields between model and ship scale.

Wang et al (2015b) used double body RANS simulations to investigate the scale effects on the nominal wake shape and mean values across a wide range of Reynolds numbers. They found that the mean nominal wake fraction reduced by almost 50% at full scale and there were significant changes in circumferential variation in nominal wake with scale, especially at inner radii. Recommendations are made regarding how similar simulations could be used to help

model scale experiments in the future. A comparison of the CFD method with model scale experiments shows agreement within 10%. No validation of the method is available for the full scale simulations.

In a similar study vein, Guiard (2013) describe how the Mewis Duct is designed using both model and full scale CFD, where the model scale CFD is compared with model test data. This paper discusses the challenges associated with full scale CFD predictions and the impact of different turbulence models used.

More recently Kok et al (2020) used both model scale and full scale CFD to investigate the scale effects in self-propelled containership squat. Again the CFD method was validated at model scale with the full scale CFD compared against the model data scaled up using the ITTC1978 extrapolation method and other empirical methods. They concluded that scale effects on squat were minimal due to the strong dependency on the Bernoulli wave.

These papers highlight the potential insights that can be gained from full scale CFD, especially the detailed flow fields, but ultimately highlight the need for full scale EFD data to validate such methods to fully realise their potential.

Another area where CFD can provide increased insight is to provide detailed flow field and pressure data to complement an experiment. This can help understand the flow physics behind trends observed in the experimental data.

Tian et al (2017) present a detailed experimental study of blade vibration conducted in different wake flows within a cavitation tunnel. Wire meshes upstream are used to generate either 4 or 6 cycle wake patterns. CFD is then used to provide greater understanding of the forces acting on individual blades and explain the differences in dynamic strain observed in different test cases.

Carrica et al (2016) conducted an experimental and numerical study of a zigzag manoeuvre for the KCS in shallow water. This work provided good quality experimental results to validate numerical tools, which in turn can be used to get significant insight of the hydrodynamics occurring during the manoeuvre. The velocity, pressure fields and vortex structures obtained from the CFD are very challenging to obtain experimentally and could help to understand the detailed flow physics in these type of manoeuvres.

4.4 Use CFD to help design or correct experimental test processes

It is now often standard practice to use CFD for the design of a new hull form, with experimental tests being reserved for evaluating final designs. This process increases the efficiency of the experimental test campaigns but can also be used to identify specific areas of the design or operating conditions which need to be evaluated during the experiments.

Another example of using CFD as part of an experimental procedure is the blockage correction method proposed by Raven (2019). This approach uses numerical simulations to determine the blockage effects for shallow water model tests conducted in a basin of limited width. Such a combined approach improves the accuracy of the experimental prediction accounting for some of the limitations often present when conducting a model scale tests.

4.5 Conclusions

It can be seen from the previous publications discussed in this chapter that there are many opportunities to be gained from combined CFD and EFD methods. These can range from CFD providing greater insight to flow physics, the development of new empirical relationships that improve scaling predictions to CFD calculations becoming an integral part of the scaling or correction process. In all cases it is clear however that to adopt such combined methods a clear validation and verification process is

needed to ensure the potential benefits are achieved.

5. SUGGESTED IMPROVEMENT OF CURRENT RECOMMENDED PROCEDURES BY USING CFD IN COMBINATION WITH MODEL TEST

5.1 CFD-based form factors

This section describes work that was carried out in close cooperation between the Resistance and Propulsion Committee and the Specialist Committee on CFD and EFD Combined Methods.

As described in Section 2 above, there are a number of known issues with the existing scaling methodologies that could possibly be improved with CFD/EFD combined methods. One of them is the form factor used in the “1978 ITTC Performance Prediction Method” (ITTC 7.5-02-03-01.4). The possibility to use CFD instead of the Prohaska method has been suggested in literature by several authors as described in Chapter 4. The Committees decided to investigate whether a modification of the 1978 Power Prediction method regarding the possibility to use CFD for the form factor could be beneficial. The motivation for selecting this issue from the list is that it was regarded as a major error source in EEDI and contract power prediction, and it is believed to have a potential to be improved with CFD, since state-of-the-art CFD can handle model scale resistance computations well. Improving the form factor determination is to be preferred rather than returning to “2D” ITTC 1957 Power Prediction Method (where form factor is not used). It was shown in the seventies that the prediction accuracy was improved with the 1978 Performance Prediction Method and it was selected as the recommended method. Since then, the 1978 method has been the standard method and modern databases are built upon it.

Several aspects needed to be studied before the committees could submit a proposal for this modification:

1. Whether CFD-derived form factors can be shown to improve, or at least not deteriorate, the scatter of full-scale predictions compared to sea trials
2. If any general recommendations on how to perform the CFD-simulations can be formulated.
3. Which friction line should be used to derive the form factor?

5.1.1 Comparison with sea trials

When the “1978 Performance Prediction method” was originally derived, several versions were compared and the criterion for selecting the best method was the amount of scatter of full-scale power predictions compared to a large number of sea trials. It was therefore relevant to investigate whether any organisations recently have been able to demonstrate that using CFD-derived form factors improves, or at least does not deteriorate, the scatter. Only two ITTC members reported back on this aspect. MARIN reports that it has now become standard to compute the form factor for each tank project, using the RANS code Parnassos in double-body mode. The $1+k$ obtained is well correlated with what they get from a Prohaska plot of low-speed tests, though not precisely equal. MARIN has no concrete information on whether and how the sea trial correlation improves but believes it is more solid, less subjective, and also more efficient. SSPA claims that CFD-based form factors reduce the scatter compared to the original 1978 Performance Prediction method as well as the method without the form factor (“2D-method”). As presented in Korkmaz et al. (2021b), full scale speed-power-rpm relations between 78 speed trials and the corresponding full scale predictions based on model tests carried out at SSPA were compared. The probability density functions (PDFs) of the normalized correlation factors (where the value of 1 indicates predictions and the speed trials are equal) were calculated as can be seen in Figure 12. The comparison of the standard deviations for the power predictions indicates that the scatter is reduced when the CFD based form factors from

the EASM turbulence model are used compared to the Prohaska method. The improvements were larger when the ITTC-1957 model-ship correlation is replaced with the numerical friction line of the same turbulence model and the code used for the double body computations.

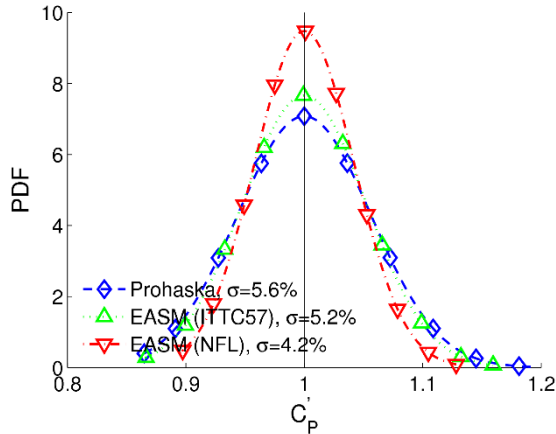


Figure 12: The probability density functions (PDFs) of the normalized correlation factor for power using the Prohaska Method, CFD based form factors with the ITTC-1957 model-ship correlation and the numerical friction lines using EASM turbulence model (Korkmaz et al., 2021b)

5.1.2 How to perform the CFD-simulations

According to ITTC 7.5-03-02-04 "Practical Guidelines for Ship Resistance CFD", a form factor can be computed as

$$(1 + k) = \frac{C_T}{C_F} \quad (1)$$

where C_T is the resistance from double body RANS computation (i.e. friction and viscous pressure resistance)

C_F is the 2D flat plate friction resistance at the same Reynolds number.

CFD-simulations for the form factor can be performed with different codes, turbulence models, grid sizes and so on. In order to investigate if any general recommendations on the set-up could be given, a benchmark study for ITTC members was launched. Initially, 4 members submitted computational results. One computation from published literature could be added. This data collection was the basis for the

initial recommendations to modifications of the recommended procedures. In late 2019, the study was expanded to include 9 participants with 286 submissions. The work is published in a journal article (Korkmaz et al., 2021a), which includes more detailed results and discussions than what can be comprised here.

The test cases were the two open hull forms KVLCC2 and KCS (Van, 2011) at design draught and KVLCC2 at ballast draught (Korkmaz et al., 2021a).

CFD computations were performed using double model RANS at specified Reynolds numbers, and the form factors derived from the fraction between the CFD viscous resistance coefficient and the 2D flat plate friction resistance from the ITTC-1957 model-ship correlation line.

The participating organisations and their codes are listed in Table 1.

Over-all results summary

Summaries of the form factor predictions are shown in Figure 13. Even though there is some spread between the submissions, the mean is very close to the experimentally derived form factor. This means that if the CFD-based form factor is used in a power prediction, the correlation factors (C_a or C_p) derived from earlier model test statistics, can still be used. Additionally, majority of the CFD-based form factor predictions for KVLCC2 in ballast draught are within the experimental uncertainty of the form factor (1.9% of $1 + k$ for the 95% confidence interval) determined by Prohaska method (Korkmaz et al 2021a).

Code

All participating codes were well-known, established RANS codes, widely used for marine applications. No general difference could be detected between the codes except for one code, which initially gave obviously unrealistic results. The code developers were contacted and found one error in the friction

integration algorithm and a bad cell distribution in the default setting (see more below). Participants that used that code re-submitted with the updated code and mesh, which resulted in comparable results. The lesson learned is that even well-established codes may have weak points and the users must carry out their own validation work for their specific task.

Table 1: Participants in form factor benchmark study

Organisation	Code	Initial study	Extended study
Centrale Nantes	ISIS-CFD	x	x
SSPA	Shipflow	x	x
University of Strathclyde	Star-CCM+	x	x
NMRI	NAGISA	x	x
MARIN	ReFresco	x	
University of Michigan	Open FOAM / Helyx		x
China Ship Scientific Research Centre	NaViiX		x
Ocean, Coastal and River Engineering, NRC-OCRE	Open FOAM		x
Shanghai Ship and Shipping Research Institute	Star-CCM+		X
Yokohama National University	SURF		x

Cell distribution

Variation in longitudinal and vertical cell distribution was studied by one participant (also reported in Korkmaz 2019). The form factor is rather robust with regards to cell distribution, even for a very coarse grid in the fore body the differences in form factor were within 0.02. The only grid that gave inaccurate result was when

the cell distribution in the aft body was extremely coarse.

Grid type and wall treatment

106 submissions were carried out using wall functions and 180 using wall-resolved grids. Vast majority of the structured grids utilized wall resolved grids, while most of the unstructured grids used wall functions. The type of grid and wall treatment showed somewhat indicative trends on the form factor: form factors from wall resolved and structured grids were higher than the simulations with wall functions and unstructured grids on average.

Normalized wall distance y^+

Except very few simulations, the submissions used recommended average $y^+ < 1$ for wall resolved and $y^+ > 23$ for wall functions). The identified y^+ (first cell size normal to the wall) did not show general trends but different codes indicated varying tendencies. (UofM used adaptive wall functions and provided results that spanned $1 < y^+ < 100$.)

Number of cells

All submissions had more than 0.4 million cells. No difference in scatter or level could be detected based on number of cells, although as the cell number increases for a given code, the results for that code converge.

Turbulence model

Five turbulence models were represented: $k-\omega$ SST, realizable $k-\epsilon$, RNG $k-\epsilon$, Spalart-Allmaras and EASM. Turbulence modelling is identified as one of the most influential aspect of the CFD set-up. However, no general trends are observed but different codes indicated varying tendencies, sometimes opposite trends among to codes.

Speed (Reynolds number)

When a Prohaska plot from model test is used to derive the form factor, a straight line is

extrapolated using mainly the measurements at the lowest speed practically possible. It means that the correlation factors (Ca/C_p) are derived based on these points. Ideally, it should not matter, as the form factor should be independent of speed. However, a known flaw of the ITTC-1957 model-ship correlation line is that it is too steep at the lower Reynolds numbers (see for example Korkmaz et al., 2021a). Therefore, the CFD based form factor is different when derived at the Reynolds number corresponding to the model scale design speed compared to a Reynolds number corresponding to the low speed points of a resistance test. For the test cases in the study, the differences in form factors are about 0.011 and 0.015 for KVLCC2 and KCS, respectively (Figure 13). When using CFD based form factors for power predictions in combination with the correlation factors (Ca or C_p) derived from earlier model tests, the CFD computations can be done either at the Reynolds number corresponding to the lower end of the

model test speed range or to the design speed. This is because the correlation between the form factors derived from the earlier model tests and the CFD based form factors are both based on the EFD techniques (turbulence stimulation, hull openings, inclusion of appendages such as rudders) and test characteristics (such as the typical Reynolds number range) in the case of EFD, and the CFD set-up (such as the choice of the turbulence model, the type of wall treatment). Additionally, some members report numerical instabilities when attempting double model computations at low speeds for hulls with pronounced bulbous bows. For those cases, it may help to run at a higher Reynolds number, corresponding to design speed. Another option is to increase the forward trim in the computations. It can also be argued that the form factor should be derived at the most important speed, i.e. design speed. These discussions would be resolved with a friction line other than the ITTC-1957 model-ship correlation line.

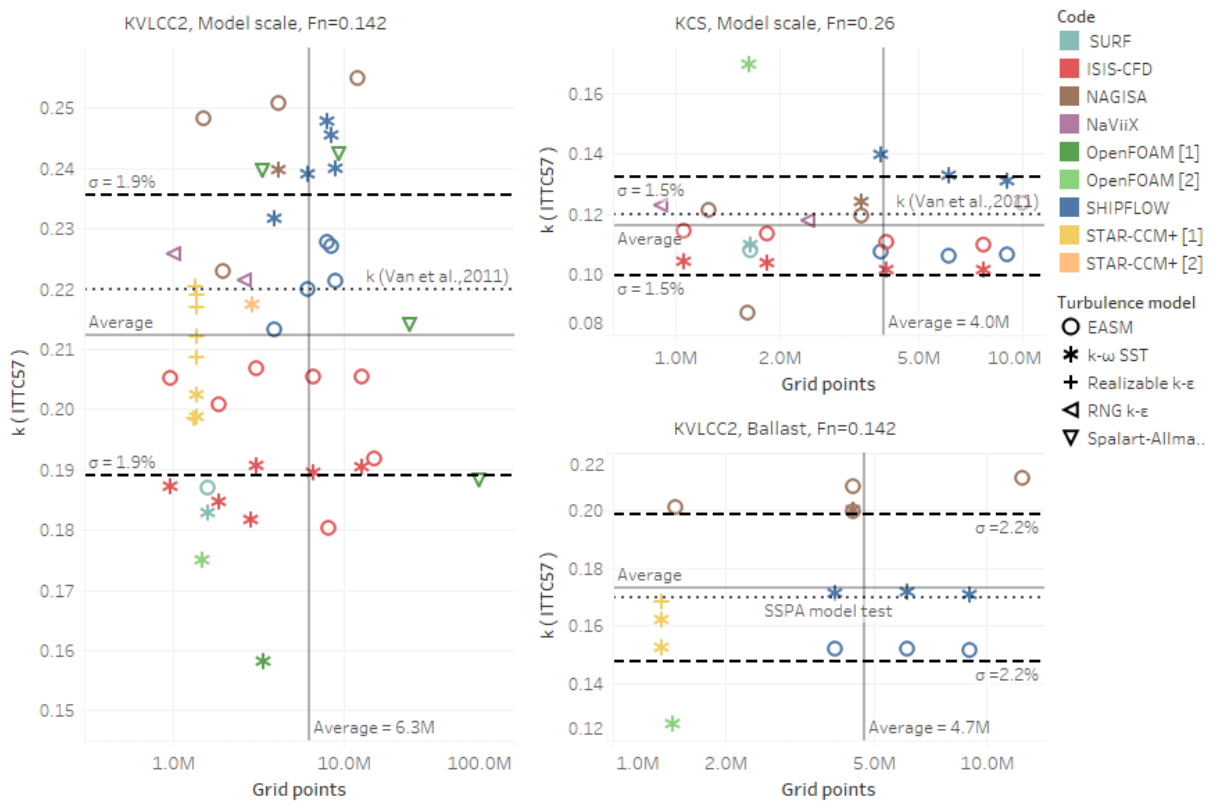


Figure 13: Form factor, k , based on ITTC-1957 model-ship correlation line versus grid size for KVLCC2 hull in design loading condition at $Fn=0.142$ (left), KCS hull in design loading condition at $Fn=0.26$ (top right) and KVLCC2 in ballast loading condition $Fn=0.142$ (bottom right) (Korkmaz et al., 2021a)

Draft and trim

It can be argued that the form factor should be derived at the resultant draft after dynamic sinkage and trim that the ship will have at the design speed. However, since the experimentally based form factor is derived by extrapolating to zero speed wave resistance, this also means extrapolating to the zero speed draft, which may be different from the draft at the design speed due to dynamic sinkage and trim. When using a form factor for power prediction in combination with the correlation factors derived from earlier model tests, then the form factor should be derived at the static draft. In the presence of a bulb close to or piercing the water surface, the computation may be problematic due to suppression of large waves especially at low speed. Imposing a slight forward trim so that the bulb is sub-merged may help.

Transom

A deeply submerged transom may be problematic for RANS codes. Raven 2019 suggests that adding a wedge with slip condition is a possible solution. No distinctive effect of slightly submerged transom (submerged transom area divided by maximum midship cross-section up to 0.015) were found on the correlation between the predictions and the speed trials (Korkmaz et al., 2021b). More studies are needed to be able to give general recommendations. In the meantime, each organisation should develop their own validated solution.

Flow separation

Flow separation that occurs at model scale but not at full scale is a known scaling problem that may occur on full hull forms. Raven 2019 suggests that one way to detect and possibly correct for this is to compute the CFD-based form factor at both model and full scale. The model scale form factor is used to derive the wave resistance and the full scale form factor is used to compute the full scale viscous resistance. This suggestion has been tested in

Korkmaz et al. (2021b), and it has been confirmed that the prediction accuracy is increased for the hulls exhibiting separation. This is a promising option that should be investigated further by other members.

5.1.3 Which friction line that should be used to derive the form factor

As described in Section 2, the ITTC-1957 model-ship correlation line has been criticised by several authors in the literature as well as in internal discussions in the ITTC community. It is now clear that the reported scale dependency of the form factor is caused by the non-physical shape of the ITTC 1957 line, rather than the form factor concept itself. Some authors propose to overcome this by either using another friction line, for example Katsui as in Raven (2009), or by omitting the use of a friction line as in Wang et al. (2015). Korkmaz (2021b) showed that adoption of numerical friction lines can introduce improvements to the power predictions compared with a large number of sea trials. However, the main cause of the gain in the accuracy of the predictions were not due to elimination of the scale effects on form factors but another minor contributing factor. As concluded in Korkmaz (2021b), the usage of numerical friction lines led to a readjustment of the full scale viscous resistance predictions which can be obtained by modifying the correlation allowance (C_a) to a large extent. It has also been suggested that each user derive its own friction line based on CFD, using the same turbulence model and CFD method as used for the hull. If this can be shown to give higher accuracy, ITTC should formulate a Recommended Procedure for deriving such a friction line.

It has to be stressed that replacing the ITTC-1957 model-ship correlation line in the power prediction methods implies that the correlation factors (C_a or C_p) are no longer valid. It would mean a very large work effort for the individual model test institutes to derive new correlation factors, and it can only be motivated if the accuracy can be shown to be improved. For this

reason, it was decided for the time being to recommend to continue using the ITTC-1957 model-ship correlation line, also for CFD based form factors.

5.2 Conclusions and recommendations

The mentioned joint committee study, as well as published papers, some of them with committee members as authors, forms the motivation for the final suggested Recommended Procedures. The following was concluded:

Since the study contains only limited number of test cases and only one organisation's comparison with a large number of sea trials, it can neither be concluded nor rejected that that CFD-based form factors should *replace* the Prohaska method.

It should be suggested that CFD-based form factors can be used to *support* the conventional Prohaska method.

ITTC should encourage the use of CFD-based form factors to support the conventional method, as it seems likely that it improves the accuracy of the predictions on average.

When more institutes gain experience with CFD-based form factors, the recommendations should be re-evaluated.

To start with, C_F should be recommended to be derived from the ITTC-1957 model-ship correlation line, in spite of its drawbacks. In this way, each organisations' correlation factors (C_a or C_p) can be kept unchanged.

The use of alternative friction lines for C_F should be investigated further:

- What are the implications of changing to a published line such as Katsui or Grigson?
- Is it more accurate to use a CFD-based friction line using the same CFD-models as for the hull?

No general recommendation on how to perform the CFD computations for form factor can be given. Suitable choice of mesh, turbulence model etc. is code dependent. Therefore to ensure the quality of CFD prediction of form factor, refer to the new "Quality assurance in Ship CFD Application", 7.5-03-01-02.

Based on the study and considerations described above, improvements of the following Recommended Procedures were suggested to the Resistance and Propulsion Committee:

ITTC 7.5-03-02-04 "Practical Guidelines for Ship Resistance CFD", Section 3.1

ITTC 7.5-02-03-01.4 "1978 ITTC Performance Prediction Method", Section 2.4.1

The committee recommends the full conference to adopt the modifications of the procedures.

6. REVIEW OF CURRENT ITTC PROCEDURES FOR POTENTIAL USE OF COMBINED EFD AND CFD

In this section, the current ITTC Procedures are reviewed for possible benefits from combined EFD and CFD in the future.

6.1 An Overview

In the 2017 Edition of the ITTC procedures (2017), there are a total 79 procedures, among which 60 are related to EFD only, seven are related to both EFD and CFD, five are only related to CFD, and the rest of them are routine work related. Among 39 guidelines in 2017 ITTC, there are 25 that are only related to EFD, four are related to both EFD and CFD, and five are related to only CFD. Also, of the 13 work instructions, one is about the introduction of suggested formats, and the rest are about calibration of testing equipment.

6.2 Resistance, Propulsion and Powering Performance

Guideline 7.5-01-03-04 is about benchmarking for PIV and SPIV setups. This guideline mentions using RANS simulation to assist in testing by calculating flow separation. Procedure 7.5-03-02-02 lists the resistance and propulsion benchmark database that can be used for CFD validation.

Guideline 7.5-02-03-02.5 mentions the method of using combined CFD (RANS) and EFD to tune a model scale wake field in a cavitation tunnel towards a full-scale wake field. Similarly, procedure 7.5-02-03-03.7 talks about how to use combined methods of simulation, as well as model tests, to predict cavitation and erosion damage on "unconventional" rudders and on rudders behind highly loaded propellers. Procedure 7.5-02-05-3.2 mentions the use of CFD and model test combination to determine the head rise across the pump, and the inlet duct loss for waterjet system performance analysis.

The phenomenon of wave breaking and the resistance in waves is currently being studied in detail with unsteady RANS.

Exact simulation is not achievable due to insufficient knowledge of the actual full-scale flow field and simulation approximations due to Reynolds number, Froude number, and non-geosim hull representations, therefore, further research is required to understand how to use CFD at full scale for resistance, propulsion, and powering.

Also, CFD is being used to study cavitation in detail. With regards to gap cavitation, the viscous effect in the gap is currently of focus with unsteady RANS. Rigorous procedures for the numerical modelling of cavitating flows will be formed in the next 3 years.

6.3 Manoeuvring and Seakeeping

Guideline 7.5-03-04-02 introduces validation and verification of RANS solutions in the prediction of manoeuvring capabilities,

using methods from QM 7.5-02-06-04 "Uncertainty Analysis for Manoeuvring Predictions based on Captive Manoeuvring Testing" and QM 7.5-02-06-05 "Uncertainty Analysis for Free Running Manoeuvring Model Test".

Procedure 7.5-02-07-02.5 addresses verification and validation of linear and weakly non-linear seakeeping computer codes. This procedure mainly discusses using experiments for CFD validation, with multiple mentions of 7.5-02-07-02.3 "Experiments on Rarely Occurring Events". One typical example of CFD/EFD combined method is mentioned in procedure 7.5-02-07-02.8, which calculates the weather factor f_w for the decrease of ship speed in wind and waves. This procedure includes methods of experiment, numerical computation, and empirical formulae.

A standard simulation procedure of free running, and the calculation of hydrodynamic coefficients in calm water, can be formed in the next 3 years. The manoeuvring hydrodynamic coefficients in waves, especially the coupling effects between different coefficients can be obtained based on unsteady RANS simulations. The general procedures may be formed in the next few years. Scale effects, including the larger model wake fraction, and the larger model resistance, can be studied based on the unsteady RANS, and the non-similar rudder inflow between model and full scale can be further studied.

The numerical procedure of sloshing can be formed in the next three years. The simulation of added resistance in head waves based on unsteady RANS has been widely carried out by many scholars, especially the cases in short waves. Based on these research results, the added resistance in oblique waves can be studied in the next three years. The numerical simulation for ship motion with green water based on CFD method has been widely used in recent years, and it can be extended to the research for the large amplitude motion with green water. Simulation of multidirectional irregular wave spectra and modelling of

complex ice environment can be achieved based on unsteady RANS.

6.4 Stability and Hydrodynamic Noise

The numerical simulation of large amplitude roll damping using CFD is the focus of much current research, and the numerical prediction of free rolling based on unsteady RANS has been widely accepted for many cases. However, instructions on how to calculate roll damping coefficients for different types of ship has still not been recommended by the ITTC. A procedure for the prediction of roll damping coefficients based on the free rolling should be determined in the next 3 years. At present, the simulation of large roll damping based on unsteady RANS is mostly concentrated in calm water, and more attention should be paid for the calculation process of large amplitude roll damping in waves.

The direct simulation of different failure modes based on unsteady RANS, such as parametric rolling, pure loss of stability, dead ship, excessive acceleration, surfing riding/broaching has been attempted in recent years. More complex and accurate simulations will be possible in the next few years, and simulation procedures for parametric rolling and dead ship can also be formed in the ensuing years.

For stability in waves, the capsize boundary is an important quantity. However, the capsize boundary is difficult to quantify because of the chaotic behaviour due to nonlinearity of restoring moment. Therefore, CFD is recommended for the determination of capsize boundary. This can also help to further develop the model test procedures for the determination of the capsize boundary.

Numerical simulation based on CFD method can be used to understand of the physics and behaviour of the motion of a damaged ship and the flooding process. Air compressibility is an important factor that affects damage flooding, and the study of the influence of air compressibility through model test requires high

test conditions. Therefore, the influence of air compressibility can be systematically studied based on CFD method in the next few years, and the numerical research can provide guidance for the study of this mechanism.

Besides physical tests, numerical methods for structure-borne noise will be more involved in the next years. As the excitation source, the spatial-temporal distribution of turbulent flow will be more detailed and accurately CFD predicted. These demanding requirements still require a great deal of effort on future CFD.

6.5 General Recommendations

6.5.1 Elimination of the scale effect by combined EFD and CFD

Scale effects have been mentioned in many procedures for different phenomena, and the combination of EFD and CFD method can play an important role in the study of such problems.

Two scale effect phenomena including the larger model wake fraction and the larger model resistance have been mentioned in the procedure of manoeuvring. The scale effect can be eliminated by the combination of EFD and CFD.

Scale effects in manoeuvring have yet to be fully understood, and they are mainly due to a non-similar rudder inflow between model and full scale. Therefore, we can also use the combination of EFD and CFD for research on the role of non-similarity.

The procedure of ‘Validation of Manoeuvring Simulation Models_7.5-02-06-03’, describes the development of simulation models, and the ways that they are validated. This procedure is in fact a classical case for the combination of CFD and EFD. We suggest more detailed or improved validation methods.

The procedure ‘Seakeeping Experiments 7.5-02-07-02.1’, mentions scale effects and the key factors that can also be studied by the combination of EFD and CFD.

In the procedure ‘Cavitation Induced Pressure Fluctuations: Numerical Prediction Methods 7.5-02-03-03.4’, the accurate and reliable full-scale predictions of cavitation-induced pressure fluctuation should be confirmed by the combination of CFD and EFD.

For the procedure of ‘Cavitation Induced Erosion on Propellers, Rudders and Appendages Model Scale Experiments 7.5-02-03-03.5’, the scale effects related to fluid effects and bubble dynamic effects in cavitation testing can be investigated by the combination of CFD and EFD.

For the procedure of ‘Prediction of Cavitation Erosion Damage for Unconventional Rudders or Rudders Behind Highly-Loaded Propellers 7.5-02-03-03.7’, the gap cavitation scale effect, the viscous effect within the gap, and vortex cavitation can be studied by the combination of EFD and CFD.

For the procedure of ‘Modelling the Behaviour of Cavitation in Waterjets’ 7.5-02-03-04.8, numerical modelling has been paid more and more attention due to the high cost required for experimental modelling. The highest quality results in modelling the behaviour of cavitation in waterjets can be obtained by combination of EFD and CFD.

6.5.2 Uncertainty analysis

Almost all model tests and simulations must be accompanied by uncertainty analysis. Future work should be directed towards improved and unified uncertainty analyses.

For the guideline of ‘Underwater Noise from Ships, Full Scale Measurements _7.5-04-04-01’, the sources of uncertainty and variability can be studied by the combination of EFD and CFD.

For the procedure of ‘Experiments on Rarely Occurring Events 7.5-02-07-02.3’, the rarely occurring events can be first studied by CFD, and then further validated through the combination of CFD and EFD.

For the procedure of ‘Laboratory Modelling of Multidirectional Irregular Wave Spectra 7.5-02-07-01.1’, the verification and validation procedure for added resistance codes can be realized by the combination of EFD and CFD methods.

For the procedure of ‘Cavitation Induced Pressure Fluctuations: Numerical Prediction Methods 7.5-02-03-03.4’, there is just one rigorous verification and validation procedure. Therefore, universally-accepted V&V procedures for CFD should be established.

For the procedure of ‘Floating Offshore Platform Experiments 7.5-02-07-03.1’, many parameters cause uncertainties in floating offshore platform tests, and CFD can be utilized to study the influence of different factors of uncertainty.

7. UNCERTAINTY ASSESSMENT METHODS FOR CFD SIMULATIONS

In this chapter, various uncertainty assessment methods for CFD simulations are reviewed with applications to naval hydrodynamics in mind. Firstly, the ITTC Procedure and Guidelines (2017) and the American Society of Mechanical Engineers (ASME) standard procedures are compared and their differences are discussed. Yao et al. (2013) proposed verification and validation based on the orthogonal design approach and it is described in detail. Other recent approaches, such as N-version and Roy’s method, are also reviewed. Finally, the ISO procedures are presented and compared with the ASME procedures.

7.1 Difference In ITTC and ASME Procedures

7.1.1 Grid refinement ratio (r_i)

In ITTC Procedure and Guidelines (2017), iterative and parameter convergence studies are conducted using multiple solutions, at least

three, with systematic parameter refinement by varying the i^{th} input parameter Δx_i while holding all other parameters constant. Many common input parameters are of this form, e.g., grid spacing, time step, and artificial dissipation. Iterative errors must be accurately estimated or negligible in comparison to errors due to input parameters before accurate convergence studies can be conducted.

Careful consideration should be given to the selection of uniform parameter refinement ratio, r_i in terms of the element size, Δx_i .

$$r_i = \Delta x_{i,2}/\Delta x_{i,1} = \Delta x_{i,3}/\Delta x_{i,2} = \Delta x_{i,m}/\Delta x_{i,m-1} \quad (2)$$

The most appropriate values for industrial CFD are not yet fully established. Small values, i.e., very close to one, are undesirable since solution changes will be small and sensitivity to input parameter may be difficult to identify compared to iterative errors. Large values alleviate this problem; however, they also may be undesirable since the finest step size may be prohibitively small, i.e., require many steps, if the coarsest step size is designed for sufficient resolution such that similar physics are resolved for all solutions. Also, similarly as for small values, solution changes for the finest step size may be difficult to identify compared to iterative errors, since iterative convergence is more difficult for the small step size. Another issue is that for parameter refinement ratio other than $r_i = 2$, interpolation to a common location is required to compute solution changes, which introduces interpolation errors. However, in cases of industrial CFD, $r_i = 2$ may often be too large. A good alternative may be $r_i = \sqrt{2}$, as it provides a fairly large parameter refinement ratio and at least enables prolongation of the coarse parameter solution as an initial guess for the fine parameter solution.

In the ASME procedure, Roache (1998) defines a representative cell, mesh, or grid size, h . For example, for three-dimensional, structured, geometrically similar grids, which is not necessarily a Cartesian one,

$$h = [(\Delta x_{max})(\Delta y_{max})(\Delta z_{max})]^{1/3} \quad (3)$$

For unstructured grids one can define

$$h = \left[\left(\sum_{i=1}^N \Delta V_i \right) / N \right]^{1/3} \quad (4)$$

where N is the total number of cells used for the computations and ΔV_i is the volume of the i^{th} cell.

It is desirable that the grid refinement factor, $r = h_{coarse}/h_{fine}$, should be greater than 1.3 for most practical problems. This value of 1.3 is again based on experience and not on some formal derivation. The grid refinement should, however, be made systematically; that is, the refinement itself should be structured even if the grid is unstructured.

7.1.2 Uncertainty (U_i) and order of accuracy (p_i)

In Uncertainty Analysis in CFD Verification and Validation Methodology and Procedures 7.5-03-01-01 (ITTC, 2017), the generalized Richardson Extrapolation (RE) is used to estimate the error δ_i^* for the selection of the i^{th} input parameter and order of accuracy p_i . The error is expanded in a power series expansion with integer powers of Δx_i as a finite sum. The accuracy of the estimates depends on how many terms are retained in the expansion, the magnitude (or importance) of the higher order terms, and the validity of the assumptions made in the RE theory.

With three solutions, only the leading term can be estimated, which provides one term estimates for error and order of accuracy.

$$\delta_{RE,1}^{*(1)} = \frac{\varepsilon_{i,21}}{r_i^{p_i} - 1} \quad (5)$$

$$p_i = \frac{\ln(\varepsilon_{i,32}/\varepsilon_{i,21})}{\ln(r_i)} \quad (6)$$

where $\varepsilon_{i,32} = \varphi_{i,3} - \varphi_{i,2}$ is changes between coarse-medium solutions and $\varepsilon_{i,21} = \varphi_{i,2} - \varphi_{i,1}$ is changes between medium-fine solutions.

Although not proposed by Roache (1998), the factor of safety F_s approach can be used for situations where the solution is corrected with an error estimate from RE as

$$U_i = (F_s - 1) |\delta_{RE,1}^*| \quad (7)$$

The exact value for factor of safety is somewhat ambiguous and $F_s = 1.25$ is recommended for careful grid studies.

In the ASME procedure, let $h_1 < h_2 < h_3$ and $r_{21} = h_2/h_1$, $r_{32} = h_3/h_2$ and calculate the apparent (or observed) order, p , of the method from reference

$$p = [1/\ln(r_{21})][1/\ln|\varepsilon_{32}/\varepsilon_{21}| + q(p)] \quad (8)$$

$$q(p) = \ln\left(\frac{r_{21}^p - s}{r_{32}^p - s}\right) \quad (9)$$

$$s = 1 \cdot \sin(\varepsilon_{32}/\varepsilon_{21}) \quad (10)$$

where $\varepsilon_{32} = \varphi_3 - \varphi_2$, $\varepsilon_{21} = \varphi_2 - \varphi_1$, and φ_k denote the simulation value of the variable on the k^{th} grid. Note that $q(p) = 0$ for a constant r . This set of three equations can be solved using fixed point iteration with the initial guess equal to the first term, i.e., $q = 0$.

For example, suppose that we need to calculate and report the following error estimates along with the observed order of the method p . Approximate relative error may be cast as a dimensionless form or in a dimensioned form, respectively as follows:

$$e_a^{21} = \left| \frac{\varphi_1 - \varphi_2}{\varphi_1} \right| \quad (11)$$

$$e_a^{21} = |\varphi_1 - \varphi_2| \quad (12)$$

The error was estimated from the equation

$$U_i = \frac{F_s \cdot e_a^{21}}{r_{21}^p - 1} = F_s |\delta_{RE,1}^*| \quad (13)$$

For the factor of safety, F_s , Roache (1998) recommended a less conservative value for $F_s = 1.25$, but only when using at least three grid solutions and the observed p .

7.2 CFD results verification based on orthogonal design

Based on the orthogonal design and the statistical inference theory, Yao et al. (2013) developed a new verification method and the related procedures in the CFD simulation. It is shown that the new method can be used for the verification in the CFD uncertainty analysis and can reasonably and definitely judge the credibility of the simulative result. The concept of the validation process recommended by ITTC is vague. The turbulence model of the CFD simulation should be an important source of uncertainty, which is the greatest contribution to the CFD uncertainty. However, the turbulence model's uncertainty evaluation method is not included in the recommended procedure. The interactions between the calculated factors are not considered in the validation method in the recommended procedures, and it is assumed that the calculated parameters are independent of each other. But the interactions will affect the estimation of the combined standard uncertainty and the validation process.

7.2.1 Orthogonal design method

The orthogonal design method refers to the method used in a physical test involving multiple elements. Provided that the numerical simulation could be regarded as a virtual physical test, this method may as well be used to design and analyse the virtual test process and the results.

Firstly, the calculation factors to be examined should be divided into the controlled calculation factors and the out-of-control calculation factors. The former are the major elements that affect the simulation result, and the latter include all minor elements other than the controlled calculation factors.

When the controlled calculation factors and their interaction and the level are set, the orthogonal array should be chosen to ensure that all controlled factors and some blank columns are included. The statement heading should be designed in a way that the controlled factors and the interaction scheduled to be examined in every column should not be overlapped in the effect.

7.2.2 Variance analysis method

The variance analysis refers to a method, which distinguishes the experiment results affected by different factor level (including interaction) changes or errors. The F test is the basis of the variance analysis and is mainly used to check whether there is a significant difference among levels of calculation factors.

Assume that F is the ratio of the average sum of squares of deviations caused by the factor level change and the average sum of squares of deviations caused by errors, as

$$F = \frac{\frac{S_j}{f_j}}{\frac{S_e}{f_e}} \quad (14)$$

where f is the degrees of freedom and S is the sum of squares of deviations. Therefore, if the ratio of the effect on the simulation result attribution of the controlled calculation factors and the out-of-control calculation factors can be identified as F , then F can be used to check whether some major calculation factors are omitted. Meanwhile, S_j and S_e represent the influence of the controlled factors and their interactions on the simulation result and that of the out-of-control factors and their interaction on the simulation result, respectively.

7.2.3 Type A evaluation of standard uncertainty

When \bar{y} is the estimated value of the simulated physical quantity y and obtained

based on the statistical method, $u(y)$ is the standard uncertainty of Type A and can be obtained through statistical analysis of y

$$u(y) = s(\bar{y}) = \frac{s(y)}{\sqrt{n}} = \sqrt{\frac{\sum_{i=1}^n (y_i - \bar{y})^2}{n(n-1)}} \quad (15)$$

In the process of the numerical simulation under a certain statistical control, if \bar{y} is the arithmetic mean value and serves as the estimated value of y , n is the number of independent simulations, i.e., the number of calculations on the orthogonal table, y_i is the calculation result of independent simulations at i^{th} time, the combined standard deviation, S_p , can be used as a token and the standard uncertainty of the simulation result is

$$u(y) = \frac{S_p}{\sqrt{n}} = \sqrt{\frac{\sum_{i=1}^n (y_i - \bar{y})^2}{n(n-1)}} \quad (16)$$

where S_p represents the combined standard deviation, S_i the sample standard deviation, p the sampling frequency, i.e., the number of calculations at the same level, and n the total number of samples.

If the controlled calculation factor A is put on column j in the orthogonal table, its number of levels being l , the repeated number of each level being p , and the degree of freedom being $f_A = l - 1$, the sum of squares of the deviations S_A and u_A the uncertainty of Type A can be calculated and so can $S_{A \times B}$ of the interaction of the calculation Factors A and B , the out-of-control calculation factor or the random error standard deviations s_e and uncertainty u_e .

$$S_A = \sqrt{\frac{S_A}{f_A}}, u_A = \frac{S_A}{\sqrt{N}} \quad (17)$$

$$S_{AxB} = \sqrt{\frac{S_{AxB}}{f_{AxB}}}, u_{AxB} = \frac{S_{AxB}}{\sqrt{N}} \quad (18)$$

$$S_e = \sqrt{\frac{S_{blankrow}}{f_{blankrow}}}, u_e = \frac{S_e}{\sqrt{N}} \quad (19)$$

where S_j the sum of squares of deviations on any column j in the orthogonal table, which can be calculated as follows

$$S_j = \frac{I_j^2 + II_j^2 + \dots + (l_j)^2}{p} - \frac{(\sum_{i=1}^N y_i)^2}{N} \quad (20)$$

In this formula, I_j , II_j , represent the sum of y numbers listed on levels “1”, “2” on column j . As to the interaction, the following formula is used

$$S_{AxB} = \sum_j S_j, f_{AxB} = (l - 1)^2 \quad (21)$$

7.2.4 Type B evaluation of standard uncertainty

When y is the estimated value of the simulated physical quantity Y and is not obtained based on the statistical method, its estimated variance, $u^2(y)$, and $u(y)$, the uncertainty components for Type B, can be evaluated according to the methods such as those based on the historical data, the experience, the adopted error correction formula, the CFD software instruction and other information provided by other documentation.

Based on the information above, the evaluation methods of the uncertainty for Type B are to judge the probable interval $(-a, a)$ of the simulated value, by using the confidence level (including the probability) to estimate the coverage factor k and then to calculate the uncertainty by the formula as follows:

$$u(y) = \frac{a}{k} \quad (22)$$

In the CFD simulation, the uncertainty component for Type B comes mostly from the uncertainty caused by known and correctable system errors and the imperfection in the correction method. The truncation error and the iterative error of the numerical computation can have an approximate correction and its uncertainty u_G and u_I can be calculated by k factor formula. The mathematical model error and the accumulation of the rounding error that are not clear or not possible to correct will be classified into the uncertainty components of Type A.

The formula of truncation uncertainty and iterative uncertainty are as follows:

$$u_G = \frac{\delta_{RE}}{\sqrt{3}} \quad (23)$$

$$u_I = \frac{y_U - y_L}{2\sqrt{6}} \quad (24)$$

where y_U and y_L are the upper bound and the lower bound of the simulation result that can meet the condition of convergence.

7.2.5 Calculation of combined standard uncertainty

The u_c , combined standard uncertainty of CFD, is the sum of the variances of all standard component uncertainties $u_i(x)$. If there is a significance interaction, the covariance can be used

$$u_c = \sqrt{\sum_{i=1}^n u_i^2} \quad (25)$$

$$u_c = \sqrt{\sum_{i=1}^n u_i^2 + 2 \sum_{i=1}^n \sum_{j=i+1}^n r(x_i, x_j) u(x_i) u(x_j)} \quad (26)$$

In this formula, $u(x_i)$ and $u(x_j)$ are the standard uncertainties of x_i and x_j , r is the estimated value of the correlation coefficient of x_i and x_j .

7.2.6 Evaluation of expanded uncertainty

For the combined uncertainty, u_c , corresponding to the standard deviation, the probability of containing the true value is 68% at the interval of the simulation results $y \pm u_c$. In some engineering applications, a high confidence probability level is required so that the simulation falls into the interval, and in the hope that the interval contains with a great probability the simulated value reasonably endowed. To meet this requirement, the expanded uncertainty, U , can be calculated by multiplying the combined uncertainty and the coverage factor k . The following formula is used

$$U = ku_c(y) \quad (27)$$

Therefore, the result is represented as $Y = y \pm u$, where y is the estimate of the simulated value, the interval $y - U \leq Y \leq y + U$ is the extent containing with a great probability the reasonably endowed y distribution. The coverage factor, k , ranges from 2 to 3 based on the confidence level required by the interval $y \pm U$. if k is 2, it means that the simulation result value, which obeys the normal distribution, will be in the range of the estimated value $\pm U$ according to 95% of probability level of that interval can reach up to 99%.

7.3 Validation method and process in CFD uncertainty assessment

After the CFD simulation result is verified, it is usually required to be validated. The validation method proposed by Yao et al. (2013) is described in the following. The validation may be characteristic parameters of the simulation results and the experiment results by using the statistical inference theory. In fact, the results of the physical experiment or the numerical simulation are random variables, and

it can be assumed that they obey the normal distribution $N(\mu, \sigma)$. The comparison of two random variables should be made by the concepts and the means of the statistical inference. Strictly speaking, only if the statistical characteristic parameters μ and σ of the two random variables are equal. No significant differences between them can be validated.

7.3.1 Statistical inference method for validation

The statistical inference is based on one or several sub-samples to infer or judge the statistical characteristics of its population. The degree of confidence is an important index to measure the reliability. Here, the problem is to use the statistical inference method to judge whether the expectation, μ_c , and the variance, σ_c^2 , of the numerical simulation population inferred from the small sample are the same as the expectation, μ_T , and the variance, σ_T^2 , of the population of the experiment. If so, then the numerical simulation results are validated.

7.3.2 F-test

In the CFD validation process, one first judges whether the variance of the population of the numerical simulation, σ_c^2 , and that of the experiment, σ_T^2 , in the statistical sense is the same or not, by means of the F-test of the statistical inference theory.

Define the following F variable

$$F = \frac{\widehat{\sigma}_c^2}{\widehat{\sigma}_T^2} = \frac{S_c^2}{S_T^2} = \frac{\frac{S_c}{f_c}}{\frac{S_T}{f_T}} \quad (28)$$

where $\widehat{\sigma}_T$ is the estimate of the population of the experiment σ_T , S_T^2 is the experimental standard deviation, which can be obtained from the database of the benchmark test or the historical information. Suppose that it is known and its degree of freedom is ∞ . $\widehat{\sigma}_c$ is the estimate of the CFD simulation results, s_c is the sum of the squares of the deviations of the simulation

results. f is the degree of freedom, $f_c = N - 1$, N is the size of the numerical simulation sub-sample, and is called the program number of the orthogonal design.

The data can be obtained from the verification process of the CFD simulation based on the orthogonal design, as in Equations (26) and (27).

$$S_j = S_j = \frac{I_j^2 + II_j^2 + \dots + (l_j)^2}{\frac{p}{(\sum_{i=1}^N y_i)^2} - \frac{1}{N}} \quad (29)$$

where l is the level of the calculation factor, p is each level's repetitive number, y is the simulation results, I_j , II_j , represent the sum of y numbers listed on levels "1", "2" on column j . For the interaction, we have

$$S_{AxB} = \sum S_j, f_{AxB} = (l - 1)^2 \quad (30)$$

Although N cannot be very large, the full factor program information can be obtained, because it is a sample from the orthogonal design and the overall information can be obtained from a part of the implementation. So its F-test confidence is higher than the common sample. If $F > F_a(f_c, \infty)$, then the statistical hypothesis $\sigma_c^2 = \sigma_T^2$ is untrue, otherwise, it can be believed that $\sigma_c^2 = \sigma_T^2$, which means that the population variances of the numerical simulation and the experiment are equal.

7.3.3 t-test

From the law of large numbers, the best unbiased estimator of the expectation, μ , of random variables is the arithmetic mean. So in the validation process, the average of the population of two random variables, i.e., the results of the numerical simulation and the physical experiment, are compared.

If the two samples are relatively large and equal, even the variances are different, the t-test

method can be approximately applied. In fact, the experiment sub-sample is assumed to be a big sub-sample from the benchmark test, and the sub-sample of the numerical simulation is an approximate large sub-sample obtained by the orthogonal design, so the requirements of a relatively large number for the two sub-sample of the same size can be approximately met.

The statistical hypothesis goes like this: "The averages of the population of the sub-samples from the numerical simulation and the experiment are equal, $\bar{X}_c = \bar{X}_T$ ". Here, \bar{X}_c and \bar{X}_T are the averages of the results from the numerical simulation and the experiment, N_c and N_T are the sizes of the sub-samples. Define the t variable as

$$t = \frac{\bar{X}_c - \bar{X}_T}{\sqrt{\frac{N_c \hat{\sigma}_c^2 + N_T \hat{\sigma}_T^2}{N_c + N_T - 2} \sqrt{\frac{1}{N_c} + \frac{1}{N_T}}}} \quad (31)$$

$$f = (N_c - 1)(N_T - 1) \quad (32)$$

With the general aspects, $N_c = N_T = N$ and N is large enough, the Equation (29) can be rewritten as

$$t = \frac{\bar{X}_c - \bar{X}_T}{\sqrt{\frac{\hat{\sigma}_c^2 + \hat{\sigma}_T^2}{N}}} = \frac{\bar{X}_c - \bar{X}_T}{\sqrt{\frac{s_c^2 + s_T^2}{N}}} \quad (33)$$

$$= \frac{\bar{X}_c - \bar{X}_T}{\sqrt{u_c^2 + u_T^2}}$$

where u_c and u_T are the combined uncertainty of the CFD simulation and the experiment, respectively.

Considering that the current CFD simulation accuracy cannot reach the level of the experiment, so for simplicity, the term u_T can be omitted, Equation (28) can be simplified as

$$t = \frac{|\bar{X}_c - \bar{X}_T|}{u_c}, \quad f_c = N - 1 \quad (34)$$

According to the t variable degrees of freedom f and the confidence level α , $t_\alpha(f_c)$, the critical value of the variable t can be obtained. If $t < t_\alpha$, then $\bar{X}_c = \bar{X}_T$, the statistical hypothesis is not untrue. The simulation results can be validated.

7.3.4 Validation process

For the simulation results, it is necessary to judge by the statistical inference method whether the expectation and the variance of the population of the simulation results obtained from a small sub-sample are the same as those of the population of the experiment results. If they are equal, the simulation results are validated. The proposed validation methodology and its process of the CFD numerical simulation can be summarized as in the Figure 14.

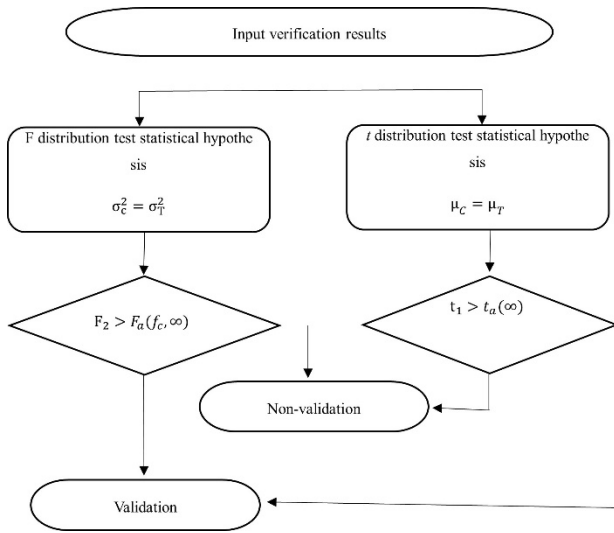


Figure 14: Flow chart of CFD simulation result's validation

7.4 Methods for grid convergence

7.4.1 Least square root method

Where the use of unstructured grids leads to variability in the grid, the error can be estimated using a Least Squares Root (LSR) method (Eça at al., 2010; Larsson at al., 2013). This requires at least four solutions to perform a curve fit of

$$\varphi_i = \varphi_0 + \alpha h_i^p \quad (35)$$

where i is the grid number from 1 to the number of grids and h_i is the size ratio.

The convergence condition is determined based on the observed order of accuracy, p , such that $p > 0$ indicates monotonic convergence and $p < 0$ indicates monotonic divergence. Oscillatory convergence is defined as being when the solution is alternately above and below the exact solution.

Since p is strongly influenced by the amount of scatter in the solutions, such that it may be larger than the theoretical order of accuracy, leading to an underestimate of the error, three alternative error estimates are provided, also found by curve fitting.

$$\delta_{RE} = \varphi_i - \varphi_0 = \alpha h_i^p \quad (36)$$

where φ_i is the numerical solution of any local or integral scalar quantity on a given grid, φ_0 is the estimated exact solution, and α is a constant.

If results on more than three grid are available, φ_0 , α and p are obtained with a Least Squares Root method that minimizes the function:

$$S(\varphi_0, \alpha, p) = \sqrt{\sum_{i=1}^{n_g} (\varphi_i - (\varphi_0 + \alpha h_i^p))^2} \quad (37)$$

where n_g is the number of grids available. The minimum of $S(\varphi_0, \alpha, p)$ is found by setting its derivatives with respect to φ_0 , p_j and α_j equal to zero, (Eca at al., 2007). The standard deviation of the fit, U_s , is given by

$$U_s = \sqrt{\frac{\sum_{i=1}^{n_g} (\varphi_i - (\varphi_0 + \alpha h_i^p))^2}{n_g - 3}} \quad (38)$$

LSR method establishes the apparent order of convergence p from the least squares solution. Oscillatory convergence or divergence is identified by n_{ch} , the number of times the difference between consecutive solutions changes sign, i.e. $(\phi_{i+1} - \phi_i) \times (\phi_i - \phi_{i-1}) < 0$. The apparent convergence condition is then decided as follows:

- (1) $p > 0$ for $\phi \rightarrow$ Monotonic convergence.
- (2) $p < 0$ for $\phi \rightarrow$ Monotonic divergence.
- (3) $n_{ch} \geq INT(n_g) \rightarrow$ Oscillatory convergence or divergence.

The only condition which allows an error estimation based on Richardson extrapolation is monotonic convergence. But even then small perturbations in the data may lead to significant changes in the estimated value of p , and thus sometimes to unsatisfactory results when the GCI in the LSR method.

In an attempt to overcome this, the maximum difference between all the solutions Δ_M is introduced.

$$\Delta_M = \max(|\phi_i - \phi_j|) \quad \text{with } 1 \leq i \leq n_g \wedge 1 \leq j \leq n_g \quad (39)$$

Two error estimators based on power series expansion with fixed exponents are:

$$\delta_{RE}^{12} = \phi_i - \phi_j = \alpha_1 h_i + \alpha_1 h_i^2 \quad (40)$$

$$\delta_{RE}^{02} = \phi_i - \phi_o = \lambda_1 h_i^2 \quad (41)$$

δ_{RE}^{12} and δ_{RE}^{02} are also calculated in the LSR method and so we will have standard deviations given by

$$U_S^{12} = \sqrt{\frac{\sum_{i=1}^{n_g} (\phi_i - (\phi_o + \alpha_1 h_i + \alpha_1 h_i^2))^2}{n_g - 3}} \quad (42)$$

$$U_S^{02} = \sqrt{\frac{\sum_{i=1}^{n_g} (\phi_i - (\phi_o + \lambda_1 h_i^2))^2}{n_g - 3}} \quad (43)$$

LSR method procedure for the estimation of the numerical uncertainty, valid for a nominally second-order accurate method, is as follows:

(1) The observed order of accuracy p is estimated with the LSR method to identify the apparent convergence condition according to the definition given above.

(2) For monotonic convergence:

For $0.95 \leq p < 2.05$

$$U_\phi = 1.25(\delta_{RE} + U_S) \quad (44)$$

For $0 < p < 0.95$

$$U_\phi = \min(1.25(\delta_{RE} + U_S), 1.25 \min\left(1.6, \frac{2.28}{p} - 1.4\right) (\delta_{RE}^{12} + U_S^{12})) \quad (45)$$

For $p \geq 2.05$

$$U_\phi = \max(1.25(\delta_{RE} + U_S), 1.25 \min(1.6, 3p - 5.15) (\delta_{RE}^{02} + U_S^{02})) \quad (46)$$

(3) For monotonic convergence:

$$U_\phi = 3\Delta_M \quad (47)$$

7.4.2 Richardson extrapolation

In Eça and Hoekstra (2014), Richardson Extrapolation (RE) is based on the assumption that discrete solutions have a power series representation in the grid spacing. RE approach requires at least three grids. Three grids are in the asymptotic range and the data have no scatter. The basic estimation equation of discretization error is:

$$\epsilon_\phi \cong \delta_{RE} = \phi_i - \phi_o = \alpha h_i^p \quad (48)$$

ϕ_i stands for any integral of other functional of a local flow quantity, ϕ_o is the estimate of the exact solution, α is a constant to be determined, h_i is the typical cell size and p is the observed order of grid convergence (Roache, 1998). The estimation of ϵ_ϕ requires the determination of ϕ_o , α and p . Therefore, the minimum number of grids (n_g) required for the estimation of ϵ_ϕ is three, unless p is assumed equal to a theoretical value, which is often not justified for practical problems.

The assumptions inherent in the application of Equation (47) are:

The grids must be in the “asymptotic range” to guarantee that the leading term of the power series expansion is sufficient to estimate the error.

The density of the grids is representable by a single parameter, the typical cell size of the grids, h_i . This requires the grids to be geometrically similar, i.e. the grid refinement ratio must be constant in the complete field and grid properties like the deviation from orthogonality, skewness, etc. must remain unaffected.

With equal grid refinement ratios between medium/fine and coarsest/medium grids, i.e. $h_2/h_1 = h_3/h_2$, a grid triplet suffices to estimate the apparent grid convergence behavior based on the discriminating ratio:

$$R = \frac{\phi_1 - \phi_2}{\phi_2 - \phi_3} \quad (49)$$

where the subscripts 1, 2 and 3 stand for fine, medium and coarse grid, respectively (Roache, 1998).

- Monotonic convergence for $0 < R < 1$.
- Monotonic divergence for $R > 1$.
- Oscillatory convergence for $R < 0$ and $|R| < 1$.
- Oscillatory divergence for $R < 0$ and $|R| > 1$.

In fact, the discriminating ratio R is related to the observed order of grid convergence p and the grid refinement ratios $h_2/h_1 = h_3/h_2$ by

$$R = \left(\frac{h_1}{h_2}\right)^p \left(\frac{\left(\frac{h_2}{h_1}\right)^p - 1}{\left(\frac{h_3}{h_2}\right)^p - 1}\right) R = \frac{\phi_1 - \phi_2}{\phi_2 - \phi_3} \quad (50)$$

which for $h_2/h_1 = h_3/h_2$ reduces to

$$\log(R) = p \log\left(\frac{h_1}{h_2}\right) \quad (51)$$

Hence, in such conditions, $p > 0$ is equivalent to $0 < R < 1$ and $p < 0$ to $R > 1$.

In order to be able to deal with the shortcomings of “practical calculations”, three other error estimators can be used.

$$\epsilon_\phi \cong \delta_1 = \phi_i - \phi_o = \alpha h_i \quad (52)$$

$$\epsilon_\phi \cong \delta_2 = \phi_i - \phi_o = \alpha h_i^2 \quad (53)$$

$$\epsilon_\phi \cong \delta_2 = \phi_i - \phi_o = \alpha h_i + \alpha h_i^2 \quad (54)$$

These three alternatives are only used if the estimation with Equation (47) is impossible or not reliable, i.e. the observed order of grid convergence is either too small or too large. The first two options, Equations (51) and (52), are suitable for monotonically converging solutions only, whereas the latter can be used as well with non-monotonic convergence.

7.4.3 Square root extrapolation

The error estimators presented above require three grids, using Equations (47) and (53), or two grids, using Equations (51) and (52), to estimate an error (Eça and Hoekstra, 2014). But error estimation based on three or two grids is not reliable for noisy data due to the extreme sensitivity of the determination of p to small perturbations (Eça and Hoekstra, 2002).

Therefore, it is virtually impossible to decide whether or not a given set of data is in the “asymptotic range”. Note that in the presence of scatter, an observed order of grid convergence equal to the formal order of grid convergence may be fortuitously obtained and is not sufficient to label the data set as being in the “asymptotic range”. Furthermore, a single grid triplet gives only one instance of p , because Equation (47) has three unknowns. Redundancy, and thus the possibility of a quality check on the value of p , only occurs when the fourth grid is added. Therefore, it is highly recommendable to use at least four grids when some scatter in the data is expected, i.e. for most engineering flow problems.

In such conditions ($n_g \gg 4$), it is possible to do the error estimation in the least-squares sense, i.e. to determine ϕ_o from the minimum of the functions:

$$S_{RE} = \sqrt{\sum_{i=1}^{n_g} w_i (\phi_i - (\phi_o + \alpha h_i^p))^2} \quad (55)$$

$$S_1 = \sqrt{\sum_{i=1}^{n_g} w_i (\phi_i - (\phi_o + \alpha h_i^p))^2} \quad (56)$$

$$S_2 = \sqrt{\sum_{i=1}^{n_g} w_i (\phi_i - (\phi_o + \alpha h_i))^2} \quad (57)$$

$$S_{12} = \sqrt{\sum_{i=1}^{n_g} w_i (\phi_i - (\phi_o + \alpha h_i + \alpha h_i^2))^2} \quad (58)$$

The least-squares minimization of Equations (58) to (61) is presented as follows, which also includes the definition of the standard deviation of the fits, σ , that will be used as a measure of the quality of the fits (Rawlings et al., 1998).

$$w_i = \frac{1/h_i}{\sum_{i=1}^{n_g} 1/h_i} \log(R) = p \log\left(\frac{h_1}{h_2}\right) \quad (59)$$

$$\sigma_{RE} = \sqrt{\frac{\sum_{i=1}^{n_g} n_g w_i (\phi_i - (\phi_o + \alpha h_i^p))^2}{(n_g - 3)}} \quad (60)$$

$$\sigma_1 = \sqrt{\frac{\sum_{i=1}^{n_g} n_g w_i (\phi_i - (\phi_o + \alpha h_i^p))^2}{(n_g - 3)}} \quad (61)$$

$$\sigma_2 = \sqrt{\frac{\sum_{i=1}^{n_g} n_g w_i (\phi_i - (\phi_o + \alpha h_i))^2}{(n_g - 3)}} \quad (62)$$

$$\sigma_{12} = \sqrt{\frac{\sum_{i=1}^{n_g} n_g w_i (\phi_i - (\phi_o + \alpha h_i + \alpha h_i^2))^2}{(n_g - 3)}} \quad (63)$$

7.5 N-version approach

For ship hydrodynamics, verification usually uses either the Fs or LSR methods. The numerical uncertainties U_{SN_i} associated to individual code/simulation S_i use the root-sum square of the iterative U_{I_i} grid U_{G_i} , and time-step U_{T_i} uncertainties

$$U_{SN_i} = \sqrt{U_G^2 + U_{T_i}^2 + U_{I_i}^2} \quad (64)$$

where i indicates an individual code and S_i is the solution on the finest grid. ASME (2009) advocates adding $U_{I_i}^2$ with $U_{G_i}^2$ and $U_{T_i}^2$. Iterative and grid/time verification studies are difficult and unfortunately often neglected. The Fs method requires monotonic convergence and ratio of the Richardson extrapolation and theoretical order of accuracy $P = P_{RE}/P_{th} \leq 2$, due to lack of data for $P > 2$ used for estimation of the required factor of safety. LSR method allows for oscillatory convergence, but there are differences of opinion on some aspects of the procedures.

The comparison error E_i is

$$E_i = D - S_i \quad (65)$$

D is the experimental data. Validation compares E_i with the validation uncertainty

$$U_{V_i}^2 = U_{E_i}^2 - U_{SM_i}^2 = U_{SN_i}^2 + U_D^2 \quad (66)$$

U_{SM} and U_D are the simulation modelling and experimental data uncertainties, respectively. The simulations are validated at an interval U_{V_i} if

$$|E_i| \leq U_{V_i} \quad (67)$$

If $U_{V_i} \ll |E_i|$, the sign and magnitude of $E_i \approx \delta_{SM}$ can be used to make modelling improvements. U_{V_i} includes all estimable uncertainties in the data and the simulations, and is the key metric in the validation process, which sets the interval at which validation can be achieved and may or may not meet programmatic requirements/tolerances.

Individual code solution V&V provides metrics for both the error E_i and its uncertainty U_{V_i} , from which conclusions can be made concerning acceptability or improvement strategies. The experimental uncertainty U_D usually includes both systematic and random components, whereas the numerical uncertainty U_{SN_i} is based solely on the systematic error and uncertainty estimates. Sensitivity and UQ studies using random perturbations of CFD code input parameters fail to provide an accurate simulation random uncertainty estimate as not representative of the inherent randomness in the CFD process as applied by different codes and/or users for different applications.

N multiple solutions from different codes and/or users for specified benchmark test cases provide the necessary data for assessment of CFD SoA capability, including individual solution and man code errors and estimates for simulation and absolute error random uncertainties. The assumption is made that the scatter of the CFD results represents the reproducibility of the computations. Results from many users of the same code are similar to

N-order replication level experiments (individual facility and measurement systems), whereas results from many different codes are similar to M×N-order replication level experiments (multiple facilities and measurement systems).

7.5.1 N-version verification

At the multiple code/user level, the individual code/solution uncertainty includes both systematic/bias and random/precision components

$$U_{S_i}^2 = B_{S_i}^2 + P_{S_i}^2 = (B_{SM_i}^2 + B_{SN_i}^2) + P_{S_i}^2 \quad (68)$$

where bias uncertainties are estimated at the simulation (single realization) level and precision uncertainties at the code (N-version, multiple realization) level.

Equations (63) and (65) assume that correlated modelling and numerical errors are negligible as a first approximation. Thus, the systematic uncertainty should include correlated modelling and numerical errors at a higher order of approximation. In contrast, P_{S_i} includes all simulation random uncertainties, including those arising from modelling and numerical errors and their correlations, i.e., represents the random simulation uncertainty.

Equation (67) can be written for both an individual code S_i and the average of N-version codes (mean code)

$$\bar{S} = \frac{1}{N} \sum_{i=1}^N S_i \quad (69)$$

$$U_{\bar{S}}^2 = B_{\bar{S}}^2 + P_{\bar{S}}^2 \quad (70)$$

Solution V&V studies (individual code/simulation level) provide

$$B_{S_i}^2 = B_{SM_i}^2 + B_{SN_i}^2 \quad (71)$$

Usually, B_{SM_i} is not known. However, in some cases (for instance, when using fluid property data), it can be estimated and included. The mean code bias is based on the average root-sum-square for the individual codes

$$B_{\bar{S}}^2 = \frac{1}{N} \sum_{i=1}^N B_{S_i}^2 = B_{SM}^2 + B_{SN}^2 \quad (72)$$

N-version verification (code level) provides

$$P_{S_i} = 2\sigma_s \quad (73)$$

where

$$\begin{aligned} \sigma_s &= \left[\frac{1}{N-1} \sum_{i=1}^N (S_i - \bar{S})^2 \right]^{\frac{1}{2}} \\ &= \left[\frac{1}{N-1} \sum_{i=1}^N (E_i - \bar{E})^2 \right]^{1/2} = \sigma_E \end{aligned} \quad (74)$$

and

$$P_{\bar{S}} = \frac{2\sigma_s}{\sqrt{N}} \quad (75)$$

$\sigma_s \% \bar{S}$ provides a measure of the scatter in the multiple CFD solutions for the specified benchmark test case. U_{S_i} including P_{S_i} (similarly for $U_{\bar{S}}$ and $P_{\bar{S}}$) provides a simulation uncertainty estimate at the N-order replication level. The mean code is a fictitious representation of the average of the N-version population. Outliers can be identified and rejected similarly as with experimental data using, e.g., Chauvenet's criterion. Herein, for simplicity, a solution is rejected if its deviation from the mean is larger than $2\sigma_s$, i.e., $N \approx 10$.

The estimated truth $\overline{S_{ET}}$ and S_{ET} lies within the confidence intervals

$$S_i - U_{S_i} \leq S_{ET} \leq S_i + U_{S_i} \quad (76)$$

and

$$\bar{S} - \bar{U}_{\bar{S}} \leq \bar{S}_{ET} \leq \bar{S} + U_{\bar{S}} \quad (77)$$

The assumption that for $N \geq 10$ and codes/simulations sufficiently similar in modelling and numerical methods and code development that S_i distribution is approximately normal is reasonable; however, multiple peaks and skewed distributions are also realized and should be expected, e.g., clustering around turbulence models or grid types.

7.5.2 N-version validation

The CFD SoA assessment is based on N-version validation for the specified benchmark test case. The average error and average absolute error are, respectively,

$$\bar{E} = \frac{1}{N} \sum_{i=1}^N E_i \quad (78)$$

$$|\bar{E}| = \frac{1}{N} \sum_{i=1}^N |E_i| \geq |\bar{E}| \quad (79)$$

The average absolute error is always greater than or equal to the absolute value of the signed average error. Previous certification approach used average error with the sign and $\sigma_s = \sigma_E$ for estimating simulation and error random uncertainties. Bias and precision uncertainties were estimated similarly as for solution validation, i.e., treating E_i and \bar{E} as data reduction equation and using propagation of error analysis. Clearly, the average absolute error is a better indicator of CFD SoA capability, as average of large positive and negative errors leads to erroneous result that the errors are small. Herein, average absolute error and its scatter are used for the CFD SoA assessment.

The average absolute error uncertainty consists of bias and precision components

$$U_{|E|}^2 = B_{|E|}^2 + P_{|E|}^2 \quad (80)$$

The bias uncertainty is evaluated using $\overline{|E|}$ as data reduction equation and propagation of error analysis, whereas precision uncertainty uses $\overline{|E|}$ as data reduction equation and end-to-end analysis in which the standard deviation is evaluated for $\overline{|E|}$ itself. Note that this is the usual practice in experimental uncertainty analysis. Thus, the bias uncertainty is comprised of contributions for both the experimental and simulation uncertainties

$$B_{|E|}^2 = U_D^2 + B_S^2 = U_D^2 + B_{SM}^2 + B_{SN}^2 \quad (81)$$

The precision uncertainty is approximated as

$$P_{|E|} = \frac{2\sigma_{|E|}}{\sqrt{N}} \quad (82)$$

where average absolute error standard deviation is

$$\sigma_{|E|} = \sqrt{\frac{1}{N-1} \sum_{i=1}^N (|E_i| - \overline{|E|})^2} \quad (83)$$

with the absolute value statistical property of the folded normal distribution

$$\sigma_{|E|}^2 = \sigma_E^2 + \overline{E}^2 - \overline{|E|}^2 \leq \sigma_E^2 = \sigma_S^2 \quad (84)$$

$\sigma_{|E|}\%D$ provides a measure of the scatter in the multiple solution absolute errors for the specified benchmark test case.

Following the same reasoning and approach used for solution validation, SoA uncertainty U_{SoA} is defined as:

$$U_{SoA}^2 = U_{|E|}^2 - B_{SM}^2 = U_D^2 + B_{SN}^2 + P_{|E|}^2 \quad (85)$$

U_{SoA} includes all estimable uncertainties in the data and the simulations and is the key metric in the assessment of the CFD SoA. It sets the interval at which the SoA can be achieved and may or may not meet programmatic requirements/tolerances.

$$\overline{|E|} \leq U_{SoA} \quad (86)$$

For the mean code is N-version validated at the interval of the SoA uncertainty U_{SoA} , whereas for

$$\overline{|E|} > U_{SoA} \quad (87)$$

the mean code is not N-version validated due to modelling assumptions. In theory, \overline{E} can be used for modelling assumptions improvements. In particular,

$$\overline{|E|} \gg U_{SoA} \quad (88)$$

$$\overline{E} \approx \delta_{SM} \quad (89)$$

The sign of \overline{E} may be of value; however, clearly improvements are made at the individual code/simulation level.

Similar analysis can be done for the individual code/simulation

$$U_{|E_i|}^2 = B_{|E_i|}^2 + P_{|E_i|}^2 \quad (90)$$

$$B_{|E_i|}^2 = U_D^2 + B_{S_i}^2 = U_D^2 + B_{SM_i}^2 + B_{SN_i}^2 \quad (91)$$

$$P_{|E_i|} = k\sigma_{|E_i|} \quad (92)$$

$$\begin{aligned} U_{SoA_i}^2 &= U_{|E_i|}^2 - B_{SM_i}^2 \\ &= U_D^2 + B_{SN_i}^2 + P_{|E_i|}^2 \end{aligned} \quad (93)$$

Note that the coverage factor k in Equation (91) follows the folded normal distribution quantiles and is asymmetric for lower and upper bound. Depending on the mean and standard deviation of the signed error, k ranges from 1.3 to 2 for the lower bound and from 2 to 2.4 for the upper bound. For simplicity, hereafter, the approximated value $k = 2$ is used.

$$|E_i| \leq U_{SoA_i} \quad (94)$$

For individual code/simulation is N-version validated at interval U_{SoA_i} , whereas for

$$|E_i| > U_{SoA_i} \quad (95)$$

individual code/simulation is not N-version validated due to modelling assumptions. E_i can be used for modelling assumptions improvements.

$$|E_i| \gg U_{SoA_i} \quad (96)$$

$$E_i \approx \delta_{SM_i} \quad (97)$$

The equations for N-version validation are similar to those for individual solution validation, except therein $P_{|E_i|}$ is not included

$$U_{SoA_i}^2 - P_{|E_i|}^2 = U_{V_i}^2 = U_D^2 + B_{SN_i}^2 \quad (98)$$

N-version validation provides additional confidence compared to individual solution validation, since it is additionally based on statistics of the normal distribution of N-versions. State-of-the-art uncertainty is also an improvement over simply identifying outliers based on σ_S alone, since additionally includes considerations of bias uncertainties. As with experimental uncertainty analysis, maximum confidence is achieved if both bias and precision uncertainties are considered. Subgroup analysis procedures can be used for isolating and assessing differences due to the use of different models and/or numerical methods.

Programmatic requirements/tolerances U_{req} can be considered similarly as for solution validation, but with U_V replaced by U_{SoA_i} . Since U_{SoA_i} is $\geq U_V$, it will always be a more conservative assessment. There are six possible combinations of $|E_i|$, U_{SoA_i} , and U_{req} assuming none are equal

$$\begin{aligned} \text{Case 1 } & |E_i| < U_{SoA_i} < U_{req} \\ \text{Case 2 } & |E_i| < U_{req} < U_{SoA_i} \\ \text{Case 3 } & U_{req} < |E_i| < U_{SoA_i} \\ \text{Case 4 } & U_{SoA_i} < |E_i| < U_{req} \\ \text{Case 5 } & U_{SoA_i} < U_{req} < |E_i| \\ \text{Case 6 } & U_{req} < U_{SoA_i} < |E_i| \end{aligned} \quad (99)$$

In cases 1, 2, and 3, N-version validation is achieved at the U_{SoA_i} interval, i.e., the comparison error is below the noise level. From an uncertainty perspective, modelling errors cannot be isolated. In cases 4, 5, and 6, the comparison error is larger than the noise level, i.e., $U_{SoA_i} < |E_i|$ such that from an uncertainty perspective, the sign and magnitude of E can be used to estimate δ_{SM} . If $U_{SoA_i} \ll |E_i|$, $E = \delta_{SM}$. Only cases 1 and 4 meet the programmatic requirements.

Consideration of programmatic requirements/tolerances resolves two paradoxes of the Coleman and Stern (1998) solution validation approach: (1) that only when validation is not achieved it is possible to have confidence that the error equals the modelling error; and (2) validation is easier to achieve for large U_V , i.e., noisy experiments and/or simulations. These paradoxes are mentioned at the individual code/simulation level but are also true for N-version validation with U_V replaced by U_{SoA_i} .

The reason for paradox (1) is that only for $U_V = 0$ it is true that $E = \delta_{SM}$, which only can occur for cases 4 to 6. For case 4, even though validation is not achieved both $|E_i|$ and U_V are $< U_{req}$ such that programmatic requirements are met and no action is needed. For case 5, $E = \delta_{SM}$ can be used to guide improvements in modelling in order to meet programmatic requirements. For case 6, similar as for case 5, $E = \delta_{SM}$ can be used to guide improvements in modelling and reduction in U_V , i.e., U_D and/or U_{SN} (depending on their relative magnitudes) are required in order to meet programmatic requirements.

The reason for paradox (2) is that, without U_{req} , U_V is unrestricted, whereas once restricted by U_{req} , there is no possibility for acceptance of the achievement of validation by a large U_V . For case 1, both $|E_i|$ and U_V are $< U_{req}$ such that programmatic requirements are met and no action is needed. For case 2, reduction in U_V , i.e., U_D and/or U_{SN} (depending on their relative magnitudes), is required in order to meet programmatic requirements. For case 3, reduction in both $|E_i|$ and U_V , i.e., U_D and/or U_{SN} (depending on their relative magnitudes), is required in order to meet programmatic requirements. Thus, case 3 is the most difficult as one cannot discriminate between different models with $|E_i| < U_V$ from an uncertainty perspective.

The processes for determining U_{req} and U_V/U_{SoA_i} are very different; therefore, meeting or not U_{req} should not be confused with individual code/simulation and multiple codes/N-version validation. Solution validation is a process for assessing simulation modelling errors/uncertainties. N-version validation extends this concept for multiple codes/simulations, which enables inclusion of the random absolute error uncertainty in assessing the CFD SoA. Presumably, the process for determining U_{req} is dominated by financial (beyond design testing and simulation), safety, environmental, and other concerns which may or may not take into consideration E_i and U_V/U_{SoA_i} .

7.6 Roy's approach

7.6.1 Coding verification

Software quality assurance

In Roy (2005), Software Quality Assurance, or SQA, is a formal set of procedures developed to ensure that software is reliable. SQA utilizes analysis and testing procedures including static analysis, dynamic analysis, and regression testing. Static analysis is an analysis conducted without actually running the code and includes

such activities as compiling the code (possibly with different compilers on different platforms) and running external diagnostic software to check variable initialization and consistency of argument lists for subroutines and functions. Dynamic analysis includes any activity which involves running the code. Examples of dynamic analysis include run-time compiler options (such as options for checking array bounds) and external software to find memory leaks. While numerical algorithm testing is technically a form of dynamic testing, it is such an important aspect of code verification for a computational simulation that it will be addressed in a separate section. Finally, regression tests involve the comparison of code output to the output from earlier versions of the code and are designed to find coding mistakes by detecting unintended changes in the code. It is important that the regression test suite be designed to obtain coverage of as much of the code as possible (i.e., all models and coding options). The results of SQA testing should be logged so that failures can be reported and corrected. Finally, code documentation is a critical area and includes documentation of code requirements, the software development plan, the verification, and testing plan, governing and auxiliary equations, and available coding options.

Consistency and convergence

For a numerical scheme to be consistent, the discretized equations must approach the original (continuum) partial differential equations in the limit as the element size (Δx , Δt , etc.) approaches zero. For a stable numerical scheme, the errors must not grow in the marching direction. These errors can be due to any source (round-off error, iterative error, etc.). It should be noted that typical stability analyses are valid for linear equations only. Finally, convergence addresses the issue of the solution to the discretized equations approaching the continuum solution to the partial differential equations in the limit of decreasing element size. Convergence is addressed by Lax's equivalence theorem (again valid for linear equations only)

which states that given a properly-posed initial value problem and a consistent numerical scheme, stability is the necessary and sufficient condition for convergence. Thus, consistency addresses the equations, while convergence deals with the solution itself. Convergence is measured by evaluating (or estimating) the discretization error. For verification purposes, it is convenient to define the discretization error as the difference between the solution to the discretized equations f_k and the solution to the original partial differential equation f_{exact}

$$DE_k = f_k - f_{exact} \quad (100)$$

where k refers to the mesh level. For the purposes of this paper, the round-off and iterative convergence error are addressed separately, therefore their contributions to the overall discretization error are neglected.

Method of exact solutions

Code verification has traditionally been performed by using the method of exact solutions. This approach involves the comparison of a numerical solution to an exact solution to the governing partial differential equations with specified initial and boundary conditions. The main disadvantage of this approach is that there are only a limited number of exact solutions available for complex equations (i.e., those with complex geometries, physics, or nonlinearity). When exact solutions are found for complex equations, they often involve significant simplifications. For example, the flow between parallel plates separated by a small gap with one plate moving is called Couette flow and is described by the Navier–Stokes equations. In Couette flow, the velocity profiles are linear across the gap. This linearity causes the diffusion term, a second derivative of velocity, to be identically zero. In contrast to the method of manufactured solutions discussed in the next sub-section, the method of exact solutions involves the solution to the forward problem. That is given a partial differential equation, boundary conditions, and initial conditions, the goal is to find the exact solution.

Method of manufactured solutions

The method of manufactured solutions, or MMS, is a general and very powerful approach to code verification. Rather than trying to find an exact solution to a system of partial differential equations, the goal is to “manufacture” an exact solution to a slightly modified set of equations. For code verification purposes, it is not required (in fact, often not desirable) that the manufactured solution be related to a physically realistic problem; recall that verification deals only with the mathematics of a given problem. The general concept behind MMS is to choose the solution a priori, then operate the governing partial differential equations onto the chosen solution, thereby generating analytical source terms. The chosen (manufactured) solution is then the exact solution to the modified governing equations made up of the original equations plus the analytical source terms. Thus, MMS involves the solution to the backward problem: given an original set of equations and a chosen solution, find a modified set of equations that the chosen solution will satisfy. The initial and boundary conditions are then determined from the solution.

The use of manufactured solutions and grid convergence studies for the purpose of code verification was first proposed by Roache and Steinberg (1984). They employed symbolic manipulation software to verify a code for generating three-dimensional transformations for elliptic partial differential equations. These concepts were later extended by Roache et al. (1990). The term “manufactured solution” was coined by Oberkampf and Blotner (1998) and refers to the fact that the method generates (or manufactures) a related set of governing equations for a chosen analytic solution. An extensive discussion of manufactured solutions for code verification was presented by Salari and Knupp (2000) and includes both details of the method as well as application to a variety of partial differential equation sets. This report was later refined and published in book form by Knupp and Salari (2002). A recent review/tutorial was given by Roache (2002),

and the application of the manufactured solutions procedure for the Euler and Navier–Stokes equations for fluid flow was presented by Roy et al. (2004).

The procedure for applying MMS with the order of accuracy verification can be summarized in the following six steps:

Step 1. Choose the form of the governing equations

Step 2. Choose the form of the manufactured solution

Step 3. Derive the modified governing equations

Step 4. Solve the discrete form of the modified governing equations on multiple meshes

Step 5. Evaluate the global discretization error in the numerical solution

Step 6. Apply the order of accuracy test to determine if the observed order of accuracy matches the formal order of accuracy

The fourth step, which includes the solution to the modified governing equations, may require code modifications to allow arbitrary source terms, initial conditions, and boundary conditions to be used. Manufactured solutions should be chosen to be smooth, analytical functions with smooth derivatives. The choice of smooth solutions will allow the formal order of accuracy to be achieved on relatively coarse meshes, and trigonometric and exponential functions are recommended. It is also important to ensure that no derivatives vanish, including cross-derivatives. Care should be taken that one term in the governing equations does not dominate the other terms. For example, when verifying a Navier–Stokes code, the manufactured solution should be chosen to give Reynolds numbers near unity so that convective and diffusive terms are of the same order of magnitude. Finally, realizable solutions should be employed, that is, if the code requires the temperature to be positive (e.g., in the evaluation of the speed of sound which involves the square root of the temperature), then the manufactured solution should be chosen as such.

MMS has been applied to the Euler equations, which govern the flow of an inviscid (frictionless) fluid (Roy, 2004). The two-dimensional, steady-state form of the Euler equations is given by

$$\frac{\partial(\rho u)}{\partial x} + \frac{\partial(\rho v)}{\partial y} = f_m \quad (101)$$

$$\frac{\partial(\rho u^2 + p)}{\partial x} + \frac{\partial(\rho uv)}{\partial y} = f_x \quad (102)$$

$$\frac{\partial(\rho uv)}{\partial x} + \frac{\partial(\rho v^2 + p)}{\partial y} = f_y \quad (103)$$

$$\frac{\partial(\rho u e_t + pu)}{\partial x} + \frac{\partial(\rho v e_t + pv)}{\partial y} = f_e \quad (104)$$

where arbitrary source terms f are included on the right-hand side, and e_t is the specific total energy, which for a calorically perfect gas is given by

$$e_t = \frac{1}{\gamma - 1} RT + \frac{u^2 + v^2}{2} \quad (105)$$

The final relation needed to close the set of equations is the equation of state for a calorically perfect gas

$$p = \rho RT \quad (106)$$

The manufactured solution for this case is chosen as

$$\rho(x, y) = \rho_0 + \rho_x \sin\left(\frac{a_{\rho x} \pi x}{L}\right) + \rho_y \cos\left(\frac{a_{\rho y} \pi y}{L}\right) \quad (107)$$

$$u(x, y) = u_0 + u_x \sin\left(\frac{a_{u x} \pi x}{L}\right) + u_y \cos\left(\frac{a_{u y} \pi y}{L}\right) \quad (108)$$

$$v(x, y) = v_0 + v_x \sin\left(\frac{a_{v x} \pi x}{L}\right) + v_y \cos\left(\frac{a_{v y} \pi y}{L}\right) \quad (109)$$

$$w(x, y) = w_0 + w_x \sin\left(\frac{a_{wx}\pi x}{L}\right) + w_y \cos\left(\frac{a_{wy}\pi y}{L}\right) \quad (110)$$

The subscripts here refer to constants (not differentiation) with the same units as the variable, and the dimensionless constants generally vary between 0.5 and 1.5 to provide smooth solutions over an $L \times L$ square domain. For this case, the constants were chosen to give supersonic flow in both the positive x and positive y directions. While not necessary, this choice simplifies the inflow boundary conditions to Dirichlet values at the inflow and Neumann (gradient) values at the outflow. The inflow boundary conditions are determined from the manufactured solution.

7.6.2 Solution verification

Sources of numerical error

The three main sources of numerical error in a computational simulation are round-off error, iterative convergence error, and discretization error. The latter error source includes both errors in the interior discretization scheme as well as errors in the discretization of the boundary conditions. These error sources are discussed in detail in the following sub-sections.

Round-off error

Round-off errors occur due to the use of finite arithmetic on digital computers. For example, in a single-precision digital computation, the following result is often obtained

$$3.0 * \left(\frac{1.0}{3.0}\right) = 0.999999 \quad (111)$$

while the true answer is of course 1.0. Round-off error can be important for both ill-conditioned systems of equations as well as time-accurate simulations. The adverse effects of round-off error can be mitigated by using more significant digits in the computation.

Standard computers employ 32 bits of memory for each storage location. In a double-precision calculation, two storage locations are allocated for each number, thus providing 64 bits of memory. Higher-precision storage can be accessed through variable declarations, by using appropriate compiler flags, or by employing one of the recently developed 64-bit computer architectures.

Iterative convergence error

Iterative convergence error arises due to incomplete iterative convergence of a discrete system. Iterative methods are generally required for complex nonlinear systems of equations, but are also the most efficient approach for large, sparse linear systems. The two classes of iterative approaches for linear systems are stationary iterative methods (Jacobi, Gauss–Seidel, line relaxation, multigrid, etc.) and Krylov subspace methods (GMRES, conjugate gradient, Bi-CGSTAB, etc.). Nonlinear systems of equations also employ the above iterative methods, but generally in conjunction with a linearization procedure (e.g., Picard iteration, Newton’s method).

Discretization error

The discretization error was defined in Equation (99) as the difference between a numerical solution and the exact solution to the continuum partial differential equations. It arises due to the conversion of the differential equations into an algebraic system of equations (i.e., the discretization process). This process necessarily introduces discretization parameters such as the element size ($\Delta x, \Delta y$ and Δz) and/or the time step (Δt). The discretization error can be clearly related to the truncation error for linear problems; however, for nonlinear problems, this relationship is not straightforward. There are two main reasons for evaluating the discretization error. The first reason is to obtain an assessment of the discretization error associated with a given solution, which might be needed during an analysis of simulation results or for a model validation study. This error assessment can take three distinct forms: an

error estimate (e.g., the most likely value for the error is -5%), an error band (e.g., a confidence level of 95% that the error is within $\pm 8\%$), or an error bound (e.g., the error is guaranteed to be within $\pm 8\%$). The second reason for evaluating the discretization error is to drive a grid adaptation process. Grid adaptation can involve locally adding more elements (h-adaptation), moving points from a region of the low error to a region of high error (r-adaptation), or locally increasing the formal order of accuracy (p-adaptation).

Discretization error estimation

There are several methods available for estimating discretization error. These methods can be broadly categorized as a priori methods and posteriori methods. The a priori methods are those that allow a limit to be placed on the discretization error before the numerical solution is calculated, i.e., find C and p such that $DE < Ch^p$. Here p is simply the formal order of accuracy and can be determined by the methods discussed earlier. The determination of the constant C is challenging and generally problem-dependent, and can be very large (and thus not useful) for complex problems. The majority of research today is focused on posteriori methods for estimating the discretization error. These methods provide an error estimate only after the numerical solution is computed. The posteriori methods can be further sub-divided into finite-element-based error estimators and extrapolation-based error estimators. Although a brief overview of the former is given in the next sub-section, this paper focuses on the latter approach since it is equally applicable to finite-difference, finite-volume, and finite-element methods.

In general, the level of maturity for all of the posteriori error estimation methods is heavily problem-dependent (Stewart, 2003). As a whole, they tend to work well for elliptic problems, but are not as well-developed for parabolic and hyperbolic problems. The level of complexity of the problem is also an important issue. The error estimators work well for smooth, linear problems with simple physics and geometries;

however, strong nonlinearities, discontinuities, singularities, and physical and geometric complexity can significantly reduce the reliability and applicability of these methods.

Finite-element-based error estimator

Two fundamentally different types of discretization error estimators have been developed from the finite-element method (Stewart, 2003). The most widely-used are recovery methods, which involve post-processing of the solution gradients (Zienkiewicz and Zhu, 1992) or nodal values (Zhang et al., 2002) on patches of neighbouring elements. The former approach is often referred to as the ZZ error estimator, while the latter as polynomial preserving recovery (PPR). The basic formulations provide error estimates only in the global energy norm; extensions to quantities of interest must generally be done heuristically (e.g., a 5% error in the global energy norm may correspond to a 10% error in heat flux for a given class of problems). Although difficult to analyse mathematically, recovery-based error estimators do provide ordered error estimates. That is, the error estimate gets better with mesh refinement. Recovery-based methods can be extended to finite-difference and finite-volume schemes, but this process generally requires additional effort.

The second class of error estimators that have arisen from finite elements are residual-based methods. These methods take the form of either explicit residual method (Eriksson and Johnson, 1987) or implicit residual methods (Babuska and Miller, 1984). These methods were originally formulated to provide error estimates in the global energy norm. Extension of both the explicit and implicit residual methods to provide error estimates in quantities of interest generally requires the solution to the adjoint system (i.e., the dual problem). The explicit method has been extended to finite-volume schemes by Barth and Larson (2002). For more information on residual-based posteriori error estimators for finite-elements (Ainsworth and Oden, 2000; Babuska, 1986).

Extrapolation-based error estimators

The extrapolation-based error estimators come in two different forms. The most popular approach is based on Richardson extrapolation (Richardson, 1910; Richardson, 1927) and requires numerical solutions on two or more meshes with different levels of refinement. The numerical solutions are then used to obtain a higher-order estimate of the exact solution. This estimate of the exact solution can then be used to estimate the error in the numerical solutions. The second type of extrapolation-based error estimator is order extrapolation (p-extrapolation). In this approach, solutions on the same mesh, but with two different formal orders of accuracy, are used to obtain a higher-order accurate solution, which can again be used to estimate the error. The drawback to order-extrapolation is that it requires advanced solution algorithms to obtain higher-order numerical schemes, which can be difficult to code and expensive to run. The main advantage of the extrapolation-based error estimators is that they can be applied as a post-processing step to any type of discretization, whether it be a finite-difference, finite-volume, or finite-element method.

Richardson extrapolation

Richardson extrapolation is based on the series expansion of the discretization error which can be rewritten as

$$\begin{aligned} DE_k &= f_k - f_{exact} \\ &= g_1 h_k + g_2 h_k^2 + g_3 h_k^3 \\ &\quad + g_4 h_k^4 + HOT \end{aligned} \quad (112)$$

where g_i is the coefficient of the i^{th} order error term and the exact solution f_{exact} is generally not known. The assumptions that are required for using Richardson extrapolation are that (1) the solutions are smooth, (2) the higher-order terms in the discretization error series expansion are small, and (3) uniform meshes are used. The second assumption regarding the higher-order terms is true in the asymptotic range, where h is sufficiently small that the lower-order terms in

the expansion dominate. While the last assumption regarding uniform meshes appears to be quite restrictive, transformations (either local or global) can be used if the order of accuracy of the transformation is equal to (or higher than) the order of the numerical scheme. Transformations will be discussed in detail in a later subsection.

Standard Richardson extrapolation

The standard Richardson extrapolation procedure assumes that the numerical scheme is second-order accurate, and that the mesh is refined or coarsened by a factor of two. Consider a second-order discretization scheme which is used to produce numerical solutions on two meshes: a fine mesh ($h_1 = h$), and a coarse mesh ($h_2 = 2h$). Since the scheme is second-order accurate, the g_1 coefficient is zero, and the discretization error equations on the fine and coarse meshes can be rewritten as

$$\begin{aligned} f_1 &= f_{exact} + g_2 h^2 + O(h^3) \\ f_2 &= f_{exact} + g_2 (2h)^2 + O((2h)^3) \end{aligned} \quad (113)$$

Neglecting higher-order terms, these two equations can be rewritten as

$$\begin{aligned} f_1 &= f_{exact} + g_2 h^2 \\ f_2 &= f_{exact} + g_2 (2h)^2 \end{aligned} \quad (114)$$

Solving the first equation for g_2 yields

$$g_2 = \frac{f_1 - f_{exact}}{h^2} \quad (115)$$

and solving the second equation for f_{exact} gives

$$f_{exact} = f_2 - g_2 (2h)^2 \quad (116)$$

Substituting Equation (115) into Equation (116) gives

$$\begin{aligned}
 f_{\text{exact}} &= f_2 - \left[\frac{f_1 - f_{\text{exact}}}{h^2} \right] (2h)^2 \\
 &= f_2 - 4f_1 + 4f_{\text{exact}} \\
 &= f_2 - g_2(2h)^2
 \end{aligned}
 \tag{117}$$

Or simply

$$f_{\text{exact}} = f_1 + \frac{f_1 - f_2}{3}
 \tag{118}$$

Standard Richardson extrapolation thus provides a ‘‘correction’’ to the fine grid solution. This expression for the estimated exact solution f_{exact} is generally third-order accurate. This expression for the estimated exact solution f_{exact} is generally third-order accurate. In Richardson’s original work (Richardson, 1910), he used this extrapolation procedure to obtain a higher-order accurate solution for the stresses in a masonry dam based on two second-order accurate numerical solutions. In Richardson’s case, he employed central differences which cancelled out the odd powers in the truncation error. His estimate for the exact solution was thus fourth-order accurate.

Generalized Richardson extrapolation

Richardson extrapolation can be generalized to p th-order accurate schemes with solutions on a fine mesh (spacing h_1) and a coarse mesh (spacing h_2), which are not necessarily different by a factor of two. Introducing the general grid refinement factor

$$r = h_2/h_1
 \tag{119}$$

and setting $h_1 = h$, the discretization error equations can be written as

$$f_1 = f_{\text{exact}} + g_p h^p + O(h^{p+1})
 \tag{120}$$

$$f_2 = f_{\text{exact}} + g_p (rh)^p + O((rh)^{p+1})
 \tag{121}$$

Neglecting the higher-order terms, these two equations can be solved for f_{exact} to give

$$f_{\text{exact}} = f_1 + \frac{f_1 - f_2}{r^p - 1}
 \tag{122}$$

which is generally a $(p+1)$ th order accurate estimate. Again, it should be emphasized that Richardson extrapolation relies on the assumption that the solutions are asymptotic (i.e., the observed order of accuracy matches the formal order).

Observed order of accuracy

When the exact solution is not known (which is generally the case for solution verification), three numerical solutions on different meshes are required in order to calculate the observed order of accuracy. Consider a p th-order accurate scheme with numerical solutions on a fine mesh (h_1), a medium mesh (h_2), and a coarse mesh (h_3). For the case of a constant grid refinement factor

$$r = h_2/h_1 = h_3/h_2
 \tag{123}$$

we can thus write

$$h_1 = h, h_2 = rh, h_3 = r^2h
 \tag{124}$$

The three discretization error equations can be written as

$$f_1 = f_{\text{exact}} + g_p h^p + O(h^{p+1})
 \tag{125}$$

$$f_2 = f_{\text{exact}} + g_p (rh)^p + O((rh)^{p+1})
 \tag{126}$$

$$\begin{aligned}
 f_3 &= f_{\text{exact}} + g_p (r^2h)^p \\
 &\quad + O((r^2h)^{p+1}) \\
 &= f_{\text{exact}} + g_p (r^2h)^p + O((r^2h)^{p+1})
 \end{aligned}
 \tag{127}$$

Neglecting the higher-order terms, these three equations can be used to solve for the observed order of accuracy p to give

$$p = \frac{\ln\left(\frac{f_3 - f_2}{f_2 - f_1}\right)}{\ln(r)}
 \tag{128}$$

Note that here the observed order of accuracy is calculated and does not need to be assumed (as with Richardson extrapolation).

For the case of non-constant grid refinement factors

$$r_{12} = \frac{h_2}{h_1}, r_{23} = \frac{h_3}{h_2} \quad (129)$$

where $r_{12} \neq r_{23}$, the determination of the observed order of accuracy p is more complicated. For this case, the following transcendental equation (Roache, 1998) must be solved

$$\frac{f_3 - f_2}{r_{23}^p - 1} = r_{12}^p \left(\frac{f_2 - f_1}{r_{12}^p - 1} \right) \quad (130)$$

This equation can be easily solved using a simple Picard-type iterative procedure.

Richardson extrapolation as an error estimator

In some cases, researchers mistakenly report discretization error estimates by giving the relative difference between two numerical solutions computed on different meshes, i.e.,

$$\text{Diff} = \frac{f_2 - f_1}{f_1} \quad (131)$$

This relative difference can be extremely misleading when used as an error estimate. To see why, let us first develop a discretization error estimator using generalized Richardson extrapolation. The relative discretization error (RDE) is simply the difference between the numerical solution and the exact solution, normalized by the exact solution, which for the fine grid ($k = 1$) can be written as

$$RDE_1 = \frac{f_1 - f_{exact}}{f_{exact}} \quad (132)$$

Substituting the generalized Richardson extrapolation result from Equation (115) into the numerator gives

$$\begin{aligned} RDE_1 &= \frac{f_1 - f_{exact}}{f_{exact}} \\ &= \frac{f_1 - \left[f_1 + \frac{f_1 - f_2}{r^p - 1} \right]}{f_{exact}} \\ &= \frac{f_{exact}}{f_2 - f_1} \end{aligned} \quad (133)$$

The reason for leaving f_{exact} in the denominator will be apparent shortly. Consider two numerical solutions where some quantity of interest has a relative difference (from Equation (130)) of 5%. For a third-order accurate scheme with $r = 2$, the error estimate based on Richardson extrapolation (Equation (132)) is 0.71%. However, for a first-order accurate numerical scheme with a grid refinement factor of 1.5, the error estimate based on Richardson extrapolation is 9.1%. Thus, a 5% relative difference in the two solutions can mean very different values for the relative discretization error, depending on the order of accuracy of the scheme and the grid refinement factor. This example illustrates the importance of accounting for the $(r^p - 1)$ factor for obtaining accurate error estimates. This understanding led to the development of Roache's Grid Convergence Index, to be discussed in a later sub-section.

Roache's grid convergence

Roache (1994) proposed the Grid Convergence Index, or GCI, as a method for uniform reporting of grid refinement studies. The GCI combines the often reported relative difference between solutions (Equation (130)) with the $(r^p - 1)$ factor from the Richardson extrapolation-based error estimator (Equation (132)). The GCI also provides an error band rather than an error estimate.

Definition of GCI

The GCI for the fine grid numerical solution is defined as

$$GCI = \frac{F_s}{r^p - 1} \left| \frac{f_2 - f_1}{f_1} \right| \quad (134)$$

where F_s is a factor of safety that is usually set to three ($F_s = 3$). Comparing the GCI to the extrapolation-based RDE estimator given in Equation (132), we see that the GCI uses a factor of safety F_s , it employs absolute values to provide an error band, and it replaces f_{exact} in the denominator of Equation (132) with f_1 . Most importantly, the GCI correctly accounts for the (assumed) order of accuracy p and the grid refinement factor r .

Relation between of GCI and a Richardson extrapolation-based error band

The relative discretization error estimate from Equation (132) can easily be converted to an error band (RDE_{band}) by taking the absolute value and multiplying by a factor of safety F_s , resulting in

$$RDE_{band} = \frac{F_s}{r^p - 1} \left| \frac{f_2 - f_1}{f_1} \right| \quad (135)$$

Now, the only difference between the Richardson extrapolation-based error band (RDE_{band}) and the GCI is the use of f_{exact} in the denominator rather than f_1 . Will this make a significant difference? It was shown by Roy (2001) that the error in the GCI relative to the RDE_{band} is given by

$$\begin{aligned} \left| \frac{GCI - RDE_{band}}{RDE_{band}} \right| &= \frac{F_s}{r^p - 1} \left(\frac{f_2 - f_1}{f_1} \right) \\ &= \frac{GCI}{F_s} \end{aligned} \quad (136)$$

The error in the GCI relative to the RDE_{band} is thus an ordered error, meaning that it is reduced with mesh refinement (i.e., as $h \rightarrow 0$).

Factor of safety in the GCI

It is important to include the factor of safety in the GCI and the RDE_{band}. Both of these error bands are based on Richardson extrapolation, and we do not know a priori whether the estimated exact solution is above or below the true exact solution to the continuum partial

differential equations. In general, there is an equal chance that the true exact solution is above or below the estimated value. Thus a factor of safety of $F_s = 1$ centred on the fine grid numerical solution will only provide 50% confidence that the true error (f_{exact}) is within the error band. Increasing the factor of safety should increase the confidence that the true error is within the error band. The value for the factor of safety that would provide a 95% confidence band is currently a subject of debate. When only two numerical solutions are performed, the observed order of accuracy cannot be calculated and must be assumed. For this case, Roache (1998) recommends $F_s = 3$. When three solutions are performed, the observed order of accuracy can be calculated. If the observed order matches the formal order of accuracy, Roache (1995) recommends a smaller factor of safety of $F_s = 1.25$. However, when the solutions are far outside the asymptotic range, the accuracy of the extrapolation procedure is unpredictable and possibly random. In this case, no choice for the factor of safety is sure to be conservative.

Practical aspects of grid refinement

Grid refinement versus grid coarsening for structured meshes

In theory, it should not make a difference whether we start with the coarse mesh or the fine mesh. However, in practice, grid coarsening on structured meshes is often easier than grid refinement, especially for complex meshes. Here, complex meshes are defined as those with complex geometries and/or significant grid clustering. For uniform meshes, refinement can be performed by simply averaging neighbouring spatial locations. For stretched meshes, this type of refinement will lead to discontinuities in the ratio of neighbouring element sizes near the original coarse grid nodes. A better strategy for stretched meshes is to use higher-order interpolation to obtain smooth stretching distributions; however, this process can be challenging on highly complex grids. The primary problems that arise during mesh refinement are due to a loss of geometric definition at object surfaces, especially at sharp

corners. Furthermore, for structured grid approaches requiring point-to-point match-up at inter-zone boundaries, the refinement strategy must ensure that these points are co-located. Thus for complex, structured meshes, it is often easier to simply start with the fine mesh and successively remove every other point in each of the coordinate directions.

Grid refinement versus grid coarsening for unstructured meshes

For unstructured meshes, it is generally easier to start with the coarse mesh, then refine by sub-dividing the elements. This is due to the difficulties of merging elements in a manner that preserves the element type while enforcing the requirement of a constant grid refinement factor over the entire domain. While refinement for unstructured grid approaches inherits all of the drawbacks of refinement for structured grids discussed in the previous section, there are currently efforts underway to make surface geometry information directly available to mesh refinement routines (Tautges, 2001).

The choice of methods for refining the elements will determine the effective grid refinement factor. In two dimensions, triangular elements can easily be refined by connecting the midpoints of the edges, thereby creating four new triangular elements.

Non-integer grid refinement

It is not necessary to use grid refinement factors of two, a process referred to as grid doubling or grid halving (depending on whether one starts with the fine mesh or the coarse mesh). For simple meshes, grid refinement factors as small as $r = 1.1$ can be employed (Roache, 1998). Using non-integer grid refinement factors may increase the chance of getting all mesh solutions into the asymptotic grid convergence range. However, non-integer grid refinement factors are difficult to apply to complex meshes, especially those involving significant mesh stretching. For simulations on complex, structured meshes, the grid generation can sometimes make up the majority of the overall

analysis time. Thus, relying on the original grid generation procedure for grid refinement can be expensive; furthermore, it is difficult to enforce a constant grid refinement factor over the entire domain. Higher-order interpolation can be used for non-integer grid refinement. Here it is again better to start with the fine mesh and then coarsen (at least for structured meshes); however, the same geometry definition problems discussed earlier still exist. When a grid refinement factor of two is employed, there is only significant effort involved in generating the fine mesh; the coarser meshes are found by simply removing every other point. The drawback is not only that the fine mesh may be unnecessarily expensive, but there is also an increased chance that the coarse mesh will be outside the asymptotic grid convergence range.

Independent coordinate refinement

It is sometimes the case that the discretization errors come primarily from just one of the coordinate directions. In such cases, it can be helpful to perform independent refinement in the coordinate directions to determine which one is the primary contributor to the overall discretization error. For independent refinement in x and y , we can write

$$f_k = f_{exact} + g_x(\Delta x_k)^p + g_y(\Delta y_k)^q + HOT \quad (137)$$

where the error terms for each direction are included. In order to keep the analysis general, the order of accuracy in the x direction is p and the order of accuracy in the y direction is q , where the two may or may not be equal. Note that for some numerical schemes, a cross term (e.g., $g_{xy}(\Delta x)^s(\Delta y)^t$) may also be present. As in Richardson extrapolation, assume that p and q are equal to the formal order of accuracy. Consider the case of two solutions ($k = 1$ and $k = 2$) with refinement only in the x direction by a factor of r_x . As the Δx element size is refined, the term $g_y(\Delta y_k)^q$ will be constant. We are now unable to solve for the exact solution f_{exact} , but instead must solve for the quantity

$$f_{exact,x} = f_{exact} + g_y(\Delta y_k)^q \quad (138)$$

which includes the error term due to the Δy discretization. Neglecting higher-order terms, the following two equations

$$f_1 = f_{exact,x} + g_x(\Delta x)^p \quad (139)$$

$$f_2 = f_{exact,x} + g_x(r_x \Delta x)^p \quad (140)$$

can be solved for $f_{exact,x}$

$$f_{exact,x} = f_1 + \frac{f_1 - f_2}{r_x^p - 1} \quad (141)$$

and the leading x-direction error term

$$g_x(\Delta x)^p = \frac{f_2 - f_1}{r_x^p - 1} \quad (142)$$

Similarly, introducing a third solution ($k = 3$) with coarsening only in the y direction allows us to solve for the y -direction error term

$$g_y(\Delta y)^q = \frac{f_3 - f_1}{r_y^q - 1} \quad (143)$$

The size of the two error terms from Equations (141) and (142) can then be compared to determine the appropriate direction for further mesh refinement.

7.7 Comparison of ASME and ISO procedures

In Oberkampf and Roy (2010), the definitions accepted by AIAA (1998) and ASME (2006) for verification and validation as applied to scientific computing address the mathematical accuracy of a numerical solution (verification) and the physical accuracy of a given model (validation); however, the definitions used by the software engineering community (e.g., ISO, 1991; IEEE, 1991) are different. In software engineering, verification

is defined as ensuring that software conforms to its specifications (i.e., requirements), and validation is defined as ensuring that software actually meets the customer's needs. Some argue that these definitions are really the same; however, upon closer examination, they are in fact different.

The key differences in these definitions for verification and validation are since, in scientific computing, we begin with a governing partial differential or integral equation, which we will refer to as our mathematical model. For problems that we are interested in solving, there is generally no known exact solution to this model. It is for this reason that we must develop numerical approximations to the model (i.e., the numerical algorithm) and then implement that numerical algorithm within scientific computing software. Thus the two striking differences between how the scientific computing community and the software engineering community define verification and validation are as follows. First, in scientific computing, validation requires a comparison to experimental data. The software engineering community defines validation of the software as meeting the customer's needs, which is, in our opinion, too vague to tie it back to experimental observations. Second, in scientific computing, there is generally no true system-level software test (i.e., a test for correct code output given some code inputs) for real problems of interest. The "correct" output from the scientific software depends on the number of significant figures used in the computation, the computational mesh resolution and quality, the time step (for unsteady problems), and the level of iterative convergence.

7.7.1 ASME procedure

ASME procedure (2009) follows a five-step procedure proposed by Knupp & Salari (2002).

Step 1: Define a representative cell, mesh, or grid size, h . For example, for three-dimensional, structured, geometrically similar grids (not necessarily Cartesian),

$$h = [(\Delta x_{max})(\Delta y_{max})(\Delta z_{max})]^{1/3} \quad (144)$$

For unstructured grids one can define

$$h = \left[\left(\sum_{i=1}^N \Delta V_i \right) / N \right]^{1/3} \quad (145)$$

where N=total number of cells used for the computations and ΔV_i =volume of the *i*th cell.

Step 2: It is desirable that the grid refinement factor, $r = h_{coarse}/h_{fine}$, should be greater than 1.3 for most practical problems. This value of 1.3 is again based on experience and not on some formal derivation. This value of 1.3 is again based on experience and not on some formal derivation. The grid refinement should, however, be made systematically; that is, the refinement itself should be structured even if the grid is unstructured.

Step 3: Let $h_1 < h_2 < h_3$ and $r_{21} = h_2/h_1$, $r_{32} = h_3/h_2$ and calculate the apparent (or observed) order, *p*, of the method from reference

$$p = [1/\ln(r_{21})][1/\ln|\varepsilon_{32}/\varepsilon_{21}| + q(p)] \quad (146)$$

$$q(p) = \ln \left(\frac{r_{21}^p - s}{r_{32}^p - s} \right) \quad (147)$$

$$s = 1 \cdot \sin(\varepsilon_{32}/\varepsilon_{21}) \quad (148)$$

where $\varepsilon_{32} = \varphi_3 - \varphi_2$, $\varepsilon_{21} = \varphi_2 - \varphi_1$, and φ_k denotes the simulation value of the variable on the *k*th grid. Note that $q(p) = 0$ for $r = \text{constant}$. This set of three equations can be solved using fixed point iteration with the initial guess equal to the first term (i.e., $q = 0$).

Step 4: Calculate the extrapolated values from the equation

$$\varphi_{ext}^{21} = (r_{21}^p \varphi_1 - \varphi_2) / (r_{21}^p - 1) \quad (149)$$

Step 5: Calculate and report the following error estimates along with the observed order of

the method *p*. Approximate relative error may be cast as a dimensionless form or in a dimensioned form, respectively as follows:

$$e_a^{21} = \left| \frac{\varphi_1 - \varphi_2}{\varphi_1} \right| \quad (150)$$

$$e_a^{21} = |\varphi_1 - \varphi_2| \quad (151)$$

The error was estimated from the equation

$$U_i = \frac{F_s \cdot e_a^{21}}{r_{21}^p - 1} = F_s |\delta_{RE,1}^*| \quad (152)$$

For the Factor of Safety, *F_s*, Roache (1998) recommended a less conservative value for $F_s = 1.25$, but only when using at least three grid solutions and the observed *p*.

7.7.2 ISO procedure

ISO 16730 (2008) provides a framework for assessment, verification, and validation of all types of calculation methods. It does not address specific models, but is intended to apply to both analytical models and complex numerical models that are addressed as calculation methods in the context of these international standards. It is not a step-by-step procedure, but does describe techniques for detecting errors and finding limitations in a calculation method. the standards include the following:

-A process to ensure that the equations and calculation methods are implemented correctly (verification) and that the calculation method being considered in solving the appropriate problem (validation);

-Requirements for documentation to demonstrate the adequacy of the scientific and technical basis of a calculation method;

-Requirements for data against which a calculation method's predicted results shall be checked

The example in ISO/TR 16730-3 (2013) describes the application of procedures given in

ISO 16730-1 for a computational fluid dynamics (CFD) model (ISIS). The main objective of the specific model treated in ISO/TR 16730-3:2013 is the simulation of a fire in an open environment or confined compartments with a natural or forced ventilation system.

8. SUGGESTED PROCEDURES TO ENSURE THE QUALITY OF CFD/EFD COMBINED PREDICTIONS

This section describes work that was carried out mainly by a joint working group with members from the Resistance and Propulsion Committee and the Specialist Committee on CFD and EFD Combined Methods.

8.1 General considerations

ITTC's recommended procedures for model tests are sometimes referenced in legal texts such as the EEDI regulations and in commercial contexts such as building contracts. Similar references for CFD computations have up to now not been requested. The introduction of CFD/EFD combined methods in, for example power predictions, will call for adequate procedures in order to ensure that accurate results are delivered.

A number of possible measures to take to ensure accurate results were discussed in the Joint Working Group:

1. Formulate detailed Recommended Procedures on how to perform the CFD simulations
2. Introduce a certification of CFD codes or certification of organisations conducting CFD simulations
3. Require that code vendors provide locked settings for certain type of computations.
4. Require that each organisation carries out quality control of their own CFD process

Option 1-3 were rejected with the following motivations:

A detailed prescribed procedure how to perform CFD simulations is not feasible. A definition of a "correct" procedure depends on the code, the type of grid, the type of case and so on. It would be a tremendous work to formulate recommended procedures that cover even the most common codes and cases. Moreover, since the technology is developing rapidly, such recommended procedures would soon be outdated. Some general *guidelines* could be given based on the outcome of international benchmark studies. However, these alone cannot ensure that the results are accurate.

Certification of CFD-codes would not be a sufficient requirement, as the uncertainty mainly stems from the users, not the codes. The available codes must be assumed to be verified by the vendors. Certification of the users would require an independent authority and we cannot see who that would be. Certification is not in line with ITTC praxis for model test. However, the committees can formulate a set of Competency Guidelines to assist customers of CFD-work when selecting the provider. See Section 8.4.

To require the CFD code vendors to provide locked standard settings for certain tasks would again require an independent authority that formulate test criterion. Very few commercial code vendors would probably spend effort on producing such settings.

The only option that the Joint Working Group deemed feasible for ITTC is to prescribe how each organisation should carry out quality control of their own CFD process, and how to demonstrate it. Currently there is no ITTC Guideline or Recommended Procedures describing this and therefore the Joint Working Groups decided to cover this gap. The following section describes the consideration behind the new suggested procedure.

8.2 A new procedure for Quality Assurance in Ship CFD Solutions

The existing ITTC Recommended Procedures 7.5-03-01-01 “Uncertainty Analysis in CFD Verification and Validation Methodology and Procedures” describes the CFD verification and validation process thoroughly. Such a process is useful for code developers and researchers when demonstrating the uncertainty of a solution or a methodology. It is however not very useful for the daily work such as performance evaluation in the design process. The *verification* process requires that computations are carried out for multiple refined grids. This is often regarded as not feasible for commercial reasons and it is often assumed not necessary for routine work, when it has been done once for a similar case. The *validation* process assumes that benchmark data is available, which is normally not the case during consultant or design work. For these reasons, it is unclear how the existing procedure should be applied in the daily work for clients. Instead, the Joint Working Group decided to formulate a new procedure that is useful for consultant or design work for clients especially when organizations regularly carry out CFD predictions of cases that are similar to each other. The procedure could be used by organizations that wish to demonstrate their ability to carry out CFD. It could also be used as purchase condition by clients who order CFD work. Finally, such procedure can be referenced within the ITTC framework.

The principle for the suggested process is that each organisation:

1. develops their own Best Practice Guideline (BPG)
2. assesses that it gives acceptable uncertainties
3. follows the BPG in consultancy services to clients

8.2.1 Best Practice Guideline

The BPG is a detailed description of how to set-up, run and interpret a CFD simulation for a

specific type of prediction and for a required uncertainty. The new procedure lists the minimum content of a BPG.

The BPG should give differentiated instructions depending on the type of case and required uncertainty. As an example, BPG for wave resistance computations cannot be used for form factor computations, planing hulls must be treated differently from displacement hull etc. In the new procedure we define the term “case type” as:

- Type of prediction; resistance, propulsion power, nominal wake, detailed flow, performance in waves etc.
- Ship type and condition; determining factors are e.g. relative size of resistance components (related to CB , Fr , Re), propulsion type, unusual hull forms and hull features

The definition of a “case type” at each organisation is in their responsibility and should follow the findings of state of the art experimental and computational maritime fluid dynamics. To define a case type, an organisation can follow the above mentioned criteria but is not limited to them.

8.2.2 Quality assessment

The organization should assure that the BPG is formulated such that it gives the requested uncertainty level *for the specified case type* by the following steps.

Numerical and modelling uncertainty

Verification and validation against measured data can be carried out for a few typical cases of the actual case type according to ITTC 7.5-03-01-01. This gives important knowledge to the organization which grid and solver settings have to be used for a defined case type with respect to a desired uncertainty level.

Total uncertainty

The Verification and Validation process, according to the existing ITTC Recommended Procedure Uncertainty Analysis in CFD, Verification and Validation Methodology and Procedures 7.5-03-01-01, is strictly speaking only valid for the investigated case, to which we already have a measured result. Can this be valid for the other cases in our daily work? The Recommended Procedure 7.5-03-01-01 leaves the question open: *“Whether to and how to associate an uncertainty level at a validated condition with a prediction at a neighbouring condition is very much unresolved and is justifiably the subject of much debate at this time”*.

The solution that was selected for the new procedure is a so called “big sample approach”, as for example demonstrated in Zhao et al 2017. This gives an indication of the “uncertainty of applying at a neighbouring condition”. It can also be seen as a way to capture the random part of the uncertainty due to difference in the CFD set-up. In the model test world, the repeated test with a standard model, which is common practice in ITTC community, is used to capture the random part of the uncertainty. The new procedure hence requires that the BPG is assessed using a large number of samples of similar type and preferably by different users in the organization.

The result should be presented in the form of statistics of the comparison error, E , given by the difference between the measured data, D , and simulation, S :

$$E = D - S \quad (153)$$

Note that E contains uncertainty of the simulation as well as the measured data.

The comparison error should be based on the same variable and same condition, including scale, as the CFD-simulation aims to predict, i.e. for full scale CFD-predictions, full scale measurements are needed.

The data for comparison can be provided by the same organisation that performs the CFD simulations. Due to the larger number of samples, the precision of each measurement may be less than for benchmark cases. For full scale measurements the precision is often very low. This needs to be considered in the comparison.

The number of cases that are required depends on the scatter of the result and the required accuracy. In practice, it is likely to be limited to the number of available measured data points. The more cases that an organization can include, the higher the confidence they can claim to have in their predictions.

8.2.3 Demonstration

The new ITTC Recommended Guidelines 7.5-03-01-02 Uncertainty Analysis in CFD, Guidelines for RANS Codes also provides guidelines for implementation of Quality Management procedure 7.5-03-01-01. This includes presenting the comparison error in a statistical way, for example as in Figure 15. If the number of data points permits, the probability for an error within the required level can be given.

The case type, for what that comparison is valid for, needs to be included in the quality assessment demonstration, as well as the number of cases that is used for the statistics.

8.3 Suggested new Recommended Procedure

Based on the work and considerations described above, a new Recommended Procedure was suggested, which is expected to replace the existing recommended guideline Uncertainty Analysis in CFD, Guidelines for RANS Codes 7.5-03-01-02:

7.5-03-01-02 “Quality Assurance in Ship CFD Applications”

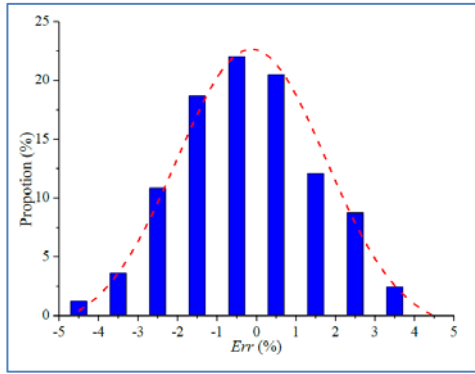


Figure 15. Example of quality assessment demonstration. Distribution of comparison error (Zhao et al 2017)

8.4 Advice to customers of CFD services

The following advice is directed to parties who are in the process of contracting for CFD consultancy services.

It is advisable to choose a CFD-service provider that:

1. follows either the existing ITTC Recommended Guidelines 7.5-03-01-02 “Uncertainty Analysis in CFD, Guidelines for RANS Codes” or when approved the new ITTC Recommended Guideline 7.5-03-01-02 “Quality Assurance in Ship CFD Applications”
2. uses a CFD-code that is considered to be established and state-of-the-art for hydrodynamics; with documented verification and validation, preferable demonstrated by participation in international benchmark studies
3. has a validation and correlation strategy against measured data, (including feedback from full scale data if full scale predictions are delivered)
4. has demonstrated expertise in maritime hydrodynamics

8.5 Conclusions

The introduction of CFD/EFD combined methods in, for example power predictions, will call for adequate procedures in order to ensure that accurate results are delivered.

A procedure that is useful for the daily work such as performance evaluation in the design process is needed.

To write a detailed description how to carry out CFD simulations is not a feasible option.

The committee has together with the Resistance and Propulsion Committee suggested a new Recommended Guideline “Quality Assurance in Ship CFD Applications”. The principle is that each organization derive their own Best Practice Guidelines and demonstrate their ability using multiple comparisons with measured values.

It is recommended that the full conference to adopt the new guideline.

8.6 Recommendations for further work

It is recommended that statistical techniques be used to assess the quality and accuracy of CFD analysis. Does the errors in general fit to the normal distribution as in Figure 15? How many cases are required? In case that no known distributions can be fit to the data, what is the alternative way? Can the mean error be an alternative way to assess?

ITTC can assist by providing a commonly agreed list of what different simulation “cases types” are and what the main parameters for BPG definition could be. An evaluation of CFD work as well as CFD benchmark workshops is required.

9. LIAISON WITH THE ITTC TC OF RELATED TECHNICAL AREAS

The committee collaborated with the Resistance and Propulsion Committee in two matters:

1. The proposed application of combined methods for form factor, which resulted in modifications to several procedures. (See Section 5)

2. Methods for CFD quality assurance, which was discussed in a joint working group between the two committees and resulted in a new proposed guideline for Quality Assurance and Ship CFD (see Section 8)

To complete TOR 5, all committee members were in contact with representatives from most of the other Technical Committees (see Section 6).

One of the committee members attended the meeting of the Specialist Committee on Ships in Operation at Sea in September 2018. Discussions and suggestions were made on the benchmark study for the evaluation of CFD applicability to determine the wind resistance.

As a Specialist committee, we have also reviewed the ITTC Manoeuvring Committee's revisions to the following guidelines and procedures:

- The Recommended Guideline 7.5-03-04-01 "Guideline on Use of RANS Tools for Manoeuvring Prediction"
- The Recommended Procedure 7.5-02-06-03 "Validation of Manoeuvring Simulation Models"
- The Recommended Guideline 7.5-03-04-02 "Validation and Verification of RANS Solutions in the Prediction of Manoeuvring Capabilities"

10. LIAISON WITH OTHER GROUPS OUTSIDE ITTC

10.1 CFD Workshop Committee

Since the first CFD Workshops in ship hydrodynamics held in 1980 at Gothenburg, Sweden (Larsson, 1981), the subsequent Workshops have been organized at approximately five year intervals at Gothenburg and Tokyo, Japan, alternately. The common objective of these Workshops was the assessment of up-to-date numerical methods for ship hydrodynamics to aid code development,

establish best practices and guide industry. Currently the CFD Workshops are being organized by the Steering Committee which consists of the hosts of the previous and next workshops and the area representatives in America, Europe and Asia. The committee summarised the evaluations of the last CFD Workshop, "Tokyo 2015" (Hino, 2015), and published the book (Hino, 2020). Also, the committee is working of the planning of the next Workshop, "Wageningen 202X" which was initially planned to be held in 2021 at Wageningen, Netherland hosted by MARIN but postponed to the later year due to the delay of SIMMAN Workshop and the circumstances related to COVID-19.

The present Specialist Committee on CFD and EFD Combined Methods was in contact with the Steering Committee of CFD Workshop through the common committee member.

Test cases for the "Wageningen 2021" Workshop are being discussed in the Steering Committee and Japan Bulk Carrier (JBC), KRISO Container Ship (KCS), ONR Tumblehome (ONRT) and a full-scale ship (not decided yet) have been selected as ship hulls. During the process, several suggestions were made from the Specialist Committee. In particular, the Specialist Committee proposed a blind test for which two members of Specialist Committee offered to provide tank test data. Unfortunately, the detailed local flow data demanded by the CFD workshop could not be offered and this suggestion was abandoned.

The information exchange on the benchmark data for full-scale ships between two committees was extremely useful. The communication between ITTC and the CFD Workshop Committee should continue in the future.

11. TOR 10

"Act as a research coordinator for other researchers who wish to contribute: Suggest research topics that lead towards the given

committee goals, assembly and review of ongoing work.”

11.1 List of Potential Research Topics

The CFD/EFD committee has been working as a research coordinator among the committee members, their respective institutions, and the greater international ship hydrodynamics community. The committee has initiated a form-factor study in which it is investigating the possibility of calculating the form factor for a ship hull using double-body CFD that can be used in tandem with EFD measurements at model scale of ship resistance and powering. The numerically-determined form factor may be superior to the current practice of an experimentally-determined form factor.

In addition to the form-factor study, the committee has compiled a list of research areas that utilize combined CFD/EFD.

- Experimental program for smooth body separation at full scale Reynolds numbers.
- Full scale field measurements of boundary layer and viscous wake.
- Use database of model scale EFD/CFD, full scale CFD, and sea trials to develop more accurate correlation allowance for extrapolation. The world-wide community collectively has an extensive database that could be studied to derive a better correlation allowance.
- Ability of CFD to predict wind resistance corrections for full scale speed trial corrections. A benchmark-study is ongoing and we encourage researchers and students to participate.
- Shallow water correction based on CFD simulations.
- Scale effects and ability of different CFD methods to predict effect of ESD and local inflow to propeller.
- Skin friction reduction methods with CFD.
- Ability of CFD to predict added resistance in waves and calm water.

- Importance of scale effects on wake and rudder force for seakeeping and manoeuvring tests.
- Using CFD to plan model test campaign for example selecting most important cases in a seakeeping program.
- Numerical models for ice loads.
- Scale effects and the ability of CFD methods to predict local propeller induced noise.
- Use EFD to tune CFD methods for roll damping, investigate scale effects for roll damping fins.
- Scale effects on appendage drag for calm water speed power predictions.
- Investigate scale effects on manoeuvring performance, e.g., propeller hull interactions. Design model scale propeller that creates correct propeller loads at model scale?
- Modelling of environmental conditions. Could CFD help understand physics involved in interactions when generating model scale waves, wind and current?
- Free surface effects on the boundary layer at full scale.

12. CONCLUSIONS AND RECOMMENDATIONS

Summary

In the maritime hydrodynamic field, EFD and CFD have up to now been seen as two separate, almost competing tools. This is reflected in ITTC’s procedures, which clearly separate CFD and model tests. Within ITTC, most organisations have the knowledge and resources to apply both EFD and CFD. This could be used to our advantage to a higher extent. Therefore, the “Specialist Committee on CFD and EFD Combined Methods” was formed in 2017 with the purpose to “initiate and support the process of introducing combined EFD/CFD methods in ITTC’s procedures”.

During these first three years, the Committee has supported the introduction of combined CFD/EFD methods in ITTC’s procedures by

performing a study on CFD based form factors to back up a proposed modification of the power prediction procedure. Furthermore, other possible improvements of the procedures using combined methods have been suggested and good examples of combined methods in the literature have been highlighted. The potential hesitation towards CFD methods in terms of uncertainty and trustworthiness have been addressed by proposing a new procedure for CFD Quality assurance.

It is concluded that the Committee has served its purpose and completed its tasks.

The Committee recommends that for the next ITTC period each committee should be requested to consider applications of combined methods in their respective fields. Each committee should also monitor and report on the uncertainty of CFD versus EFD for their relevant applications. This could be stressed by modifying The General Terms, as well as be included in each committee TOR.

Even if each committee will work with CFD and CFD/EFD combined methods in their respective fields, it would be useful to have one committee responsible for general issues of CFD and CFD/EFD and oversee that the idea of combinations is continuously developed and promoted. The Committee therefore recommends that in the next period one committee is appointed to be responsible for the CFD/EFD combined methods including CFD issues on an overview level. This includes the procedures for uncertainty assessment and quality assurance of CFD, review and highlight good examples of combined methods, suggest and initiate new applications of combined methods.

It is a common misconception in the maritime industry that the ITTC community favour experimental methods against computational. The truth is that ITTC members perform *hydrodynamic* predictions to the maritime industry with the most suitable tool available - numerical or experimental. Having access to both EFD, CFD and full scale trials,

we are in the best position to distinguish and be aware of the accuracy and capability of the different methods. ITTC could be more active in communicating this to all stakeholders. It could therefore be the task of the appointed committee to spread information in an understandable way to the maritime world outside ITTC on uncertainty of CFD versus EFD and combined methods, for example by compiling such information from the other committees.

12.1 Review of recent studies on claimed issues of model test prediction methods, for example scale effects

Model tests are still an accurate reliable way of prediction the speed power for ships. Nevertheless the computational methods can truly assist to improve the applied methods during the general scaling process by assisting and improving an individual scaling problem.

To identify which of the scaling problems would be the most suitable to be used for applying a CFD method for their improvement, the problems were listed and ranked them on different aspects. Different individual scaling problems for the calm water speed power prediction have been identified and their general uncertainty has been assessed to the level of impact on the prediction of correct trends in design as well as on the absolute powering level. The scaling problems have been rated on their frequency of occurrence in the typical business of towing tank facilities. The CFD method, which could be used in a certain scaling problem, has been assessed if it is easy to be used and state of the art for industrial CFD application. The possible improvement of the accuracy of a certain scaling problem by using CFD methods was judged as well.

All these aspects have been collected in a matrix-like overview. The determination of the form factor was addressed to be the most valuable one for further investigation to be used in combination with CFD methods.

It has to be noted here, that scaling effects and their possible assistance by CFD methods have been investigated separately here and not the combination of different scaling processes. It is known that scale effects have impact on the ranking: some scale effects are over predicting and some are under predicting. Effects are mixed and can interact in the end of a complete speed power prediction process and CFD methods could help to become aware of these effects. Picking out one scale effect and make it more robust by insights from CFD methods can result in that the final speed power prediction is not even more correct, because all scaling effects are mixed and working together hand in hand. The use of a correlation allowance finally corrects it. You have to be very careful by changing single scaling methods without checking the overall accordance with a modified correlation allowance value. Methods for checking and adapting the correlation allowance have to be available when changing individual parts of the scaling process.

The committee identified further scaling processes to be addressed in future for the consideration if CFD methods to be used in assistance for a more precise speed power prediction. The most important problems are: propeller-open-water scaling, effective wake scaling, scaling problems of immersed transoms and scaling of energy saving devices. Besides the scaling problems in the calm water speed power prediction, scaling problems in fields of manoeuvring, sea keeping and cavitation are also worth to look into them more in detail.

12.2 Review of benchmark studies, accuracy, achievements and challenges of FULL-SCALE ship CFD

- Work in the field of full-scale ship performance prediction is accelerating, based on the number of recent studies.
- Confidence in full-scale CFD simulations must be increased by demonstrating good predictive accuracy for large number of cases and over a range of conditions, consistently.

- At present, the scatter of predictions submitted to the Lloyd's Register workshop in 2016 suggests that the accuracy in power predictions with full scale CFD is still much lower than extrapolated towing tank tests. This cannot be expected to be improved simply by adding more computational power. Further work is needed to improve the computational models in full-scale simulations.
- The main challenges in full-scale CFD are identified as follows.
 - The accuracy and the resolution of the flow within a viscous and turbulent boundary layer.
 - Turbulence modelling.
 - Prohibitively large number of cells.
 - Modelling of flow separation.
- The largest barrier to improving the accuracy of full-scale CFD predictions is the lack of sea trials' data available in open literature.

The Committee recommends ITTC to continue monitoring the advances within full-scale CFD of maritime applications. Furthermore, to initiate or promote measurement campaigns of high Reynolds number flow cases.

12.3 Review of EFD/CFD combinations for relevant applications

The term CFD/EFD Combined Method could mean many different things. The Committee has categorised possible applications into the following areas:

- 1) Using CFD to derive new "empirical" relations to be used in an EFD scaling process, or verify existing ones. Examples found in literature are shallow water corrections, propeller open water scaling, and roughness allowances.
- 2) Using CFD to derive one component in a model test scaling procedure for the actual ship. An example is CFD-based form factor within the power prediction procedure.

Another example is wind resistance in speed trial evaluation.

- 3) Using CFD to design model test set-ups in order to conduct more efficient or accurate model tests. Not much is described in the literature. However, this has potential to be beneficial to ITTC members. Therefore, more attempts to collect good examples on this should be made and shared, in order to inspire other members. Examples could be:
 - a) Turbulence stimulation location
 - b) Plan calm water test by selecting most appropriate speed.
 - c) Plan seakeeping test programs (decide wave lengths, position in tank, timing of test, etc).
 - d) Pre-EFD prediction in order to give the test manager a warning if some measurement goes wrong.
 - e) Blockage correction.
 - f) Design of cavitation hull that correctly generates the scaled full-scale-wake
- 4) Tuning and validating CFD in model-scale for a specific case and use that to increase the confidence in the full scale modelling of the same case. This provides greater insight into scale effects and higher confidence in the full-scale predictions. A number of authors discuss various scale effects in the literature, especially of energy saving devices. Regarding possible tuning of CFD using EFD, one example is transition models applied to propeller blades, where the inflow turbulence level is tuned using EFD in order to get the correct transition point. There are also commercial providers of energy saving devices who claim greater confidence in the full-scale CFD prediction based on model test comparison. However, the question whether a CFD set-up that is validated at model-scale is also tuned for full-scale is not frequently discussed. This is an important knowledge gap. More full-scale validation cases are needed, not only speed trials but also details of the flow.
- 5) Using EFD to improve CFD models in general. Turbulence models and roughness models are examples of this.

It is concluded that a great deal of combined methods are already in use in the community for some years. The exact term “CFD/EFD Combined Methods” has appeared in at least two publications after the formation of our committee, but not connected to any of its committee members. Hence we believe that the committee has already had an effect to establish combined methods as a named concept and that in itself can stimulate its usage.

The Committee recommends that ITTC continues to monitor and suggest examples of CFD/EFD Combined Methods in order to inspire the community. It is suggested to continue using the categories given above when describing applications.

12.4 Suggest improvement of current recommended procedures by using CFD in combination with model test

The committee carried out a joint study with members from the Resistance and Propulsion committee on CFD form factors. The group was expanded with other external participants and included in total 9 organisations with 8 different CFD codes. The work is currently being documented in a journal paper, to be submitted in February 2020.

The following was concluded:

- Since the study contains only a limited number of test cases and only one organisation compared with a large number of sea trials, it can neither be affirmed nor rejected that that CFD-based form factors should replace the Prohaska method.
- It should be suggested that CFD-based form factors can be used to support the conventional Prohaska method.
- ITTC should encourage the use of CFD-based form factors to support the conventional method, as it seems likely that it improves the accuracy of the predictions on average.

- When more institutes gain experience with CFD-based form factors, the recommendations should be re-evaluated.
- The 1957 ship model correlation line caused the form factor to be Reynolds number dependent, which it should not be in principle. The main reason for this seems to be the too steep gradient towards lower Reynolds numbers. In practise this has minor influence on the power predictions thanks to the correlation factors, which are calibrated for each tank's individual data set. However, when using models of different size (Reynolds number) than the data set, especially for small towing tanks, this may be larger problem. The use of alternative lines should be investigated.
- To start with, C_F should be recommended to be derived from the ITTC-1957 model-ship correlation line, in spite of its drawbacks. In this way, each organisations' correlation factors (CA or CP) can be kept unchanged. The use of alternative friction lines for C_F should be investigated further.
- Ensure the quality of CFD prediction of form factor by referring to the new "Quality Assurance in Ship CFD Application", 7.5-03-01-02

Based on this study, as well as other publications, the committee proposed modifications to the Recommended Procedures:

- ITTC 7.5-03-02-04 "Practical Guidelines for Ship Resistance CFD", Section 3.1
- ITTC 7.5-02-03-01.4 "1978 ITTC Performance Prediction Method", Section 2.4.1

The proposals were implemented by the Resistance and Propulsion Committee.

The Committee recommends that ITTC adopt the modifications.

12.5 Suggestion to what parts of the ITTC procedures that could benefit from combined methods in future work

Based on discussions with members from the other committees some ideas for application of combined methods have been put forward. It is concluded that there is potential of promoting combined methods in most fields within ITTC. However, the experts in each committee are better suited to come up with the ideas, initiate and investigate them further. The Committee recommends ITTC to request each committee to consider CFD/EFD Combined Methods within their respective field.

- Ice
 - Numerical model for ice loads including accurate ice models
 - Ice paths under the hull
- Noise
 - Greater understanding of local noise sources from CFD
 - Scale effects on propeller flow fields
- Stability in Waves
 - Currently writing procedures on prediction of ship roll damping using CFD
 - Tune models based on experimental data.
- Operation of ships at sea
 - Wind resistance corrections:
 - New air resistance benchmark test cases available
 - Shallow water correction based on CFD simulations.
 - Added resistance in waves is challenging to do at this time.
- ESD
 - Local flow features at full scale
 - Scale effects on flow into the propeller
 - Skin friction reduction methods in CFD
 - Independent provider/assessor of full scale CFD
- Manoeuvring, Ocean Engineering
 - Investigate scale effects
 - Efficient planning of test

- Propeller hull interactions, design model scale propeller that creates correct propeller loads at model scale
- Sea keeping
 - Scale effects on wake and rudder force
 - Calculation of C_w using CFD
 - Use CFD to plan model test campaign (select most important cases)
 - Use EFD to tune CFD for roll damping
 - Scale effects for roll damping fins
- R&P:
 - Scale effects on appendage drag
 - Effective wake scaling
 - POW scaling
 - Numerical Friction line
 - Transom resistance scaling
 - Wave resistance scaling
 - Roughness effect
 - Pre-test prediction and planning of test
- Manoeuvring in Waves
 - Scale effects
 - Plan tests
- Marine Renewable Energy Devices
 - Scale effects, plan tests
- Modelling of Environmental Conditions
 - Produce guidelines for generating model scale waves, wind and current
 - Use CFD to help understand physics involved in interactions
- The validation and verification (V&V) standard proposed by American Society of Mechanical Engineers (ASME) or the ITTC Recommended Procedure 7.5-03-01-01 can be used to quantify numerical uncertainties and to validate CFD results for a single solution when a corresponding experimental value exists.
- How to transfer the uncertainty level to a prediction at a neighbouring condition is unresolved.
- The established procedures for verification and validation are applied in some but not all scientific publications.
- A guidance of how to deal with uncertainty assessments of CFD in routine work, such as predictions to clients, is lacking. This means that clients cannot request quality assurance in the same way as for model test. The main question marks are
 - How to deal with validation when experimental data does not exist, i.e. how to transfer the uncertainty level to a neighbouring condition.
 - Whether a grid convergence study needs to be performed for every case in routine work, or can the uncertainty level be assumed from a similar case.

12.6 Review of past work and procedures, within and outside ITTC, on CFD uncertainty, validation & verification (V&V), applied to the marine and other business sectors

The credibility of CFD simulations requires the estimation of numerical uncertainties to avoid the risk of making erroneous conclusions. To assess the reliability and accuracy of the CFD results, there are various procedures used for verification and validation.

- CFD results can be verified by performing grid and time-step convergence studies to assess numerical uncertainty.
- CFD results can be validated by comparing them with theoretical solutions and experimental data.

12.7 Suggest procedures to ensure the quality of CFD/EFD combined predictions

The introduction of CFD/EFD combined methods in for example power predictions will call for adequate procedures in order to ensure that accurate results are delivered. The review in TOR 6 concludes that a procedure useful for the daily work, such as performance evaluation in the design process, is lacking. The committee has together with the Resistance and Propulsion Committee carried out a joint study with the purpose of proposing ways to deal with this.

To write a detailed description how to carry out CFD simulations is not a feasible option. It is proposed that each organisation derive their own Best Practice Guidelines and demonstrate their ability using multiple comparisons with

measured values. This is described in a new proposed Recommended Procedure:

7.5-03-01-02 “Quality Assurance in CFD Ship Applications”

The Committee recommends to the Full conference:

- To adopt the new procedure.
- To monitor the use of the new procedure and update the Recommended Procedure if needed, especially the proposed way of presenting the comparison error.
- To continue maintaining and improving the existing Recommended Procedure 7.5-03-01-01, “Uncertainty Analysis in CFD”, which describes several options. The Full conference should consider narrowing this down, as it has to follow the development of new CFD techniques.

12.8 Liaison with the ITTC TC of related technical areas

The committee carried out joint work with the Resistance and Propulsion committee with excellent cooperation.

12.9 Liaison with other groups outside ITTC

The present Specialist Committee kept in touch with the Steering Committee of the next CFD Workshop “Wageningen 2020” through the common committee member. Some discussions have been made between two committees regarding the test cases of the workshop including full-scale benchmark data and the possibilities of the blind test cases etc. Several committee members are also members of the JoRes project for full-scale CFD.

The communication was a very useful opportunity for information exchange, and it is recommended to continue the contact with the CFD Workshop committee and JoRes, and to establish the connection with other possible groups outside ITTC.

12.10 Suggest research topics that contribute to the committee goals

The committee compiled a list of suggested research topics and unresolved questions. It was published on a committee member’s webpage and spread in social media.

It was concluded that it is easy to formulate interesting research suggestions but more difficult to disseminate them. The committee recommends ITTC to open a new page on ITTC webpage where suggested research topics from all committees can be listed. This could be very useful and inspiring for PhD students and researchers in the community. It could be the task of each committee to add to the list.

12.11 Present committee results in a public paper

The committee is requested to present the results “in a format directed towards the typical receiver of ship predictions including both ship owners and authorities.” This has been interpreted as an article in industry-involved journals and conferences.

The AC requested that the material should first be presented in the committee report to the next conference, and thereafter in a publication. The latter should be in ITTC name (actual authors may be identified) and needs the approval of the Executive Committee (which may delegate it to the AC).

It is challenging to comply with AC’s request, since the Committee will no longer exist after the next conference. The Committee will solve this by preparing as much as possible before the conference. Contribution to the articles will be done by some committee members on a voluntary basis, not by the full committee.

It is a good idea to increase the communication with the world outside ITTC, for example to explain issues like CFD versus EFD uncertainty to the stakeholders who actually *use* the results.

It is recommended that AC indicate a timeline for the approval and submission process if the next committee is given a similar task.

13. REFERENCES

- Amadeo M-G., Gonzalez-Adalid J., Perez-Sobrinho M., Gonzalez-Gutierrez L., 2017, "Open Water results comparison for three propellers with transition model, applying crossflow effect, and its comparison with experimental results", SMP 2017.
- American Institute of Aeronautics and Astronautics., 1998, "AIAA guide for the verification and validation of computational fluid dynamics simulations", American Institute of aeronautics and astronautics.
- Andersson, J., Oliveira, D.R., Yeginbayeva, I., Leer-Andersen, M., Bensow, R.E., 2020, "Review and comparison of methods to model ship hull roughness". Applied Ocean Research Vol. 99, pp. 102119. <https://doi.org/10.1016/j.apor.2020.102119>
- ASME, 2009, "Standard for Verification and Validation in Computational Fluid Dynamics and Heat Transfer", American Society of Mechanical Engineers, New York, Standard No. V&V 20-2009.
- ASME V&V 10-2006., 2006, "Guide for verification and validation in computational solid mechanics", American Society of Mechanical Engineers.
- Baltazar J., Rijpkema D., Falcao de Campos J.A.C. , 2017, "On the Use of the gamma RE_theta Transition Model for the Prediction of the Propeller Performance at Model-Scale", SMP 2017.
- Bhattacharyya A., Neitzel J.C., Stehen S. , Abdel-Maksoud M., Krasilnikov V., 2015a, "Influence of Flow Transition on Open and Ducted Propeller Characteristics", SMP 2015.
- Bhattacharyya A., Krasilnikov V., Steen S., 2015b, "Scale Effects on a 4-Bladed Propeller Operating in Ducts of Different Design in Open Water", SMP 2015.
- Bhushan, S., Xing, T., Carrica, P., Stern, F., 2009, "Model- and Full-Scale URANS Simulations of Athena Resistance, Powering, Seakeeping, and 5415 Manoeuvring". Journal of Ship Research Vol. 53, pp. 179–198.
- Bhushan, S., Xing, T., Carrica, P., Stern, F., Des, U., 2007, "Model- and Full-Scale URANS / DES Simulations for Athena R / V Resistance, Powering, and Motions", in: 9th International Conference on Numerical Ship Hydrodynamics Ann Arbor, Michigan. pp. 5–8.
- Bonfiglio L., Brizzolara S., 2015, "Effect of turbulence models on RANSE predictions of transient flow over blade sections", SMP 2015.
- Bulten, N., Nijland M., 2011, "On the development of a full-scale numerical towing tank Reynolds scaling effects on ducted propellers and wakefields", Second International Symposium on Marine Propulsors, SMP 2011.
- Bulten N., Stoltenkamp P., 2017, "Full-scale CFD: the end of the Froude-Reynolds battle", SMP 2017.
- Carrica, P.M., Mofidi, A., Eloot, K. and Defortrie, G., 2016. "Direct simulation and experimental study of zigzag maneuver of KCS in shallow water". Ocean engineering, 112, pp.117-133.
- Choi J-K., Park H-G. and Kim H-T., 2014, "A numerical study of scale effects on performance of a tractor type podded propeller", IJNAOE 2014.
- Coleman, H., Stern, F., 1998, "Closure to 'Discussion of. Uncertainties and CFD Code Validation'(1998, ASME J. Fluids Eng., 120,

- p. 635)", Journal of Verification, Validation and Uncertainty Quantification, Vol. 120(3), pp 635-636.
- Demirel Y.K., Khorasanchi M., Turan O., Incecik A., Schultz M.P., 2014, "A CFD model for the frictional resistance prediction of antifouling coatings", *Ocean Engineering*.
- Demirel Y.K., Turan O., Incecik A., 2017, "Predicting the effect of biofouling on ship resistance using CFD", *Applied Ocean Research*, Vol. 62, pages 100-118, <https://doi.org/10.1016/j.apor.2016.12.003>.
- Dong X-Q., Li W., Yang C-J., Noblesse F., 2017, "RANSE-based Simulation and Analysis of Scale Effects on Open-Water Performance of the PPTC-II Benchmark Propeller", SMP 2017.
- Duvigneau, R., Visonneau, M., Deng, G.B., 2003, "On the role played by turbulence closures in hull shape optimization at model and full scale". *Journal of Marine Science and Technology* Vol. 8, pp. 11–25. <https://doi.org/10.1007/s10773-003-0153-8>
- Duy T-N., Hino T., Suzuki K., 2017, "Numerical study on stern flow fields of ship hulls with different transom configurations", *Ocean Engineering*.
- Eça, L., Hoekstra, M., 2002, "An evaluation of verification procedures for CFD applications", In 24th Symposium on Naval Hydrodynamics, Fukuoka, Japan, July, pp 568-587.
- Eça L., Hoekstra M., 2005, "On the accuracy of the numerical prediction of scale effects on ship viscous resistance", *MARINE* 2015.
- Eça, L., Hoekstra, M., 2006, "Discretization uncertainty estimation based on a least squares version of the grid convergence index", In 2nd workshop on CFD uncertainty analysis. Lisbon, Portugal.
- Eça L., Hoekstra M., 2008, "The numerical friction line", *Journal of Marine Science and Technology*, 13, pp. 328–345, <https://doi.org/10.1007/s00773-008-0018-1>
- Eça, L., Hoekstra, M., 2014, "A procedure for the estimation of the numerical uncertainty of CFD calculations based on grid refinement studies", Journal of Computational Physics, Vol. 262, pp 104-130.
- Eça, L., Hoekstra, M., Hay, A., Pelletier, D., 2007, "A manufactured solution for a two-dimensional steady wall-bounded incompressible turbulent flow", International Journal of Computational Fluid Dynamics, Vol. 21(3-4), pp 175-188.
- Eça L., Hoekstra M. and Raven H.C., 2010, "Quantifying Roughness Effects by Ship Viscous Flow Calculations", 28th Symposium on Naval Hydrodynamics, Pasadena, California.
- Eça, L. S., Vaz, G., Hoekstra, M., 2010, "Code verification, solution verification and validation In RANS solvers", In International Conference on Offshore Mechanics and Arctic Engineering, Vol. 49149, pp 597-605.
- Farkas, A., Degiuli, N. and Martić, I., 2017, "Numerical simulation of viscous flow around a tanker model", *Brodogradnja*, 68 (2), 109-125. <https://doi.org/10.21278/brod68208>
- Farkas, A., Degiuli, N., Martić, I., 2018, "Assessment of hydrodynamic characteristics of a full-scale ship at different draughts". *Ocean Engineering* Vol. 156, pp. 135–152. <https://doi.org/10.1016/j.oceaneng.2018.03.002>
- Fujisawa, T., Tsubokura, M., Tanaka, H., 2020, "Study on Estimation of Flow Around Marine Propeller by Large-Scale LES and Affection of Grid Resolution and Reynolds

- Number", in: Proceedings of the ASME 2020 39th International Conference on Ocean, Offshore and Arctic Engineering, OMAE2020, August. Florida, US, pp. 1–8.
- Garcia-Gomez, 2000, Garcia-Gomez, A., 2000, "On the form factor scale effect", *Ocean Engineering*, (26).
- Garenaux, M., de Jager, A., Raven, H.C., Veldhuis, C., 2019, "Shallow-Water Performance Prediction: Hybrid Approach of Model Testing and CFD Calculations", in: *Practical Design of Ships and Other Floating Structures*. Springer, Singapore, pp. 63–82. https://doi.org/10.1007/978-981-15-4624-2_4
- Giannoulis, 2019, Giannoulis A., Halse K.H., 2019, "Evaluation of a practical approach for numerical propulsion tests", *OMAE 2019*
- Gornicz, T., van det Ploeg, A., Scholcz, T., 2016, "Trim wedge optimisation with viscous free surface computations", *PRADS 2016*.
- Grigson C.W.B., 1999, "A planar friction Algorithm and its use analysing hull resistance", *RINA*.
- Gudla, A.S.T., Kalyanam, S.S., Bhattacharyya, A., Sha, O.P., 2019, "Asymmetric Stern Modifications for KVLCC2", in: *Practical Design of Ships and Other Floating Structures*. Springer, Singapore, pp. 258–268. https://doi.org/10.1007/978-981-15-4624-2_15
- Guiard T., 2017, "Full-Scale Self-Propulsion Calculations Including Roughness Effects and Validation with Sea Trial Data", *Star Global conference*.
- Guiard, T., Leonard, S., Mewis, F., 2013, "The Becker Mewis Duct® - Challenges in Full-Scale Design and new Developments for Fast Ships", *Third International Symposium on Marine Propulsors smp'13*, Launceston, Tasmania, Australia.
- Guilmineau E., Deng G.B., Leroyer A., Queutey P., Visonneau M., Wackers J., 2015, "Influence of the Turbulence Closures for the Wake Prediction of a Marine Propeller", *SMP 2015*.
- Haase, M., Zurcher, K., Davidson, G., Binns, J.R., Thomas, G., Bose, N., 2016, "Novel CFD-based full-scale resistance prediction for large medium-speed catamarans". *Ocean Engineering Vol. 111*, pp. 198–208. <https://doi.org/10.1016/j.oceaneng.2015.10.018>
- Hafermann D., Schneider M., Richards J., Chao K.Y., Takai M., 2010, "Investigation of Propulsion Improving Devices with CFD", *PRADS 2010*.
- Hally D., 2017, "A RANS-BEM coupling procedure for calculating the effective wakes of ships and submarines", *SMP 2017*.
- Hasuike N., Okazaki M., Okazaki A. and Fujiyama K., 2017, "Scale effects of marine propellers in POT and self propulsion test conditions", *SMP 2017*.
- Heinke H-J., Hellwig-Rieck K., 2011, "Investigation of Scale Effects on Ships with a Wake Equalizing Duct or with Vortex Generator Finns", *Second International Symposium on Marine Propulsors, SMP11*.
- Heinke H.-J., Hellwig-Rieck K., Lübke L., 2019, "Influence of the Reynolds Number on the Open Water Characteristics of Propellers with Short Chord Lengths", *SMP 2019*.
- Helma S., 2015, "An Extrapolation Method Suitable for Scaling of Propellers of any Design", *SMP 2015*.
- Helma S., Streckwall H., Richter J., 2017, "The effect of propeller scaling methodology on the performance prediction", *SMP 2017*.
- Hino, T. (Ed.), 2015, "Tokyo 2015: A Workshop on CFD in Ship Hydrodynamics," *Workshop Proceedings, Tokyo, Dec. 2–4*.

- Hino, T. et al. (Ed.), 2020, “Numerical Ship Hydrodynamics: an assessment of the Tokyo 2015 Workshop, Springer.
- Hino T., Stern, F., Larsson, L., Visonneau, M., Hirata, N., Kim J., 2021, "Numerical Ship Hydrodynamics - An Assessment of the Tokyo 2015 Workshop", Springer 2021.
- Hiroi, T., Windén, B., Kleinwächter, A., Ebert, E., Fujisawa, J., Kamiirisa, H., Damaschke, N., Kawakita, C., 2019, "Full-Scale On-board Measurements of Wake Velocity Profiles , Underwater Noise and Propeller Induced Pressure Fluctuations". Conference Proceedings The Japan Society of Naval Architects and Ocean Engineers Vol. 29, pp. 193–198.
- Hollenbach U., 2009, "Pro’s and Con’s of the form-factor using Prohaska’s method when extrapolating the model resistance", STG Annual Meeting.
- Huang, Y.T., Lin, B.C., 2019, "Design and development of the energy saving rudder-bulb-fin combination by using computational fluid dynamics technique", in: Practical Design of Ships and Other Floating Structures. Springer, Singapore, pp. 290–302.
- IEEE Standards Coordinating Committee., 1991, “IEEE Standard Glossary of Software Engineering Terminology (IEEE Std 610.12-1990)”, Los Alamitos. CA: IEEE Computer Society, Vol. 169.
- Inukai, Y., 2019, "Full Scale Measurement of The Flow Field at The Stern by Using Multi - Layered Doppler Sonar (MLDS)", in: Sixth International Symposium on Marine Propulsors Smp’19, Rome, Italy.
- ISO, 1991, “9000-3: Quality Management and Quality Assurance Standards-Part 3: Guidelines for the Application of ISO 9001 to the Development, Supply and Maintenance of Software”, International Standards Organization, Geneva, Switzerland.
- ISO., 2008, “ISO 16730-1, Fire Safety Engineering - Assessment, Verification and Validation of Calculation Methods - Part 1: General”, International Organization for Standardization, Geneva.
- ISO., 2013, “ISO/TR 16730-3, Fire Safety Engineering - Assessment, Verification and Validation of Calculation Methods - Part 3: Example of a CFD model”, International Organization for Standardization, Geneva.
- ITTC, 1957, "Subjects 2 and 4 - Skin Friction and Turbulence Stimulation", 8th International Towing Tank Conference, (<https://itc.info/media/3107/subjects-2-4-skin-friction-and-turbulence.pdf>)
- ITTC, 1978, "Report of Resistance Committee", 15th International Towing Tank Conference , (<https://itc.info/media/2865/report-of-resistance-committee.pdf>)
- ITTC, 1990, "Report of the powering performance committee", 19th International Towing Tank Conference , (<https://itc.info/media/2304/report-of-the-power-performance-committee.pdf>)
- ITTC, 1999, "The Specialist Committee on Unconventional Propulsors", 22nd International Towing Tank Conference, (<https://itc.info/media/1516/specialist-committee-on-unconventional-propulsion.pdf>)
- ITTC, 2005, "The Specialist Committee on Azimuthing Podded Propulsion", 24th International Towing Tank Conference, (<https://itc.info/media/5864/volume-ii-specialist-committee-on-app.pdf>)
- ITTC, 2008, "The Specialist Committee on Azimuthing Podded Propulsion", 25th International Towing Tank Conference, (https://itc.info/media/3493/volume2_5azimuthingpoddedpropulsion.pdf)

- ITTC, 2011, "The Specialist Committee on Scaling of Wake Field", ITTC 2011, 2011(<https://itc.info/media/5530/10.pdf>)
- ITTC, 2017a, "7.5-02-02-01 Resistance Test", ITTC –Recommended Procedures and Guidelines, (<https://www.itc.info/media/8001/75-02-02-01.pdf>)
- ITTC, 2017b, "7.5-02-03-01.4 1978 ITTC Performance Prediction Method", ITTC – Recommended Procedures and Guidelines, (<https://www.itc.info/media/8017/75-02-03-014.pdf>)
- ITTC, 2017c, "7.5-02-03-01.3 Podded Propulsion Tests and Extrapolation", ITTC – Recommended Procedures and Guidelines, (<https://www.itc.info/media/8015/75-02-03-013.pdf>)
- ITTC, 2017d, "7.5-02-03-01.6 Hybrid Contra-Rotating Shaft Pod Propulsors Model Test", ITTC –Recommended Procedures and Guidelines, (<https://www.itc.info/media/8021/75-02-03-016.pdf>)
- ITTC, 2017e, "7.5-02-03-01.1 Propulsion/Bollard Pull Test", ITTC –Recommended Procedures and Guidelines, (<https://www.itc.info/media/8011/75-02-03-011.pdf>)
- ITTC, 2017f, "7.5-04-05-01 Guideline on the determination of model-ship correlation factors", ITTC –Recommended Procedures and Guidelines, (<https://www.itc.info/media/8185/75-04-05-01.pdf>)
- ITTC Procedures and Guidelines, 2017, "7.5-03-01-01 Uncertainty Analysis in CFD Verification and Validation, Methodology and Procedures", ITTC –Recommended Procedures and Guidelines, (<https://www.itc.info/media/>).
- Kim H-T., Kim H-T., Kim J-J. and Lee D-Y., 2019b, "Study on the skin-friction drag reduction by air injection using computational fluid dynamics-based simulations", PRADS 2019.
- Kim M-C., Shin Y-J. , Lee W-J., Lee J-H., 2017, "Study on Extrapolation Method for Self-Propulsion Test with Pre-Swirl Device", SMP 2017.
- Kim, K., Leer-Andersen, M. and Werner, S., 2019, "Roughness Effects on Ship Design and Operation", in: Practical Design of Ships and Other Floating Structures. Springer, Singapore, pp. 186–204.
- Kim, K., Leer-Andersen, M., Werner, S., Orych, M., Choi, Y., 2012, "Hydrodynamic Optimization of Pre-swirl Stator by CFD and Model Testing", 29th Symposium on Naval Hydrodynamics Gothenburg, Sweden, 26-31 August.
- Kim, K.S., Kim, Y.C., Yang, K.K., Kim, J., Hwang, S., Kim, M.S., Lee, Y.Y., Ahn, H., 2019, "Full Scale Computations for Resistance and Self-propulsion Performances of Commercial Ship by RANS Simulations", in: Practical Design of Ships and Other Floating Structures. Springer, Singapore, pp. 28–43. https://doi.org/10.1007/978-981-15-4624-2_2
- Kim, W., Jang, Y., Kim, M., 2016, "Performance analysis for DSME Cap Fin in model and full-scale", PRADS 2016.
- Kinaci O.C., Sukas O.F., Bal S., 2016, "Prediction of wave resistance by a Reynolds-averaged Navier–Stokes equation–based computational fluid dynamics approach", Journal of Engineering for the Maritime Environment, 3 (230).
- Klose R., Schulze R., Hellwig-Rieck K., 2017, "Investigation of Prediction Methods for Tip Rake Propellers", SMP 2017.

- Knupp, P., Salari, K., 2002, "Verification of computer codes in computational science and engineering. CRC Press.
- Kok, Z., Duffy, J., Chai, S. and Jin, Y., 2020, "Benchmark case study of scale effect in self-propelled container ship squat". ASME 2020 39th International Conference on Ocean, Offshore and Arctic Engineering. American Society of Mechanical Engineers Digital Collection.
- Korkmaz, K.B., Werner, S. and Bensow, R., 2019a, "Investigations for CFD Based Form Factor Methods" In Proceedings of the Numerical Towing Tank Symposium (NuTTS 2019), Tomar, Portugal, 29 September–1 October 2019.
- Korkmaz K.B., Werner S., Bensow R., 2019b, "Numerical friction lines for cfd based form factor determination", MARINE 2019.
- Korkmaz K.B., Werner S., Sakamoto N., Queutey P., Deng G., Yuling G., Guoxiang D., Maki K., Ye H., Akinturk A., Sayeed T., Hino T., Zhao F., Tezdogan T., Demirel Y.K. and Bensow R., 2021a, "CFD Based Form Factor Determination Method", Ocean Engineering, Vol. 220, 108451, <https://doi.org/10.1016/j.oceaneng.2020.108451>.
- Korkmaz, K. B., Werner S., Bensow R., 2021b, "Verification and Validation of CFD Based Form Factors as a Combined CFD/EFD Method", J. Mar. Sci. Eng., 9(1), 75; <https://doi.org/10.3390/jmse9010075>.
- Kouh, J-S., Chen, Y-J., Chau, S-W., 2009, "Numerical study on scale effect of form factor", Ocean Engineering, Vol. 36, Issue 5, pp 403-413.
- Krasilnikov V., 2013, "Self-Propulsion RANS Computations with a Single-Screw Container Ship", SMP 2013.
- Krasilnikov V., Sileo L. and Steinsvik K., 2017, "Numerical investigation into scale effect on the performance characteristics of twin-screw offshore vessels", SMP 2017.
- Krasilnikov V., Koushan K., Nataletti M., Sileo L. and Spence S., 2019, "Design and Numerical and Experimental Investigation of Pre-Swirl Stators PSS", SMP 2019.
- Larsson, L. (Ed.), 1981, "SSPA-ITTC Workshop on Ship Boundary Layers", SSPA Report 90, Gothenburg, Sweden.
- Larsson, L., Stern, F., Visonneau, M., 2013, "Numerical ship hydrodynamics: an assessment of the Gothenburg 2010 workshop", Springer Science & Business Media.
- Lee J-H., Kim M-C., Shin Y-J., Kang J-G., 2017, "Study on Performance of Combined Energy Saving Devices For Container Ship by Experiments", SMP 2017.
- Lee Y-G., Ha Y-J., Lee S-H., Kim S-H., 2018, "A study on the estimation method of the form factor for a full-scale ship", Brodogradnja, 69 (1).
- Liefvendahl, M., Fureby, C., 2017, "Grid requirements for LES of ship hydrodynamics in model and full scale". Ocean Engineering Vol. 143, pp. 259–268. <https://doi.org/10.1016/j.oceaneng.2017.07.055>
- Li D-Q., Lindell P., Werner S., 2019, "Transitional flow on model-scale propellers and their likely influence on performance prediction", SMP 2019.
- Lin T-Y. and Kouh J-S., 2015, "On the Scale Effect of Thrust Deduction in a Judicious Self-Propulsion Procedure for a Moderate-Speed Containership", J Mar Sci Technology, Vol. 20, pp 373–391, <https://doi.org/10.1007/s00773-014-0289-7>
- Lücke T., Streckwall H., 2017, "Experience with Small Blade Area Propeller Performance", SMP 2017.

- Mikkelsen, H., Steffensen, M.L., Ciortan, C., Walther, J.H., 2019, "Ship scale validation of CFD model of self-propelled ship". MARINE 2019 Computational Methods in Marine Engineering VIII pp. 718–729.
- Mikkelsen H., Walther J.H., 2020, "Effect of roughness in full-scale validation of a CFD model of self-propelled ships", Applied Ocean Research, Vol. 99, 102162.
- Müller S-B., Abdel-Maksoud M, Hilbert G., 2009, "Scale effects on propellers for large container vessel", First International Symposium on Marine Propulsors, 2009.
- Nguyen, T.V., Ikeda, Y., 2016, "Reynolds Number and Propeller effects on lift and drag forces on a high lift rudder with wedge tail", PRADS 2016.
- Niklas, K., Pruszko, H., 2019, "Full-scale CFD simulations for the determination of ship resistance as a rational, alternative method to towing tank experiments". Ocean Engineering Vol. 190, pp. 106435. <https://doi.org/10.1016/j.oceaneng.2019.106435>
- Oberkampf, W. L., Blottner, F. G., 1998," Issues in computational fluid dynamics code verification and validation", American Institute of Aeronautics and Astronautics (AIAA) Journal, Vol.36(5), pp 687-695.
- Oberkampf, W. L., Roy, C. J., 2010, "Verification and validation in scientific computing", Cambridge University Press.
- Okada Y., Katayama K., Okazaki A., Okazaki M., Fukuda K., Kobayashi Y., Kajino T., 2017, "The Battle Royal of Energy Saving Devices for a Ship", SMP 2017.
- Okazaki A., Yamasaki S., Kawanami Y., Ukon Y. and Ando J., 2015, "The Effect of Tip Rake on Propeller Open Water Efficiency and Propulsive Efficiency", SMP 2015.
- Oliva-Remolà, A., Rojas, L.P., Arribas, F.P., 2014, "A contribution to appendage drag extrapolation using computational tools", Developments in Maritime Transportation and Exploitation of Sea Resources - Proceedings of IMAM 2013, 15th International Congress of the International Maritime Association of the Mediterranean, 1, pp. 67-72
- Oliva-Remolà, Adriana & Rojas, Luis & Arribas, F.P.. (2013). "A contribution to appendage drag extrapolation using computational tools.", Developments in Maritime Transportation and Exploitation of Sea Resources, pp. 67-72, DOI:10.1201/b15813-10, Corpus ID: 53547412
- Oliveira D., Larsson A.I., Granhag L., 2018, "Effect of ship hull form on the resistance penalty from biofouling", The Journal of Bioadhesion and Biofilm Research, 34(3).
- Orihara, H., Tsujimoto, M., 2017, "Performance prediction of full-scale ship and analysis by means of on-board monitoring . Part 2 : Validation of full-scale performance predictions in actual seas". Journal of Marine Science and Technology Vol. 0, pp. 0. <https://doi.org/10.1007/s00773-017-0511-5>
- Park H-G., Choi J-K. and Kim H-T., 2014, "An estimation method of full-scale performance for pulling type podded propellers", IJNAOE, Vol. 6, Issue 4, pp 965-980.
- Park, D-W., 2015, "A study on the effect of flat plate friction resistance on speed performance prediction of full-scale", International Journal of Naval Architecture and Ocean Engineering, 2015(7).
- Pecoraro A., Di Felice F., Felli M., Salvatore F., Viviani M., 2013, "Propeller-hull interaction in a single-screw vessel", SMP 2013.
- Pena, B., Muk-Pavic, E., Ponkratov, D., 2019, "Achieving a high accuracy numerical simulations of the flow around a full scale

- ship", in: Proceedings of the International Conference on Offshore Mechanics and Arctic Engineering - OMAE. pp. 1–10. <https://doi.org/10.1115/OMAE2019-95769>
- Peravali S. K., Bensow R., Gyllenram W. and Shiri A., 2016, "An investigation on ittc 78 scaling method for unconventional propellers", ICHD 2016.
- Pereira, F.S., Eca, L., Vaz, G., 2017, "Verification and Validation exercises for the flow around the KVLCC2 tanker at model and full-scale Reynolds numbers". Ocean Engineering Vol. 129, pp. 133–148. <https://doi.org/10.1016/j.oceaneng.2016.11.005>
- Peric, M., 2019, "White paper: Full-scale simulation for marine design". Siemens White Paper.
- Ponkratov, D., 2016, "Lloyd's Register workshop on ship scale hydrodynamics", in: Ponkratov, D. (Ed.), 2016 Workshop on Ship Scale Hydrodynamic Computer Simulation. p. 2016. <https://doi.org/10.1002/ejoc.201200111>
- Ponkratov D., 2021, "Jores - Development of an industry recognised benchmark for Ship Energy Efficiency Solutions <https://jores.net/>".
- Quereda R., Bernal L., Pérez-Sobrino M., González-Adalid J., 2019, "Critical values of Rn defining transitional flow", SMP 2019.
- Quereda R., Pérez-Sobrino M., González-Adalid J., Soriano C., 2017, "Conventional propellers in CRP-POD configuration. Tests and extrapolation", SMP 2017.
- Raven H., van der Ploeg A., Starke B., 2004, "Computation of free-surface viscous flows at model and full-scale by a steady iterative approach", 25th Symposium on Naval Hydrodynamics.
- Raven, C.H., Ploeg, A., Starke, A.R., 2008, "Towards a CFD-based prediction of ship performance - Progress in predicting full-scale resistance and scale effects", RINA - International Conference - Marine CFD 2008.
- Raven, H., van der Ploeg, A., Starke, A.R., Eça, L., H. 2009 "Towards a CFD-Based Prediction of Ship Performance --- Progress in Predicting Full-Scale Resistance and Scale Effects." International Journal of Maritime Engineering 135: 12
- Raven H.C., 2017, "Combined CFD/EFD Methods-Exploiting CFD for Improving Performance Predictions", ITTC 2017.
- Raven H., Private communication, 2019
- Rawlings, J. O., Pantula, S. G., Dickey, D. A., 2001, "Applied regression analysis: a research tool", Springer Science & Business Media.
- Regener, P. B., Mirsadraee Y., and Andersen P., 2017, "Nominal vs. Effective Wake Fields and their Influence on Propeller Cavitation Performance", SMP 2017.
- Rijkema, D., Vaz, G., 2011, "Accurate model and full-scale viscous flow computations on propulsors", The Naval Architect, Issue (JULY-AUGUST), pp. 52-55
- Rijkema D., Baltazar J., de Campos J.F., 2015, "Viscous flow simulations of propellers in different Reynolds number regimes ", SMP 2015.
- Roache, P.J., 1998, "Verification and Validation in Computational Science and Engineering", Hermosa publishers, Albuquerque, New Mexico.
- Roache, P. J., 2002, "Code verification by the method of manufactured solutions", Journal of Fluids Engineering, Vol. 124(1), pp 4-10.

- Roache, P. J., Knupp, P. M., Steinberg, S., Blaine, R. L., 1990, "Experience with benchmark test cases for groundwater flow", In 1990 Spring Meeting of the Fluids Engineering Division, Toronto, Ont, Can, 06/04-07/90, 49-56.
- Roache, P. J., Steinberg, S., 1984, "Symbolic manipulation and computational fluid dynamics", American Institute of Aeronautics and Astronautics (AIAA) Journal, Vol. 22(10), pp 1390-1394.
- Roy, C. J., Nelson, C. C., Smith, T. M., Ober, C. C., 2004, "Verification of Euler/Navier–Stokes codes using the method of manufactured solutions", International Journal for Numerical Methods in Fluids, Vol. 44(6), pp 599-620.
- Sakamoto, N., Ohashi, K., Kobayashi, H., 2019, "Overset RaNS Computation of Flow around Bulk Carrier with ESD in Full Scale and its Validation". Conference Proceedings The Japan Society of Naval Architects and Ocean Engineers Vol. 29, pp. 199–204.
- Salari, K., Knupp, P., 2000, "Code verification by the method of manufactured solutions (No. SAND2000-1444)", Sandia National Labs., Albuquerque, NM (US); Sandia National Labs., Livermore, CA (US).
- Sánchez-Caja A., Ory E., Salminen E., Pylkkänen J., Siikonen, T., 2003, "Simulation of Incompressible Viscous Flow Around a Tractor Thruster in Model and Full Scale. ", The 8th International Conference on Numerical Ship Hydrodynamics.
- Sasajima, H. and Tanaka, I., 1966, "On the estimation of wakes of ships", XI ITTC, Tokyo.
- Sasaki N., Atlar M., 2019, "Scale Effect of Gate Rudder", SMP 2019.
- Sezen, S., Cakici, F., 2019, "Numerical Prediction of Total Resistance Using Full Similarity Technique". China Ocean Engineering Vol. 33, pp. 493–502. <https://doi.org/10.1007/s13344-019-0047-z>
- Shin K-W., Andersen P., 2017, "CFD Analysis of Scale Effects on Conventional and Tip-Modified Propellers", SMP 2017.
- Song K-W., Guo C-Y., Wang C., Sun C., Li P., Zhong R-F., 2019, "Experimental and numerical study on the scale effect of stern flap on ship resistance and flow field", Ships and Offshore Structures, Vol. 15, Issue 9, pp 981-997.
- Song, S., Demirel, Y.K., Atlar, M., 2019, "An investigation into the effect of biofouling on the ship hydrodynamic characteristics using CFD". Ocean Engineering Vol. 175, pp. 122–137. <https://doi.org/10.1016/j.oceaneng.2019.01.056>
- Starke B., Raven H.C., van der Ploeg A., 2007, "Computation of transom-stern flows using a steady free-surface fitting RANS method", 9th International Conference on Numerical Ship Hydrodynamics.
- Starke, A.R., Drakopoulos, K., Toxopeus, S.L., Turnock, S.R., 2017, "RANS-based full-scale power predictions for a general cargo vessel, and comparison with sea-trial results". 7th International Conference on Computational Methods in Marine Engineering, MARINE 2017 Vol. 2017-May, pp. 353–364.
- Stewart J.R., 2003, "A posteriori error estimation for predictive models", Presentation at the Workshop on the Elements of Predictability, Johns Hopkins University, Baltimore, Maryland, November 13–14.
- Strasser G., 2018, "QSG Note on Model-Ship Extrapolation Process", Private communications

- Streckwall H., Greitsch L., Scharf M., 2013, "An advanced Scaling Procedure for Marine Propellers", SMP 2013.
- Sun, W., Hu, Q., Hu, S., Su, J., Xu, J., Wei, J., 2020, "Numerical Analysis of Full-Scale Ship Self-Propulsion Performance with Direct Comparison to Statistical Sea Trial Results". *Journal of Marine Science and Engineering* Vol. 8, pp. 1–22.
- Sun W., Hu S., Su J., Wei J., Huang G., 2019, "Numerical Analysis of Hull- Propeller and Free Surface Interaction at Model- and Full-Scale", SMP 2019.
- Tacar Z., Sasaki N., Atlar M., Korkut E., 2019, "Investigation of scale effects on gate rudder® performance", AMT 2019.
- Tahara Y., Himeno Y., Katsui T., 2003, "Computation of ship viscous flow at full-scale Reynolds number: consideration of near-wall flow model including surface roughness effect", *Journal of The Society of Naval Architects of Japan*, (192).
- Tamura, K. and Sasajima, T., 1977, "Some Investigation on Propeller Open-Water Characteristics for Analysis of Self-Propulsion Factors", *Mitsubishi Technical Bulletin*, No. 119, pp 1-12.
- Tautges, T. J., 2001, "CGM: A geometry interface for mesh generation, analysis and other applications", *Engineering with Computers*, Vol. 17(3), pp 299-314.
- Terziev, M., Tezdogan, T., Incecik, A., 2019, "A geosim analysis of ship resistance decomposition and scale effects with the aid of CFD". *Applied Ocean Research* Vol. 92. <https://doi.org/10.1016/j.apor.2019.101930>
- Terziev, M., Tezdogan, T., Incecik, A., 2020, "A posteriori error and uncertainty estimation in computational ship hydrodynamics". *Ocean Engineering* Vol. 208, pp. 107434. <https://doi.org/10.1016/j.oceaneng.2020.107434>
- Tezdogan, T., Incecik, A., Turan, O., 2016, "Full-scale unsteady RANS simulations of vertical ship motions in shallow water". *Ocean Engineering* Vol. 123, pp. 131–145. <https://doi.org/10.1016/j.oceaneng.2016.06.047>
- Toki N., 2008, "Investigations on Correlation Lines through the analysis of Geosim Model test results", *Journal of the Japan Society of Naval Architects and Ocean Engineers*.
- Townsin R. L., Medhurst J. S., Hamlin N. A., Sedat B. S., 1984, "Progress in Calculating the Resistance of Ships with Homogeneous or Distributed Roughness ", *NECIES Centenary Conference on Marine Propulsion*.
- Tsujimoto, M., Orihara, H., 2018, "Performance prediction of full-scale ship and analysis by means of on- board monitoring (Part 1 ship performance prediction in actual seas)". *Journal of Marine Science and Technology* Vol. 0, pp. 0. <https://doi.org/10.1007/s00773-017-0523-1>
- van der Ploeg A., Starke B., 2011, "Prediction of the transom flow regime with viscous free surface computations", *MARINE* 2011, (29).
- Van Hoydonck W., Delefortrie G., De Maerschack B. and Vantorre M., 2018, "Open-Water Rudder Tests using CFD", *SNH* 2018.
- Van S.-H, Ahn H., Lee Y.-Y., Kim C., Hwang S., Kim J., Kim K.-S., Park I.-R., 2011, "Resistance characteristics and form factor evaluation for geosim models of kvlcc2 and kcs", *Advanced Model Measurement Technology for EU Maritime Industry - AMT'11*.
- Veikonheimo T., Miettinen P., Huisman J., 2017, "On the advanced extrapolation method for a new type of podded propulsor via CFD simulations and model measurements", *SMP* 2017.

- Visonneau M., Queutey P. and Deng G.B., 2006, "Model and full-scale free-surface viscous flows around fully-appended ships", ECCOMAS CFD.
- Visonneau, M., G.B. Deng, E. Guilmineau, P. Queutey & J. Wackers, 2016, "Local and Global Assessment of the Flow around the Japan Bulk Carrier with and without Energy Saving Devices at Model and Full Scale", 31th Symposium on Naval Hydrodynamics.
- Wageningen 2021: a Workshop on CFD in Ship Hydrodynamics", <https://w2020.marin.nl/>
- Wang, J., Yu, H. and Feng, Y. 2019 "Feasible study on full-scale delivered power prediction using CFD/EFD combination method" *J Hydrodyn Vol 31*, pp 1250–1254 (2019).
- Wang J., Yu H., Zhang Y. and Xiong X., 2016, "CFD-Based Method of Determining Form Factor k for Different Ship Types and Different Drafts", *Journal of Marine Science Applications*, Vol. 15, pp 236–241.
- Wang W.-H, Gu M.-Y. and Wang Y.-Y., 2015, "Calculation method of form factor based on energy conservation of ship wave-making. ", *Journal of Ship Mechanics*, Vol. 19.
- Wang, Z-Z., Xiong, Y., Shi, L. and Liu, Z., 2015, "A numerical flat plate friction line and its application", *Journal of Hydrodynamics* 23, pp 383–393.
- Wang, Z-Z., Xiong, Y., Wang, R., Shen, X-R. and Zhong, C-H., 2015, "Numerical study on scale effect of nominal wake of single screw ship", *Ocean Engineering*, Vol. 104.
- Wang, Z-Z., Xiong Y., Wang R., Zhong C-H., 2016, "Numerical investigation of the scale effect of hydrodynamic performance of the hybrid CRP pod propulsion system", *Applied Ocean Research*, Vol. 54.
- Wawrzusiszyn M., Kraskowski M., Król P., Bugalski T., 2018, "Experimental and Numerical Hydrodynamic Analysis of Propulsion Factors On R/V Navigator XXI with a Pre-Swirl Stator Device", NUTTS 2018.
- Werner S., Gustafsson L., "Uncertainty of Speed Trials", In the proceedings of Hull PIC 2020, Hamburg, Germany.
- Xia, L., Lundberg J., Bensow R., 2012, "Performance Prediction of a Nozzle Propeller", 29th Symposium on Naval Hydrodynamics.
- Xing-Kaeding Y., Gatchell S. and Streckwall H., 2015, "Towards Practical Design Optimization of Pre-Swirl Device and its Life Cycle Assessment", SMP 2015
- Yamano T., Kusunoki Y., Kuratani F., Ikebuchi T. and Funeno I., 2001, "On Scale effect of the resistance due to stern waves including forward-oriented wave breaking just behind a transom stern", PRADS 2001.
- Yazaki A., 1969, "A Diagram to Estimate the Wake Fraction for a Actual Ship from a Model Tank Test", 12th ITTC, Rome.
- Yao, Z. Q., Shen, H. C., Hui, G. A. O., 2013, "A new methodology for the CFD uncertainty analysis", *Journal of Hydrodynamics*, Ser. B, 25(1), pp 131-147.
- Zhang, H., Wang, X., Chen, X., 2018, "Scale Effect Studies on Hydrodynamic Performance for DTMB 5415 Using CFD", in: Proceedings of the ASME 2018 37th International Conference on Ocean, Offshore and Arctic Engineering, June. pp. 1–7.
- Zhao et al 2017, "An Innovative Methodology of Confidence Level Assessment for Virtual Test of Ship Hydrodynamics", *The 30th American Towing Tank Conference*
- Zhou, Y., Liu, L., Cai, X., Feng, D., Guo, B., 2019, "Numerical study on scale effect of KCS", in: Proceedings of the ASME 2019

38th International Conference on Ocean,
Offshore and Arctic Engineering
OMAEO2019 June 9-14, 2019, Glasgow,
Scotland, UK. pp. 1-7.
<https://doi.org/10.3390/app9204442>

Zondervan G-J., de Jager A., Veldhuis C.,
Gareaux M., Bosschers J., Janse G., 2019,
"Advances in Design and Analysis of
Ducted Propellers for Dredging Vessels",
PRADS 2019.

Appendix A. LEVEL OF IMPACT FOR DIFFERENT ISSUES AFFECTING THE SCALING AND PERFORMANCE PREDICTION

Table 2 Determination of the level of impact for different issues affecting the scaling and performance prediction procedure of vessels. Rank 0-1-2 (2 is highest).

Item	Impact on trend and design	Impact on absolute power	Frequency of occurrence	Total impact	Possibility to improve with CFD
Hull friction determination using alternative friction or correlation line	1	0	2	3	1
Determination of the form factor	2	2	2	6	2
Wave resistance	1	0	1	2	2
Transom drag	2	1	1	4	2
Roughness allowance	0	1	2	3	1
Appendage resistance	2	1	1	4	2
Flow separation or vortex on the hull	2	1	1	4	0
Propeller open water scaling	2	0	2	4	1
Nominal wake field scaling	2	1	1	4	2
Effective wake scaling	2	1	2	5	2
Energy Saving Device	2	2	1	5	1
Ducted propeller	2	2	0	4	1